

Aus der Klinik für Innere Medizin/Kardiologie
am Deutschen Herzzentrum Berlin

DISSERTATION

Myocardial strain: On agreement and reproducibility of a new
parameter to determine ventricular function

zur Erlangung des akademischen Grades
Doctor medicinae (Dr. med.)

vorgelegt der Medizinischen Fakultät
Charité – Universitätsmedizin Berlin

von

Jennifer Sigrid Myrtle Erley

aus Tübingen

Datum der Promotion: 4. Juni 2021

Table of Contents

<u>List of Tables</u>	I
<u>List of Figures</u>	II
<u>List of Abbreviations</u>	III
<u>Abstract (English)</u>	1
<u>Abstract (Deutsch)</u>	2
<u>Introduction</u>	4
I. <u>Overthinking diagnostic procedures in cardiology</u>	4
II. <u>Non-invasive cardiovascular imaging</u>	4
III. <u>Quantifying myocardial contractility</u>	4
IV. <u>Modalities and techniques to determine myocardial strain</u>	5
a) <u>Speckle-tracking Echocardiography (STE)</u>	5
b) <u>Myocardial Tagging (TAG)</u>	6
c) <u>Myocardial Feature Tracking (FT)</u>	6
d) <u>Strain-encoding (SENC)/ fast Strain-encoding (fSENC)</u>	7
V. <u>Aims of this dissertation</u>	8
<u>Materials and Methods</u>	8
I. <u>Inter-vendor agreement</u>	8
II. <u>Test-retest reproducibility</u>	10
III. <u>Inter- and intra-observer reproducibility</u>	10
<u>Results</u>	11
I. <u>Inter-vendor agreement</u>	11
II. <u>Test-retest reproducibility</u>	11
III. <u>Inter- and intra-observer reproducibility</u>	13
<u>Discussion</u>	14
I. <u>Inter-vendor agreement</u>	15
II. <u>Test-retest reproducibility</u>	17
III. <u>Inter- and intra-observer reproducibility</u>	18
IV. <u>Outlook into the future of strain imaging</u>	19
<u>References</u>	21
<u>Eidesstattliche Versicherung</u>	26
<u>Anteilsklärung an den erfolgten Publikationen</u>	27
<u>Liste ausgewählter Publikationen</u>	29
<u>Druckexemplare der ausgewählten Publikationen</u>	30
<u>Lebenslauf</u>	75
<u>Publikationsliste</u>	78
<u>Danksagung</u>	80

List of Tables

- I. On inter-vendor agreement (page 11)
 - **Table 1:** Results of the Bland-Altman analysis demonstrating inter-vendor agreement (page 11).
- II. On test-retest reproducibility (pages 12 and 13)
 - **Table 2:** Median (IQR) strain values of scans before (1+2) and after (3+4) the break and corresponding significance values (page 12).
 - **Table 3:** Test-retest reproducibility between scans before (1+2) and after (3+4) the break, shown using ICC (95% CI) and CoV (\pm sd) (page 12).
 - **Table 4:** Test-retest reproducibility between single scans, shown using ICC (95% CI) and CoV (\pm sd) (pages 12 and 13).
- III. On inter- and intra-observer reproducibility (page 14)
 - **Table 5:** Results of the ICC and CoV (\pm sd)-analyses on inter- and intra-observer reproducibility (page 14).

List of Figures

- **Figure 1:** STE-images (4-chamber view), including the myocardial contours (left) and the corresponding longitudinal LV strain curves (right), of a healthy person (I.) and a patient with coronary artery disease (II). Strain analysis was performed using EchoInsight (Epsilon Imaging, Ann Arbor, Michigan, USA) (page 5).
- **Figure 2:** Exemplary TAG-images (short-axis and 4-chamber view), including myocardial contours (left) and corresponding LV strain curves (right), of a healthy volunteer. Circumferential strain is determined in the short-axis images and longitudinal strain in the long-axis views. Strain analysis was conducted using Segment (version 2.2 R6960 (<http://segment-heiberg.se>)) (page 6).
- **Figure 3:** Exemplary FT-images (short-axis and 4-chamber view), including the myocardial contours (left) and the corresponding LV strain curves (right), of a patient with cardiac amyloidosis, coronary artery disease and diastolic heart failure. Similar to TAG, circumferential strain is determined in the short-axis and longitudinal strain using the long-axis images. Images were analyzed with SuiteHeart (SuiteHEART, Neosoft, Pewaukee, Wisconsin, USA) (page 7).
- **Figure 4:** fSENC-images (4-ch and midventricular short-axis view) of a healthy volunteer. After post-processing, the regional strain is depicted in a color-coded outline of the heart (green and blue indicating contraction vs. yellow and red indicating relaxation). Using SENC, circumferential strain is measured in the long-axis images and longitudinal strain in the short-axis images (page 7).

List of Abbreviations

CI	confidence interval
CMR	cardiovascular magnetic resonance imaging
CoV	coefficient of variation
EF	ejection fraction
EPI	echo planar imaging
ES	end-systole
FOV	field-of-view
fSENC	fast strain-encoding
FT	feature tracking
GCS	global circumferential strain
GLS	global longitudinal strain
HFpEF	heart failure with preserved ejection fraction
HFrfEF	heart failure with reduced ejection fraction
ICC	intraclass correlation coefficient
IQR	interquartile range
LOA	limits of agreement
LV	left ventricular
Sd	standard deviation
SENC	strain-encoding
SPIR	selective fat suppression
SSFP	steady-state free precession
STE	speckle-tracking echocardiography
TA	acquisition time
TAG	tagging
TE	echo time
TR	repetition time

Abstract (English)

Background. Strain is a novel quantitative parameter to determine heart function and heart failure by measuring the shortening of the heart muscle from diastole to systole. Using cardiovascular magnetic resonance imaging (CMR), various techniques are available to quantify strain: tagging (TAG), feature tracking (FT) and strain-encoding (SENC)/ fast strain-encoding (fSENC). In echocardiography, strain can be calculated using speckle-tracking (STE). Whereas the problem of inter-vendor variability of different ultrasound systems is well analyzed for STE, it is unknown if the choice of the magnetic resonance imaging scanner influences CMR-strain measurements. Moreover, important aspects of reproducibility have not been thoroughly explored for many modalities and techniques, such as fSENC, limiting the use of strain measurements in clinical routine. This dissertation focuses on a study published by our working group to address these obstacles regarding the fSENC-technique. Furthermore, it integrates the results into a clinical context and compares the analysis to research on other modalities and techniques.

Methods. Fifteen healthy volunteers were scanned at three centers with different 3T magnetic resonance scanners from leading vendors: the German Heart Institute Berlin, the Charité University Medicine Berlin-Campus Buch and the Theresien-Hospital Mannheim. Every volunteer received four fSENC-scans with a uniform imaging protocol, interrupted by a fifteen-minute break between scan number two and three. Left ventricular (LV) global longitudinal strain (GLS) and circumferential strain (GCS) were analyzed (Myostrain 5.0, Myocardial Solutions). Inter-vendor agreement was determined using Bland-Altman analysis. Test-retest reproducibility and inter- and intra-observer reproducibility were calculated using intraclass correlation (ICC) and coefficients of variation (CoV). The results are demonstrated and compared to studies on different modalities and techniques for strain analysis.

Results. fSENC showed good to moderate inter-vendor agreement between different sites (bias of 0.01-1.88%) and excellent test-retest reproducibility, regardless of the vendor. Inter- and intra-observer agreement of all global strain analyses were excellent.

Conclusion. Our findings show that a bias should be expected when using fSENC in volunteers. Although this bias needs to be validated in a larger cohort and in patients, it should be considered when planning multi-center studies and when comparing fSENC scans that were acquired at different sites. The excellent test-retest reproducibility and intra- and inter-observer reproducibility reflect the reliability of fSENC, which is in accordance with other modalities and techniques to determine strain.

Abstract (Deutsch)

Hintergrund. „Strain“ (Verformung) ist ein neuer quantitativer Parameter zur Bestimmung von Herzfunktion und Herzinsuffizienz anhand der Messung der Verkürzung des Herzmuskels von Diastole zu Systole. In der kardiovaskulären Magnetresonanztomographie (MRT) sind verschiedene Techniken zur Quantifizierung von „Strain“ verfügbar: „Tagging“ (TAG), „Feature Tracking“ (FT) und „Strain-encoding“ (SENC)/ „fast Strain-encoding“ (fSENC). In der Echokardiographie kann „Strain“ mittels „Speckle-tracking“ (STE) berechnet werden. Während das Problem der Variabilität zwischen verschiedenen Ultraschallsystemen für „STE“ bereits gut untersucht ist, ist es ungewiss ob die Wahl des Scanners einen Einfluss auf die MRT „Strain“-Messwerte hat. Außerdem wurden wichtige Aspekte der Reproduzierbarkeit für viele Modalitäten und Techniken, wie zum Beispiel „fSENC“, noch nicht vollständig erforscht, was den Nutzen von „Strain“-Messungen in der klinischen Routine einschränkt. Diese Dissertation fokussiert sich auf eine Studie, die unsere Arbeitsgruppe publizierte, um diese Hindernisse in Bezug auf die „fSENC“ Technik zu adressieren. Darüber hinaus integriert sie die Ergebnisse in einen klinischen Kontext und vergleicht diese Analyse mit der Forschung zu anderen Modalitäten und Techniken.

Methoden. Fünfzehn gesunde Probanden wurden an drei Zentren mit verschiedenen 3T MRT-Geräten der führenden Hersteller untersucht: am Deutschen Herzzentrum Berlin; der Charité Universitätsmedizin Berlin- Campus Buch und dem Theresien-Krankenhaus Mannheim. Jeder Proband erhielt vier „fSENC“-Untersuchungen mit einem einheitlichen Bildgebungsprotokoll, unterbrochen von einer fünfzehn-minütigen Pause zwischen den Untersuchungen Nummer zwei und drei. Der linksventrikuläre (LV) globale longitudinale „Strain“ (GLS) und der LV zirkumferentielle „Strain“ (GCS) wurden analysiert (Myostrain 5.0, Myocardial Solutions). Die Übereinstimmung zwischen den Herstellern wurde mittels Bland-Altman Analyse bestimmt. Die Reproduzierbarkeit wiederholter Messungen sowie die Inter- und Intraobserver-Vergleichbarkeit wurden mit der Intraklassen-Korrelation (ICC) und dem Variationskoeffizienten (CoV) berechnet. Die dargestellten Ergebnisse werden demonstriert und mit Studien zu anderen Modalitäten und Techniken zur Messung von „Strain“ verglichen.

Ergebnisse. „fSENC“ zeigte eine gute bis moderate Übereinstimmung zwischen verschiedenen Standorten (Bias von 0.01-1.88%) und eine exzellente Reproduzierbarkeit aufeinanderfolgender Tests, ungeachtet des Herstellers. Die Interobserver und Intraobserver-Vergleichbarkeiten aller globalen „Strain“-Analysen waren exzellent.

Schlussfolgerung. Unsere Ergebnisse zeigten, dass ein Bias bei der Nutzung von „fSENC“ bei Probanden erwartet werden muss. Obwohl dieser Bias in einer größeren Kohorte und in

Patienten validiert werden muss, sollte er bei der Planung von multizentrischen Studien und beim Vergleich von „fSENC“ Messungen an verschiedenen Standorten berücksichtigt werden. Die exzellente Reproduzierbarkeit wiederholter Messungen sowie die Interobserver- und Intraobserver-Vergleichbarkeiten reflektieren die Verlässlichkeit von „fSENC“. Dies ist in Übereinstimmung mit anderen Modalitäten und Techniken zur Bestimmung von „Strain“.

Introduction

I. Overthinking diagnostic procedures in cardiology

Despite a recent decline in the mortality rates caused by cardiovascular diseases overall, a rapid increase can be observed in the incidence of heart failure with growing life expectancy of the population in Germany (1). Heart failure, the long-term consequence of many cardiovascular diseases, needs to be recognized at an early stage when treatment options are still available and the quality of life of patients is not yet irreversibly impaired. To do this, new diagnostic tools, which might allow for the early screening, reliable detection and accurate monitoring of treatment strategies in heart failure patients, should thoroughly be studied to pave the way for future use in clinical routine.

II. Non-invasive cardiovascular imaging

Echocardiography is the most widely used, practical and fastest non-invasive method to image the heart. Nevertheless, cardiovascular magnetic resonance imaging (CMR) is the current non-invasive reference standard for analysis of cardiac morphology and function (2, 3), surpassing echocardiography regarding “tissue contrast, spatial resolution and signal to noise ratio” (4, p. 1). Due to high examination costs, limited scanner access and missing skills to perform and analyze CMR, it is mostly recommended as a diagnostic modality when echocardiographic images are unsatisfactory (5). However, CMR provides added diagnostic value for many purposes, for example to differentiate between the underlying pathologies of heart failure (e.g. of infiltrative or inflammatory nature) and for the diagnostic work-up of patients with cardiomyopathies and congenital heart diseases (5).

III. Quantifying myocardial contractility

The quantification of myocardial function in both echocardiography and CMR was possible using a parameter called ejection fraction (EF), calculated by dividing the stroke volume from the end-diastolic volume, shown in percent (6). EF is currently applied to classify heart failure patients into different stages (7), despite being influenced by many factors, such as heart frequency and loading conditions (6). Due to these limitations, there is growing interest in alternative quantitative parameters with the hope to better grasp the true myocardial contractility. Myocardial strain is such a novel parameter, described as the dimensionless result of the heart muscle shortening during systole and lengthening during diastole (8, 9). It is often expressed in percent and has a negative value, as the muscle fibers reduce in length when

contracting during systole (8, 9). Because of the different orientation of the heart muscle fibers, longitudinal, radial and circumferential strain can be determined separately (9). Strain measurements can be expressed on a global basis (e.g. representing the entire left ventricle) or on a regional basis, after automatic segmentation of the heart by analysis software with respect to the model published by the American Heart Association (AHA) (10). Strain can be determined using both CMR and echocardiography. It was reported that strain is less susceptible to changes in loading conditions than EF (11) and various studies demonstrated that strain can detect fine changes in myocardial contraction when EF remains preserved (12), for example in myocarditis patients (13), in long-term heart transplanted patients (14) and also in heart failure patients (15, 16).

IV. Modalities and techniques to determine myocardial strain

a) Speckle-tracking Echocardiography (STE)

In echocardiography, strain can be determined using a technique called “speckle-tracking” (STE). STE employs the tracking of speckle artifacts in the echocardiographic image, created by “reflections, refraction and scattering of echo beams” (9, p. 718). The change in position of these speckle artifacts can then be used to calculate strain with dedicated post-processing software. Global longitudinal strain (GLS) using STE is the only parameter that is already recommended in clinical routine, for the detection of chemotherapy-related cardiotoxicity (17, 18). Importantly, STE was shown to better predict mortality than EF in different patient populations, including heart failure patients (19, 20). **Figure one** shows exemplary STE-images and left ventricular (LV) strain curves.

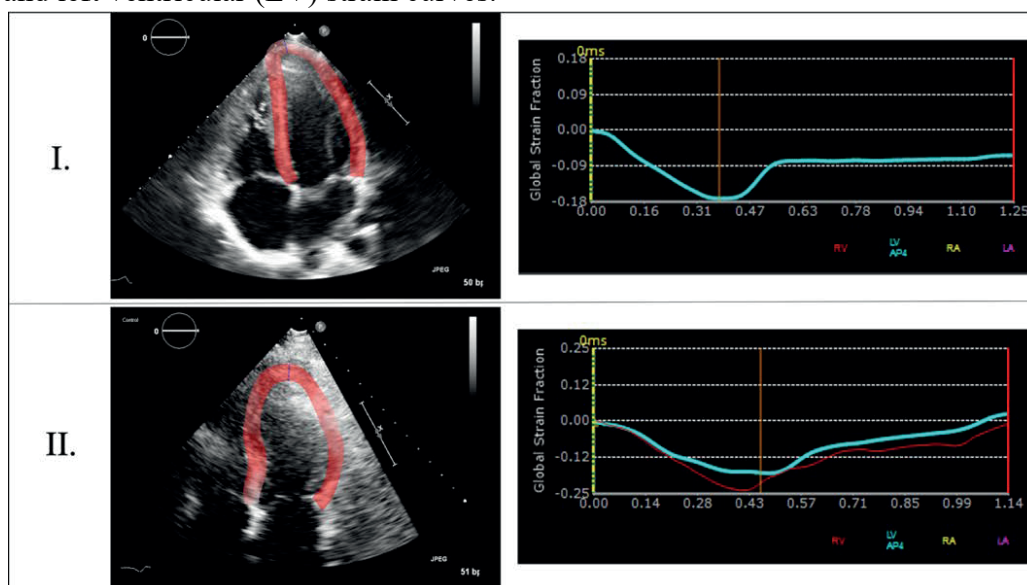


Figure 1: STE-images (4-chamber view), including the myocardial contours (left) and the corresponding longitudinal LV strain curves (right), of a healthy person (I.) and a patient with coronary artery disease (II). Strain analysis was performed using EchoInsight (Epsilon Imaging, Ann Arbor, Michigan, USA).

b) Myocardial Tagging (TAG)

Using CMR, several different techniques are available for strain analysis. Tagging (TAG) was the first pulse sequence, introduced by Zerhouni et al. (21). TAG uses “lines or grids superimposed on the myocardium” (22, p. 1381) to quantify deformation throughout the cardiac cycle, as shown in **figure two**. Despite TAG being the current reference standard for strain quantification (23) with validation in many studies, it was never widely applied in clinical routine due to many possible disadvantages, such as a low temporal resolution, low accuracy, the need for an additional pulse sequence and long, unpractical post-processing (24).

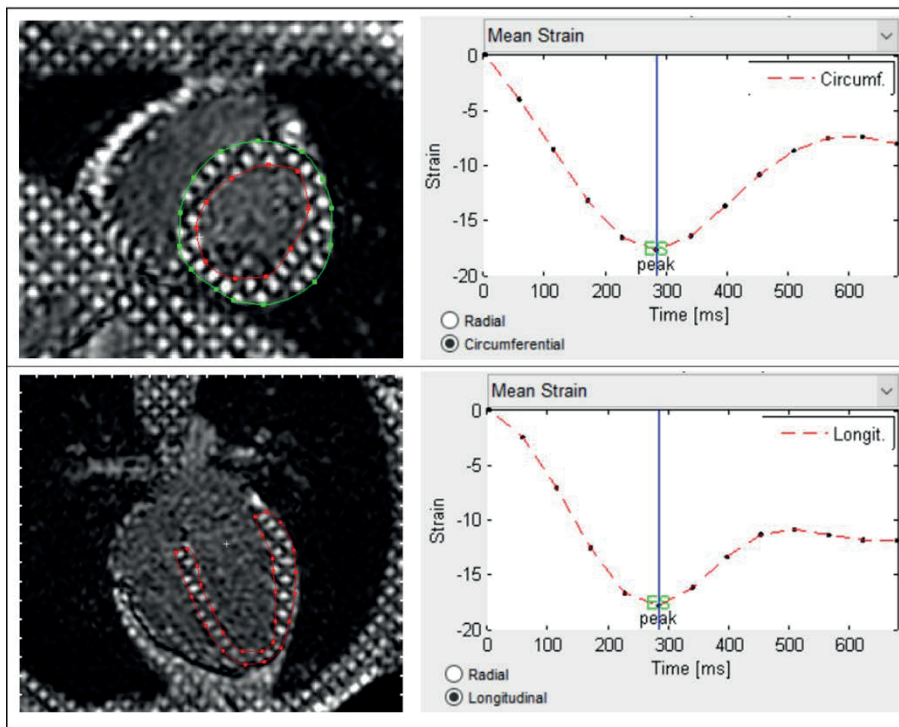


Figure 2: Exemplary TAG-images (short-axis and 4-chamber view), including myocardial contours (left) and corresponding LV strain curves (right), of a healthy volunteer. Circumferential strain is determined in the short-axis images and longitudinal strain in the long-axis views. Strain analysis was conducted using Segment (version 2.2 R6960 (<http://segment-heiberg.se>)).

c) Myocardial Feature Tracking (FT)

Another technique, called myocardial feature tracking (FT), uses the tracking of pixels throughout the cardiac cycle (25) to calculate strain. Regarding FT, there is no need to acquire additional pulse sequences, as it can be performed on conventional cine steady-state free precession (SSFP) images (24) (seen in **figure three**). FT has already been validated against TAG in different studies (26-28). Moreover, there is evidence that FT-derived strain serves as a better predictor of mortality than EF in patients with dilated cardiomyopathy (29).

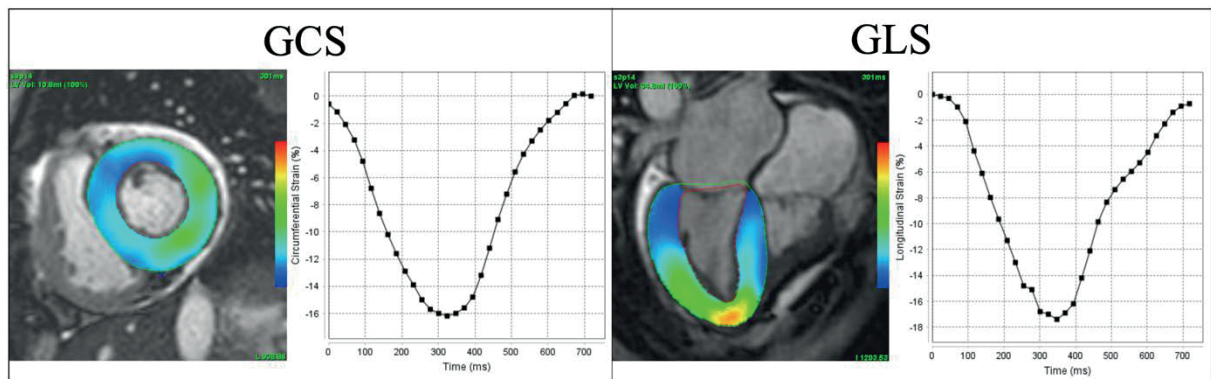


Figure 3: Exemplary FT-images (short-axis and 4-chamber view), including the myocardial contours (left) and the corresponding LV strain curves (right), of a patient with cardiac amyloidosis, coronary artery disease and diastolic heart failure. Similar to TAG, circumferential strain is determined in the short-axis and longitudinal strain using the long-axis images. Images were analyzed with SuiteHeart (SuiteHEART, Neosoft, Pewaukee, Wisconsin, USA).

d) Strain-encoding (SENC)/ fast Strain-encoding (fSENC)

Strain-encoding (SENC) is a different technique, first introduced in 2001 by Osman et al. (30). It is a dedicated pulse sequence based on TAG, but the tag planes “are initially oriented parallel to the imaging plane” (30, p. 324), which is why circumferential strain is calculated in the long-axis images and longitudinal strain in the short-axis images (4), as depicted in **figure four**. Radial strain is not measurable by SENC (24). After acquisition, the images are transferred to a post-processing software, which color-codes the heart according to the contractile strength. For SENC, a cut-off value of -17% strain is currently used to differentiate between normal and reduced contraction (23, 31).

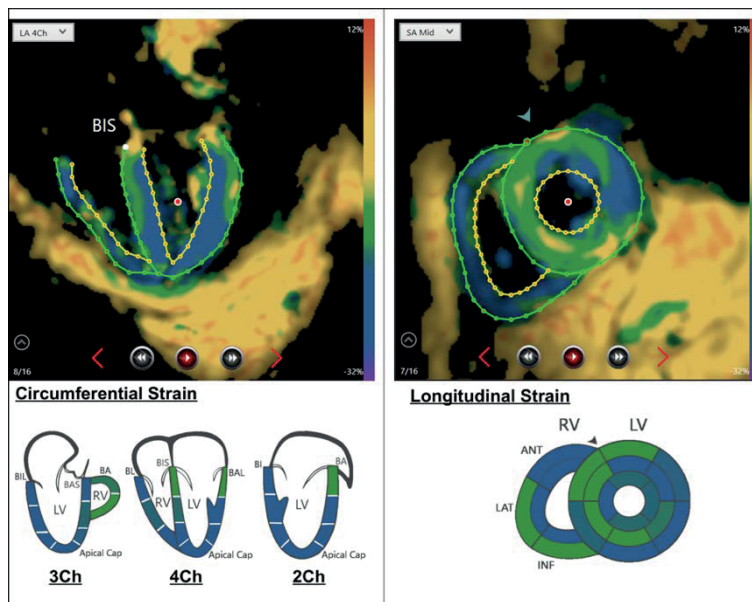


Figure 4: fSENC-images (4-ch and midventricular short-axis view) of a healthy volunteer. After post-processing, the regional strain is depicted in a color-coded outline of the heart (green and blue indicating contraction vs. yellow and red indicating relaxation). Using SENC, circumferential strain is measured in the long-axis images and longitudinal strain in the short-axis images.

Fast-SENC (fSENC) is a further development of SENC, allowing for image acquisition to be performed in a few heartbeats without the need for breath-holds (normally needed to reduce breathing artifacts) (32). This feature is particularly interesting for use in certain patient groups, such as children, uncooperative patients and patients with pulmonary or cardiovascular diseases and arrhythmias (32). SENC and fSENC were both validated against TAG in healthy subjects (33) and patients (23, 34), with the advantages of short scanning- and post-processing times (23, 24). SENC and fSENC have also been shown to provide added diagnostic value (35), for example to determine the extent of myocardial ischemia (23, 36).

V. *Aim of this dissertation*

Myocardial strain, determined using both CMR and echocardiography, has the potential to become a promising tool for quantification of myocardial function in a variety of patients with different pathologies. Nevertheless, before strain-imaging can be introduced into clinical routine, important aspects regarding the standardization and reproducibility of strain measurements need to be explored. To compare strain measurements from different centers and to plan multi-center trials, it is necessary to know if the choice of a specific CMR/echocardiography scanner impacts strain results. Recently it has been shown for STE that the choice of ultrasound scanner and post-processing software significantly influences the results of the strain analysis (37-39). However, no data existed regarding any CMR technique. Moreover, the reproducibility of repeated strain measures, or when the analysis is conducted by different readers, is also an important aspect that has not been thoroughly explored for many techniques. With the below-described study, our research group wanted to contribute to the standardization of CMR-strain analysis with focus on fSENC. In detail, our aim was to determine I) inter-vendor agreement, II) test-retest reproducibility and III) inter- and intra-observer reproducibility of fSENC LV GLS and global circumferential strain (GCS) measurements, acquired in volunteers at three different scanners from different vendors. This dissertation summarizes the results of this trial and compares our analysis to research on other modalities and techniques.

Materials and Methods

I. *Inter-vendor agreement*

The manuscript of this study has been published in the *International Journal of Cardiovascular Imaging*, including detailed information on the methods described below and the technical properties of the fSENC pulse sequence at the different scanners (40). We recruited seventeen

healthy volunteers, who were scanned at three different sites after obtaining written informed consent. The study was approved by the Ethics Committee of the Charité-University-Medicine in Berlin (EA2/208/17) and complied with the Declaration of Helsinki. The volunteers traveled to different sites within five months, including: the German Heart Institute Berlin (site I), the Theresien-Hospital Mannheim (site II) and the Max-Delbrück Center for Molecular Medicine (MDC) in collaboration with Charité University Medicine Berlin - Campus Buch (site III). Each site used a different 3T scanner of the following vendors (names in alphabetical order): Ingenia (Philips, Best, The Netherlands), MAGNETOM Verio (Siemens Healthcare GmbH, Erlangen, Germany), SIGNA Architect (GE Healthcare, Milwaukee, WI, USA). The study was registered at the German Register for Clinical Studies (DRKS) (registration number: 00013253) and the World Health Organization (WHO) (universal trial number (UTN): U1111-1207-5874). The fSENC pulse sequence was optimized with regard to the different scanners. A spiral readout was used at sites I and II and an Echo Planar Imaging (EPI) pulse sequence was used at site III. The pulse sequences at sites II and III were user-developed. Technical parameters at site I were: field-of-view (FOV) = $256 \times 256 \text{ mm}^2$, slice thickness = 10 mm, voxel size = $4 \times 4 \times 10 \text{ mm}^3$, reconstructed images at $1 \times 1 \times 10 \text{ mm}^3$, zero-filled interpolation (in-plane ZIP 1024), spiral readout (3 interleaves) with acquisition time (TA) = 10 ms, flip angle = 30° , effective echo time (TE) = 0.7 ms, repetition time (TR) = 12 ms, temporal resolution = 36 ms, typical number of acquired heart phases = 22, spectrally selective fat suppression (SPIR), total acquisition time = 1 heartbeat. Site II used the following parameters: FOV = $256 \times 256 \text{ mm}^2$, slice thickness = 7-8 mm, voxel size = $4 \times 4 \times 7 \text{ mm}^3$, reconstructed images at $1 \times 1 \times 7 \text{ mm}^3$, single-shot spiral readout (4 interleaves) with TA = 7.5 ms, flip angle = 20° , TE = 5.0 ms, TR = 9.1 ms, temporal resolution = 36.4 ms, typical number of acquired heart phases = 18, SPIR, total acquisition time = 1 heartbeat. Parameters at site III were: EPI factor = 9, FOV = $450 \times 170 \text{ mm}^2$, slice thickness = 12 mm, voxel size = $4.7 \times 4.7 \times 12 \text{ mm}^3$, reconstructed resolution at $4.7 \times 4.7 \times 12 \text{ mm}^3$, flip angle = 12° , TE = 1.18 ms, TR = 8.9 ms, temporal resolution = 35.6 ms, centric EPI recording, typical number of acquired heart phases = 22, SPIR, total acquisition time per slice = two heartbeats (one separate heartbeat used for EPI phase correction). Details on the image acquisition at the different sites can also be found in the corresponding published manuscript of the study (40). All technicians at the different sites received training on performing fSENC acquisitions and completed a written test before the study commenced. Preceding the volunteers, phantoms of similar proportions with known physical properties (41) were scanned at sites with the listed scanners after applying periodic compression and expansion, described by Osman et al. (41, 42). After the volunteers were scanned at site I, two volunteers stopped

participating in the study, so fifteen volunteers were included in total. All volunteers were scanned at the three sites according to the same imaging protocol: two consecutive fSENC acquisitions during free-breathing, a fifteen-minute break where the volunteer left the scanner and further two fSENC acquisitions. Heart rate (bpm) and blood pressure (mmHg), as well as height, weight and smoking behavior of the volunteers, were monitored closely. fSENC images were acquired in the 2-chamber (ch), 3-ch and 4-ch view to determine GCS and in three short-axis slices (basal, mid-ventricular and apical) to determine GLS. After the scans were anonymized, the images were analyzed (by J.E.) using dedicated software (Myostrain 5.0, Myocardial Solutions, Inc., Morrisville, North Carolina, USA). Scans were excluded, if no view was of sufficient quality for strain analysis (e.g. GCS could not be determined if image quality of the 2-ch, 3-ch and 4-ch images was insufficient). First, end-systole (ES) was identified in all views. Then, the endo- and epicardial contours of the LV were manually drawn at ES. After the software performed automatic propagation, the contours were corrected manually. Then, the software automatically calculated GLS and GCS, as well as segmental strain, after dividing the short-axis images into 16 segments and the long-axis images into 21 segments. The statistical analysis was performed (by J.E.) using SPSS (Version 25.0, IBM Corp., Armonk, NY, USA). All values described in this dissertation are shown with p-values and confidence intervals (CI). A p-value of ≤ 0.05 was considered significant in two-tailed tests and will be marked with an asterisk (*) in this dissertation. Inter-vendor agreement between the different scanners was determined using the Bland-Altman agreement analysis.

II. Test-retest reproducibility

Each volunteer was scanned four times, with a fifteen-minute break in between scans two and three. The test-retest reproducibility between averaged scans before (scan one and two) and after the break (scan three and four) and between single scans was calculated using intraclass correlation (ICC) and coefficient of variation (CoV). Wilcoxon test (for non-normally distributed parameters) and paired students t-test (for normally distributed measurements) were calculated to determine if the differences between strain values, acquired at the different sites, were significant.

III. Inter- and intra-observer reproducibility

A second blinded observer (V.Z.) repeated measurements for nine randomly chosen volunteers to determine inter-observer agreement. The primary observer (J.E) repeated the analysis for the same nine volunteers after two months (to prevent recall bias) to determine intra-observer

reproducibility. Scans were excluded from the analysis, if no view had sufficient image quality to determine either GCS or GLS. Both were trained by software representatives (of Myocardial Solutions) on image analysis and also completed a written test before starting with the measurements. Intra- and inter-observer reproducibility were calculated using ICC and CoV. All ICC-analyses were interpreted as previously described by others: excellent for ICC > 0.74, good for ICC 0.6-0.74, fair for ICC 0.4-0.59 and poor for ICC<0.4 (43, 44).

Results

I. Inter-vendor agreement

Tables one to five have been previously published, along with the methods described above, in this exact or modified form in the *International Journal of Cardiovascular Imaging* (40). Information on the baseline characteristics of the volunteers can also be found in the publication (40). Four scans were performed for every volunteer, with a fifteen-minute break after the first two scans, adding up to 60 scans per site. Due to artifacts, as well as technical difficulties, a total of 51 scans were considered for GLS-analysis (excluding 9 scans) and 47 scans for GCS-analysis (excluding 13 scans). **Table one** displays the results of the Bland-Altman analysis on inter-vendor agreement. The bias between strain values, acquired at the different sites, ranged from 0.01 to 1.88% strain and limits of agreement (abbreviated as LOA in the tables) ranged from -5.25 to 7.68%. The lowest and insignificant bias was found when comparing sites II and III for both GLS and GCS. The biases between both sites I and II and sites I and III were significant and higher (1.21-1.88). Limits of agreement were of a similar magnitude for all sites.

Table 1: Results of the Bland-Altman analysis demonstrating inter-vendor agreement.

	LV GLS (n=51)			LV GCS (n=47)		
	Bias (%)	LOA (%)	p	Bias (%)	LOA (%)	p
Site I vs. II	1.21	-5.25 to 7.68	0.012*	1.14	-2.34 to 4.64	<0.001*
Site I vs. III	1.24	-4.47 to 6.92	0.004*	1.88	-3.02 to 6.79	<0.001*
Site II vs. III	0.01	-4.78 to 4.81	0.968	0.61	-3.99 to 5.20	0.083

II. Test-retest reproducibility

Tables two and three show the results of the test-retest reproducibility analysis. **Table two** portrays the median and interquartile range (IQR) strain values of combined scans before and after the break and the results of the Wilcoxon test or paired student's t-test to determine if the differences in strain values were significant. The only significant difference between median

strain values of scans before and after the break was found for GLS at site I. Otherwise, differences in median strain values were marginal and insignificant.

Table 2: Median (IQR) strain values of scans before (1+2) and after (3+4) the break and corresponding significance values.

		LV GLS (n=51)		LV GCS (n=47)	
		Median (IQR) strain	p	Median (IQR) strain	p
Site I	Scans 1+2	-20.1 (-20.9 to -18.3)	0.020*	-19.0 (-21.1 to -18.3)	0.950
	Scans 3+4	-19.4 (-20.6 to -17.8)		-19.4 (-21.0 to -18.3)	
Site II	Scans 1+2	-19.9 (-21.3 to -16.8)	0.347	-17.4 (-19.0 to -16.4)	0.307
	Scans 3+4	-20.1 (-21.2 to -17.0)		-17.3 (-18.6 to -16.7)	
Site III	Scans 1+2	-18.8 (-20.2 to -15.1)	0.977	-17.2 (-18.6 to -16.3)	0.056
	Scans 3+4	-18.4 (-19.8 to -16.2)		-18.5 (-19.5 to -16.5)	

Table three shows the ICC (95% confidence interval (CI)) and CoV (\pm standard deviation (sd)) values on test-retest reproducibility of scans before and after the break, which was mostly excellent. The best ICC and CoV values were observed for GLS at site II. GLS at site I and GCS at site III showed the lowest test-retest reproducibility, which can still be classified as good.

Table 3: Test-retest reproducibility between scans before (1+2) and after (3+4) the break, shown using ICC (95% CI) and CoV (\pm sd).

	LV GLS (n=51)		
	ICC (95% CI)	p	CoV \pm sd
Site I	0.63 (0.21-0.86)	0.002*	0.06 \pm 0.05
Site II	0.97 (0.90-0.99)	<0.001*	0.03 \pm 0.02
Site III	0.82 (0.54-0.94)	<0.001*	0.09 \pm 0.07
	LV GCS (n=47)		
Site I	0.82 (0.53-0.93)	<0.001*	0.05 \pm 0.03
Site II	0.80 (0.47-0.94)	<0.001*	0.04 \pm 0.04
Site III	0.69 (0.29-0.88)	0.001*	0.07 \pm 0.05

Table four illustrates the test-retest reproducibility between single scans, which was overall good to excellent.

Table 4: Test-retest reproducibility between single scans, shown using ICC (95% CI) and CoV (\pm sd).

	Scans	LV GLS (n=51)		
		ICC (95% CI)	p	CoV (\pm sd)
Site I	1 vs. 2	0.94 (0.81-0.98)	<0.001*	0.03 \pm 0.02
	2 vs. 3	0.75 (0.16-0.92)	0.002*	0.07 \pm 0.04
	3 vs. 4	0.97 (0.91-0.99)	<0.001*	0.02 \pm 0.02
	1 vs. 3	0.70 (0.15-0.90)	0.013*	0.06 \pm 0.06

	1 vs. 4	0.74 (0.27-0.91)	0.007*	0.06 ± 0.06
	2 vs. 4	0.79 (0.33-0.93)	0.002*	0.07 ± 0.05
Site II	1 vs. 2	0.88 (0.61-0.96)	<0.001*	0.07 ± 0.07
	2 vs. 3	0.94 (0.80-0.98)	<0.001*	0.04 ± 0.05
	3 vs. 4	0.97 (0.91-0.99)	<0.001*	0.03 ± 0.03
	1 vs. 3	0.97 (0.89-0.99)	<0.001*	0.04 ± 0.03
	1 vs. 4	0.94 (0.81-0.98)	<0.001*	0.06 ± 0.04
	2 vs. 4	0.95 (0.77-0.99)	<0.001*	0.05 ± 0.04
Site III	1 vs. 2	0.92 (0.77-0.97)	<0.001*	0.08 ± 0.09
	2 vs. 3	0.84 (0.51-0.95)	0.001*	0.10 ± 0.11
	3 vs. 4	0.96 (0.90-0.99)	<0.001*	0.06 ± 0.05
	1 vs. 3	0.89 (0.67-0.96)	<0.001*	0.09 ± 0.09
	1 vs. 4	0.89 (0.68-0.97)	<0.001*	0.10 ± 0.08
	2 vs. 4	0.85 (0.55-0.95)	0.001*	0.10 ± 0.08
		LV GCS (n=47)		
Site I	1 vs. 2	0.89 (0.68-0.96)	<0.001*	0.05 ± 0.06
	2 vs. 3	0.83 (0.47-0.94)	0.002*	0.07 ± 0.06
	3 vs. 4	0.86 (0.56-0.95)	0.001*	0.05 ± 0.04
	1 vs. 3	0.79 (0.37-0.93)	0.004*	0.06 ± 0.04
	1 vs. 4	0.86 (0.58-0.95)	<0.001*	0.05 ± 0.04
	2 vs. 4	0.88 (0.62-0.96)	<0.001*	0.06 ± 0.05
Site II	1 vs. 2	0.94 (0.79-0.98)	<0.001*	0.04 ± 0.04
	2 vs. 3	0.89 (0.61-0.97)	0.001*	0.05 ± 0.03
	3 vs. 4	0.85 (0.52-0.96)	0.001*	0.05 ± 0.04
	1 vs. 3	0.79 (0.20-0.95)	0.013*	0.06 ± 0.04
	1 vs. 4	0.85 (0.46-0.96)	0.002*	0.04 ± 0.06
	2 vs. 4	0.85 (0.50-1.00)	0.002*	0.05 ± 0.05
Site III	1 vs. 2	0.90 (0.70-0.97)	<0.001*	0.06 ± 0.03
	2 vs. 3	0.71 (0.18-0.90)	0.012*	0.08 ± 0.06
	3 vs. 4	0.85 (0.56-0.95)	0.001*	0.06 ± 0.05
	1 vs. 3	0.71 (0.12-0.90)	0.005*	0.08 ± 0.06
	1 vs. 4	0.79 (0.38-0.93)	<0.001*	0.08 ± 0.05
	2 vs. 4	0.83 (0.50-0.94)	0.001*	0.07 ± 0.05

III. Inter- and intra-observer reproducibility

Both observers independently excluded one volunteer from the strain analysis due to insufficient image quality to determine GLS and GCS. The ICC and CoV results of the remaining eight volunteers, reflecting inter- and intra-observer reproducibility, are summarized and displayed in **Table five**. Inter- and intra-observer reproducibility were excellent for LV GLS and GCS, but even better for GLS.

Table 5: Results of the ICC and CoV (\pm sd)-analyses on inter- and intra-observer reproducibility.

	LV GLS		
	ICC (95% CI)	p	CoV \pm sd
Inter-Observer Reproducibility	0.96 (0.92-0.98)	<0.001*	0.03 \pm 0.04
Intra-Observer Reproducibility	0.99 (0.98-1.00)	<0.001*	0.02 \pm 0.02
	LV GCS		
Inter-Observer Reproducibility	0.82 (0.58-0.92)	<0.001*	0.04 \pm 0.03
Intra-Observer Reproducibility	0.77 (0.47-0.90)	<0.001*	0.05 \pm 0.04

Discussion

In modern cardiovascular diagnostics, non-invasive, objective and reliable methods, quantifying myocardial contractility, are necessary to provide an accurate diagnostic workup, to monitor treatment efficacy and to determine the prognosis of patients with heart failure. Currently, heart failure patients are still grouped according to their EF into patients with preserved (“HFpEF”) and reduced EF (“HFrEF”) (7). Hence, the EF of a patient has a strong influence on important diagnostic and therapeutic decisions, although half of the patients who suffer from symptoms of heart failure show no change in EF (the “HFpEF”-group) (7). Furthermore, EF cannot be applied on a regional basis and is influenced by factors such as preload, afterload and cardiac remodeling (6). With these limitations, EF bears the risk of underestimating the real extent of heart failure, potentially leading to patients being underdiagnosed and not receiving the correct therapy. There is a clear need for new objective markers to quantify cardiac performance. Strain has shown to provide important information on myocardial function in addition to EF (13-16) and resulted to be a stronger predictor of mortality and hospitalization in patients with a wide range of cardiovascular diseases (17, 19, 20, 29). Furthermore, it enables the analysis of regional myocardial contractility, which previously could only be determined after surgical implantation of physical probes into the heart (4). Over the past few years, many echocardiographic and CMR- techniques have been developed to determine strain as a novel parameter, such as 2D-STE, 3D-STE, TAG, FT, SENC and Displacement Encoding with Stimulated Echoes (DENSE), all with different benefits and disadvantages (24). Despite the rapidly evolving techniques for strain-analysis and the increasing number of studies illustrating promising results of using strain in a variety of diseases (13-16, 23, 36, 45, 46), only STE-GLS is currently recommended for clinical use (17, 18). The sparse use of strain in everyday clinical life is mostly the result of missing standardization, caused by a variety of factors. First, the influence of different vendors (e.g. of ultrasound or magnetic resonance scanners or software) on strain measurements is still unknown in the field

of CMR. Moreover, the reproducibility of repeated strain measures, or of analyses conducted by different readers, is still not thoroughly explored for most techniques. Our working group wanted to address these questions with focus on the fSENC technique, to help pave the way for future use of strain imaging in clinical routine. In detail, our work explained in this dissertation showed that: 1.) a bias of 0.01-1.88% was found after scanning a cohort of healthy volunteers at three different CMR-scanners using fSENC; 2.) test-retest reproducibility of subsequent or interrupted fSENC scans was excellent, regardless of scanner type and 3.) inter- and intra-vendor reproducibility of global strain values was also excellent, but even better for GLS than GCS.

I. Inter-vendor agreement

Although our working group conducted the first study to determine inter-vendor agreement of strain measurements using different CMR-scanners, the effect of inter-vendor and inter-software variability on strain results is well known in echocardiography (37-39). The bias we determined between fSENC scans, acquired at different CMR-scanners, was mostly similar or lower than the bias determined for different echocardiographic systems (37-39). As already explained in the corresponding published manuscript (40), a variety of factors could have influenced inter-vendor agreement in our study. First of all, the technical characteristics of the fSENC pulse sequence were modified by experts from the different scanner companies to fit the scanners and receive optimal image quality. A spiral readout was used at sites I and II and an EPI at site III. The pulse sequences employed at sites II and III were user-developed. Furthermore, the technical parameters differed between all three sites after optimization. The mean strain values of the phantoms (scanned before the volunteers), provided in the manuscript of the study, were higher at scanning systems of sites II and III than site I, similar to the distribution of strain observed in the volunteers (seen in figure 4 of the published manuscript (40)). This could show that the sole optimization of the pulse sequence could have resulted in different ranges of strain values at the different sites (for example more negative strain measurements at site I), leading to higher biases when comparing site I to either site II or III. Hence, more research is needed to find the specific impact of different scanning parameters on strain measurements.

Other factors could have impacted inter-vendor agreement as well, such as the training and scanning techniques of the different technicians and volunteer-related changes, such as changes in loading conditions (since the volunteers were scanned at different time points during the day). Nevertheless, the monitored blood pressure and heart rate of the volunteers stayed stable

throughout (table 1 of the published manuscript) and there is evidence that the hemodynamics of healthy subjects do not change over a period of up to one year, for example when investigating 4D flow in volunteers (47). Therefore, we assume that the hemodynamics of the volunteers did not have a major influence on the inter-vendor agreement in our study.

A harmonization of technical properties and scanning parameters, when adjusting the pulse sequence for the different scanners, might have resulted in more comparable strain values. However, that setting would not have given a realistic perspective on the bias that needs to be expected in the clinical routine, where pulse sequences are optimized to fit specific scanners and different clinical sites have various scanning programs, techniques and personnel. Therefore, our results on inter-vendor agreement in healthy volunteers should encourage deeper research in patients and in larger cohorts to help understand and minimize inter-vendor variability of strain measurements. Furthermore, it is important to determine inter-vendor agreement for other techniques as well, such as FT or TAG. Especially inter-vendor agreement of FT should be optimal, as FT is performed using the cine SSFP pulse sequence, universally available in all scanners without the need for optimization. In case future research should reveal significant biases regarding inter-vendor agreement in larger patient cohorts, a different approach towards standardization would be to define scanner-specific normal values, as also recommended for different genders and age groups (48). Despite improving comparability, this would not be a practical solution, as classifications and guidelines would need to be published in multiple different editions, depending on all the circumstances influencing strain. Another option to counteract inter-vendor variability, currently recommended for echocardiography (49), would be to perform repeated strain measurements of a patient using the same scanner only. This measure currently impedes the comparison of different studies and the design of multi-center studies for further validation of strain on a large scale. Therefore, vendors should aim at reducing technical differences when adjusting a pulse sequence or technique to different scanners in echocardiography and CMR.

Not only the technical differences between scanners, but also the differences between post-processing software prevents inter-vendor agreement (38, 39). Currently, only one software is available for fSENC analysis (Myostrain, Myocardial Solutions, Inc., Morrisville, North Carolina, USA). Regarding other techniques, such as STE, TAG and FT, various software is provided by different vendors for strain analysis. This aspect of inter-vendor variability could also partly explain the moderate inter-modality and inter-technique agreement between STE, SENC and FT we found in 50 patients, who received both echocardiography and CMR at the

University of Chicago (published in the *Journal of Cardiovascular Magnetic Resonance*) (50). The software providers might apply different tracking algorithms with “spatial and temporal smoothing to regularize the results in order to reduce noise” (24, p. 610), or they might calculate global strain differently or use only specific layers for strain calculation (24). Even strain measurements acquired using the same technique show significant variability when analyzed with different software (38, 39). Hence, future efforts should also be concentrated on the development of post-processing software with a standardized algorithm, which has already shown to allow for a good comparison between strain values, irrespective of technique or modality (51). With the growing importance of STE for the detection of cardiotoxicity, the problem of inter-vendor variability on strain results, caused by the increasing offer of different post-processing software, resulted in the publication of a consensus statement in favor of standardizing STE (8). Furthermore, official recommendations were published to use the same scanning equipment and post-processing software for repeated measurements of a patient (49). Unfortunately, a similar consensus statement does not exist for any CMR-technique. Therefore, it would be important to define similar recommendations for CMR as in echocardiography (49), ensuring that follow-up analyses of the same patient are conducted using the same technique and software at the moment. Moreover, it would be urgent to develop similar consensus statements for the different CMR-techniques to clarify the current state and need for standardization.

II. *Test-retest reproducibility*

We found good to excellent reproducibility between scans interrupted by a fifteen-minute break and between subsequent scans, independent of site. Giusca et al. previously reported an excellent reproducibility of strain values determined with fSENC after a median time of 63 days (12). Interestingly, they also compared the reproducibility between fSENC and EF and found better reproducibility of strain measurements (12). In a different study, previously published in the *Journal of the Heart Failure Association of the European Society of Cardiology (ESC Heart Failure)*, our working group determined test-retest reproducibility of strain using fSENC, FT and TAG after a median time of 40 days in eleven healthy volunteers and seven heart failure patients (52). We found an excellent reproducibility of fSENC strain measurements on a global (ICC:0.94-0.96) and segmental basis (52). Furthermore, it was just as excellent for FT (ICC:0.91-0.97) and TAG (ICC:0.95-0.96) (52). A better test-retest reproducibility compared to EF was described for STE as well by Barbier et al (53). We and others showed that fSENC strain measurements are not only reproducible in volunteers independent of the scanner, but

also in heart failure patients. Moreover, it seems like the test-retest reproducibility seems to be an advantage of strain measurements, regardless of modality or technique. This reflects the robustness and improved reliability of strain in comparison to EF.

III. Inter- and intra-observer reproducibility

We found an excellent intra- and inter-observer reproducibility of fSENC GLS and GCS measurements in healthy volunteers. Our findings comply with a different study conducted by our working group to analyze the effect of training on the reproducibility of fSENC strain analyses, previously published in *Scientific Reports* (54). During this trial, 10 HFpEF patients, 10 HFrEF patients and 10 volunteers were analyzed using fSENC by four observers with different levels of CMR-experience (a CMR-expert (T.L.), a CMR-beginner (V.Z.), an echocardiography-expert (H.H.) and a non-cardiac technician (J.E.)), after all observers completed the same training (54). Inter-observer reproducibility was excellent between all readers, regardless of the level of experience (54). Moreover, in the study previously published in the *Journal of Cardiovascular Magnetic Resonance*, we compared inter-modality and inter-technique agreement between STE and CMR-FT and SENC in a cohort of 50 patients who received both examinations at the University of Chicago (50). We found that the inter- and intra-observer reproducibility of SENC (ICC:0.94-0.99) was just as excellent as the reproducibility of more established techniques, such as STE (ICC:0.91-0.94) and FT (ICC:0.86-0.99) (50). Similar to our analysis in volunteers described above, the reproducibility of SENC measurements in patients was also marginally better for GLS than GCS, whereas the reproducibility of FT measures was better for GCS than for GLS (40, 50). A reason could be that the short-axis images, used to determine longitudinal strain using SENC and circumferential strain using FT, are simpler to contour. Furthermore, in the study previously published in *ESC Heart Failure*, we also determined inter- and intra-observer reproducibility of fSENC, TAG and FT in the cohort of eleven volunteers and seven heart failure patients, with excellent results as well (ICC: 0.99 for fSENC; ICC: 0.97-0.99 for TAG; ICC: 0.86-0.95 for FT) (52). Similar results were found by different authors for STE (55), FT (56), fSENC (12) and TAG (57). Better reproducibility of strain in comparison to EF has also been reported (12, 58). To conclude, the excellent inter- and intra-observer reproducibility is also an advantage of using strain compared to EF. Importantly, we showed that this reproducibility can be achieved with training, independent of experience.

The ability to determine regional deformation with good reproducibility is an important feature of strain that should be highlighted when comparing it to EF. In the study published in *ESC Heart Failure*, we analyzed the intra-observer reproducibility of pooled LV segmental longitudinal and circumferential strain in volunteers and heart failure patients using TAG, FT and fSENC (52). We found excellent intra-observer reproducibility for all techniques, similar to other authors as well (23, 56, 57). Nevertheless, the CoV values of the segmental analyses were higher compared to the global reproducibility, implicating a higher variation of segmental strain results. Other studies reported comparable findings with a similar magnitude of CoV values for segmental analyses using FT and STE (59, 60). There is evidence that the variability of segmental strain values is also impacted by the choice of scanner and post-processing software (60, 61). Our analysis revealed that the acquisition-based techniques performed better on a segmental basis than FT. A reason why FT might be less suitable to determine intramyocardial strain is the weakness to differentiate between the intramyocardial greyscale ranges, which are very alike in cine SSFP images (24). Some studies report SENC and fSENC to be superior to TAG for segmental reproducibility analyses (23, 34). This finding is particularly interesting as the temporal and spatial resolution of fSENC is lower than that of SENC to allow imaging within a few heartbeats (32, 34). We and others could show that fSENC is not inferior to TAG regarding global and segmental reproducibility, indicating that the temporal and spatial resolution is sufficient for reliable strain analysis (34). Regional assessment of deformation is currently not recommended in echocardiography, with one reason being suboptimal reproducibility (49). Although there is no clear recommendation for CMR strain-imaging, we believe that the reproducibility of segmental strain analyses still needs to be improved before clinical use by harmonizing post-processing algorithms, providing guidelines on how to thoroughly perform the strain analysis and conducting further research to improve and standardize especially the acquisition-based techniques, which might be more suitable for segmental strain analysis.

IV. Outlook into the future of strain imaging

We conducted a multi-vendor, multi-center study as a step forward towards the standardization of strain. As a result, we found a bias of 0.01-1.88% when applying fSENC to scan volunteers at different CMR-scanners from major providers. Studies with a larger cohort and in patients are needed in the future to validate these results. Nevertheless, this bias needs to be recognized when designing and interpreting multi-center studies to assess strain with any modality or technique. Moreover, we found excellent test-retest reproducibility of fSENC in volunteers,

regardless of the scanner. This excellent reproducibility can also be applied to heart failure patients and to other techniques, such as FT and TAG, as shown in a different study by our working group. Lastly, we determined an excellent inter- and intra-observer reproducibility of global strain values. Both the test-retest reproducibility and the intra- and inter-observer reproducibility are advantages of strain compared to EF. Strain is a valuable, practical and robust tool to quantify myocardial contractility. With further improvement towards standardization, strain should likely be added to CMR- and echocardiographic examinations to screen, diagnose and monitor patients with heart failure of different etiologies.

References

1. Deutsche Herzstiftung: Deutscher Herzbericht 2018. 2. Morbidität und Mortalität der Herzkrankheiten im Überblick. Frankfurt/Main: Deutsche Herzstiftung 2018.
2. Salerno M, Sharif B, Arheden H, Kumar A, Axel L, Li D, Neubauer S. Recent Advances in Cardiovascular Magnetic Resonance: Techniques and Applications. *Circ Cardiovasc Imaging*. 2017;10(6).
3. Bloom MW, Hamo CE, Cardinale D, Ky B, Nohria A, Baer L, Skopicki H, Lenihan DJ, Gheorghiu M, Lyon AR, Butler J. Cancer Therapy-Related Cardiac Dysfunction and Heart Failure: Part 1: Definitions, Pathophysiology, Risk Factors, and Imaging. *Circ Heart Fail*. 2016;9(1):e002661.
4. Ibrahim e-S. Myocardial tagging by cardiovascular magnetic resonance: evolution of techniques--pulse sequences, analysis algorithms, and applications. *J Cardiovasc Magn Reson*. 2011;13:36.
5. von Knobelsdorff-Brenkenhoff F, Schulz-Menger J. Role of cardiovascular magnetic resonance in the guidelines of the European Society of Cardiology. *J Cardiovasc Magn Reson*. 2016;18:6.
6. Konstam MA, Abboud FM. Ejection Fraction: Misunderstood and Overrated (Changing the Paradigm in Categorizing Heart Failure). *Circulation*. 2017;135(8):717-9.
7. Pfeffer MA, Shah AM, Borlaug BA. Heart Failure With Preserved Ejection Fraction In Perspective. *Circ Res*. 2019;124(11):1598-617.
8. Voigt JU, Pedrizzetti G, Lysyansky P, Marwick TH, Houle H, Baumann R, Pedri S, Ito Y, Abe Y, Metz S, Song JH, Hamilton J, Sengupta PP, Koliaas TJ, d'Hooge J, Aurigemma GP, Thomas JD, Badano LP. Definitions for a common standard for 2D speckle tracking echocardiography: consensus document of the EACVI/ASE/Industry Task Force to standardize deformation imaging. *J Am Soc Echocardiogr*. 2015;28(2):183-93.
9. Blessberger H, Binder T. NON-invasive imaging: Two dimensional speckle tracking echocardiography: basic principles. *Heart*. 2010;96(9):716-22.
10. Cerqueira MD, Weissman NJ, Dilsizian V, Jacobs AK, Kaul S, Laskey WK, Pennell DJ, Rumberger JA, Ryan T, Verani MS, American Heart Association Writing Group on Myocardial S, Registration for Cardiac I. Standardized myocardial segmentation and nomenclature for tomographic imaging of the heart. A statement for healthcare professionals from the Cardiac Imaging Committee of the Council on Clinical Cardiology of the American Heart Association. *Int J Cardiovasc Imaging*. 2002;18(1):539-42.
11. Knappe D, Pouleur AC, Shah AM, Cheng S, Uno H, Hall WJ, Bourgoun M, Foster E, Zareba W, Goldenberg I, McNitt S, Pfeffer MA, Moss AJ, Solomon SD, Investigators MADIT-CRT. Dyssynchrony, contractile function, and response to cardiac resynchronization therapy. *Circ Heart Fail*. 2011;4(4):433-40.
12. Giusca S, Korosoglou G, Zieschang V, Stoiber L, Schnackenburg B, Stehning C, Gebker R, Pieske B, Schuster A, Backhaus S, Pieske-Kraigher E, Patel A, Kawaji K, Steen H, Lapinskas T, Kelle S. Reproducibility study on myocardial strain assessment using fast-SENC cardiac magnetic resonance imaging. *Sci Rep*. 2018;8(1):14100.
13. Kostakou PM, Kostopoulos VS, Tryfou ES, Giannaris VD, Rodis IE, Olympios CD, Kouris NT. Subclinical left ventricular dysfunction and correlation with regional strain analysis in myocarditis with normal ejection fraction. A new diagnostic criterion. *Int J Cardiol*. 2018;259:116-21.
14. Syeda B, Höfer P, Pichler P, Vertesich M, Bergler-Klein J, Roedler S, Mahr S, Goliash G, Zuckermann A, Binder T. Two-dimensional speckle-tracking strain echocardiography in long-term heart transplant patients: a study comparing deformation parameters and ejection fraction derived from echocardiography and multislice computed tomography. *Eur J Echocardiogr*. 2011;12(7):490-6.

15. DeVore AD, McNulty S, Alenezi F, Ersboll M, Vader JM, Oh JK, Lin G, Redfield MM, Lewis G, Semigran MJ, Anstrom KJ, Hernandez AF, Velazquez EJ. Impaired left ventricular global longitudinal strain in patients with heart failure with preserved ejection fraction: insights from the RELAX trial. *Eur J Heart Fail.* 2017;19(7):893-900.
16. Mordi IR, Singh S, Rudd A, Srinivasan J, Frenneaux M, Tzemos N, Dawson DK. Comprehensive Echocardiographic and Cardiac Magnetic Resonance Evaluation Differentiates Among Heart Failure With Preserved Ejection Fraction Patients, Hypertensive Patients, and Healthy Control Subjects. *Jacc-Cardiovasc Imag.* 2018;11(4):577-85.
17. Potter E, Marwick TH. Assessment of Left Ventricular Function by Echocardiography: The Case for Routinely Adding Global Longitudinal Strain to Ejection Fraction. *J Am Coll Cardiol Img.* 2018;11(2 Pt 1):260-74.
18. Plana JC, Galderisi M, Barac A, Ewer MS, Ky B, Scherrer-Crosbie M, Ganame J, Sebag IA, Agler DA, Badano LP, Banchs J, Cardinale D, Carver J, Cerqueira M, DeCara JM, Edvardsen T, Flamm SD, Force T, Griffin BP, Jerusalem G, Liu JE, Magalhães A, Marwick T, Sanchez LY, Sicari R, Villarraga HR, Lancellotti P. Expert consensus for multimodality imaging evaluation of adult patients during and after cancer therapy: a report from the American Society of Echocardiography and the European Association of Cardiovascular Imaging. *Eur Heart J Cardiovasc Imaging.* 2014;15(10):1063-93.
19. Medvedofsky D, Maffessanti F, Weinert L, Tehrani DM, Narang A, Addetia K, Mediratta A, Besser SA, Maor E, Patel AR, Spencer KT, Mor-Avi V, Lang RM. 2D and 3D Echocardiography-Derived Indices of Left Ventricular Function and Shape: Relationship With Mortality. *JACC Cardiovasc Imaging.* 2018;11(11):1569-79.
20. Park JJ, Park JB, Park JH, Cho GY. Global Longitudinal Strain to Predict Mortality in Patients With Acute Heart Failure. *J Am Coll Cardiol.* 2018;71(18):1947-57.
21. Zerhouni EA, Parish DM, Rogers WJ, Yang A, Shapiro EP. Human heart: tagging with MR imaging--a method for noninvasive assessment of myocardial motion. *Radiology.* 1988;169(1):59-63.
22. Jeung MY, Germain P, Croisille P, El ghannudi S, Roy C, Gangi A. Myocardial tagging with MR imaging: overview of normal and pathologic findings. *Radiographics.* 2012;32(5):1381-98.
23. Neizel M, Lossnitzer D, Korosoglou G, Schaufele T, Peykarjou H, Steen H, Ocklenburg C, Giannitsis E, Katus HA, Osman NF. Strain-encoded MRI for evaluation of left ventricular function and transmural in acute myocardial infarction. *Circ Cardiovasc Imaging.* 2009;2(2):116-22.
24. Amzulescu MS, De Craene M, Langet H, Pasquet A, Vancraeynest D, Pouleur AC, Vanoverschelde JL, Gerber BL. Myocardial strain imaging: review of general principles, validation, and sources of discrepancies. *Eur Heart J-Card Imag.* 2019;20(6):605-19.
25. Salerno M. Feature Tracking by CMR: A "Double Feature"? *JACC Cardiovasc Imaging.* 2018;11(2 Pt 1):206-8.
26. Hor KN, Gottliebson WM, Carson C, Wash E, Cnota J, Fleck R, Wansapura J, Klimeczek P, Al-Khalidi HR, Chung ES, Benson DW, Mazur W. Comparison of magnetic resonance feature tracking for strain calculation with harmonic phase imaging analysis. *JACC Cardiovasc Imaging.* 2010;3(2):144-51.
27. Moody WE, Taylor RJ, Edwards NC, Chue CD, Umar F, Taylor TJ, Ferro CJ, Young AA, Townend JN, Leyva F, Steeds RP. Comparison of magnetic resonance feature tracking for systolic and diastolic strain and strain rate calculation with spatial modulation of magnetization imaging analysis. *J Magn Reson Imaging.* 2015;41(4):1000-12.
28. Harrild DM, Han Y, Geva T, Zhou J, Marcus E, Powell AJ. Comparison of cardiac MRI tissue tracking and myocardial tagging for assessment of regional ventricular strain. *Int J Cardiovasc Imaging.* 2012;28(8):2009-18.

29. Romano S, Judd RM, Kim RJ, Kim HW, Klem I, Heitner JF, Shah DJ, Jue J, White BE, Indorkar R, Shenoy C, Farzaneh-Far A. Feature-Tracking Global Longitudinal Strain Predicts Death in a Multicenter Population of Patients With Ischemic and Nonischemic Dilated Cardiomyopathy Incremental to Ejection Fraction and Late Gadolinium Enhancement. *JACC Cardiovasc Imaging*. 2018;11(10):1419-29.
30. Osman NF, Sampath S, Atalar E, Prince JL. Imaging longitudinal cardiac strain on short-axis images using strain-encoded MRI. *Magnet Reson Med*. 2001;46(2):324-34.
31. Koos R, Altiok E, Doetsch J, Neizel M, Krombach G, Marx N, Hoffmann R. Layer-specific strain-encoded MRI for the evaluation of left ventricular function and infarct transmuralities in patients with chronic coronary artery disease. *Int J Cardiol*. 2013;166(1):85-9.
32. Pan L, Stuber M, Kraitchman DL, Fritzges DL, Gilson WD, Osman NF. Real-time imaging of regional myocardial function using fast-SENC. *Magn Reson Med*. 2006;55(2):386-95.
33. Neizel M, Lossnitzer D, Korosoglou G, Schaufele T, Lewien A, Steen H, Katus HA, Osman NF, Giannitsis E. Strain-encoded (SENC) magnetic resonance imaging to evaluate regional heterogeneity of myocardial strain in healthy volunteers: Comparison with conventional tagging. *J Magn Reson Imaging*. 2009;29(1):99-105.
34. Korosoglou G, Youssef AA, Bilchick KC, Ibrahim e-S, Lardo AC, Lai S, Osman NF. Real-time fast strain-encoded magnetic resonance imaging to evaluate regional myocardial function at 3.0 Tesla: comparison to conventional tagging. *J Magn Reson Imaging*. 2008;27(5):1012-8.
35. Korosoglou G, Giusca S, Hofmann NP, Patel AR, Lapinskas T, Pieske B, Steen H, Katus HA, Kelle S. Strain-encoded magnetic resonance: a method for the assessment of myocardial deformation. *ESC Heart Fail*. 2019;6(4):584-602.
36. Altiok E, Tiemann S, Becker M, Koos R, Zwicker C, Schroeder J, Kraemer N, Schoth F, Adam D, Friedman Z, Marx N, Hoffmann R. Myocardial deformation imaging by two-dimensional speckle-tracking echocardiography for prediction of global and segmental functional changes after acute myocardial infarction: a comparison with late gadolinium enhancement cardiac magnetic resonance. *J Am Soc Echocardiogr*. 2014;27(3):249-57.
37. Farsalinos KE, Daraban AM, Unlu S, Thomas JD, Badano LP, Voigt JU. Head-to-Head Comparison of Global Longitudinal Strain Measurements among Nine Different Vendors The EACVI/ASE Inter-Vendor Comparison Study. *J Am Soc Echocardiogr*. 2015;28(10):1171-+.
38. Badano LP, Cucchini U, Muraru D, Al Nono O, Sarais C, Iliceto S. Use of three-dimensional speckle tracking to assess left ventricular myocardial mechanics: inter-vendor consistency and reproducibility of strain measurements. *Eur Heart J Cardiovasc Imaging*. 2013;14(3):285-93.
39. Gayat E, Ahmad H, Weinert L, Lang RM, Mor-Avi V. Reproducibility and inter-vendor variability of left ventricular deformation measurements by three-dimensional speckle-tracking echocardiography. *J Am Soc Echocardiogr*. 2011;24(8):878-85.
40. Erley J, Zieschang V, Lapinskas T, Demir A, Wiesemann S, Haass M, Osman NF, Simonetti OP, Liu Y, Patel AR, Mor-Avi V, Unal O, Johnson KM, Pieske B, Hansmann J, Schulz-Menger J, Kelle S. A multi-vendor, multi-center study on reproducibility and comparability of fast strain-encoded cardiovascular magnetic resonance imaging. *Int J Cardiovasc Imaging*. 2020.
41. Mitchell MD, Kundel HL, Axel L, Joseph PM. Agarose as a tissue equivalent phantom material for NMR imaging. *Magn Reson Imaging*. 1986;4(3):263-6.
42. Osman NF. Detecting stiff masses using strain-encoded (SENC) imaging. *Magn Reson Med*. 2003;49(3):605-8.

43. Oppo K, Leen E, Angerson WJ, Cooke TG, McArdle CS. Doppler perfusion index: an interobserver and intraobserver reproducibility study. *Radiology*. 1998;208(2):453-7.
44. Castillo E, Osman NF, Rosen BD, El-Shehaby I, Pan L, Jerosch-Herold M, Lai S, Bluemke DA, Lima JA. Quantitative assessment of regional myocardial function with MR-tagging in a multi-center study: interobserver and intraobserver agreement of fast strain analysis with Harmonic Phase (HARP) MRI. *J Cardiovasc Magn Reson*. 2005;7(5):783-91.
45. Biering-Sorensen T, Hoffmann S, Mogelvang R, Zeeberg Iversen A, Galatius S, Fritz-Hansen T, Bech J, Jensen JS. Myocardial strain analysis by 2-dimensional speckle tracking echocardiography improves diagnostics of coronary artery stenosis in stable angina pectoris. *Circ Cardiovasc Imaging*. 2014;7(1):58-65.
46. Schneeweis C, Qiu J, Schnackenburg B, Berger A, Kelle S, Fleck E, Gebker R. Value of additional strain analysis with feature tracking in dobutamine stress cardiovascular magnetic resonance for detecting coronary artery disease. *J Cardiovasc Magn Reson*. 2014;16:72.
47. Lorenz R, Bock J, Barker AJ, von Knobelsdorff-Brenkenhoff F, Wallis W, Korvink JG, Bissell MM, Schulz-Menger J, Markl M. 4D flow magnetic resonance imaging in bicuspid aortic valve disease demonstrates altered distribution of aortic blood flow helicity. *Magn Reson Med*. 2014;71(4):1542-53.
48. Andre F, Steen H, Matheis P, Westkott M, Breuninger K, Sander Y, Kammerer R, Galuschky C, Giannitsis E, Korosoglou G, Katus HA, Buss SJ. Age- and gender-related normal left ventricular deformation assessed by cardiovascular magnetic resonance feature tracking. *J Cardiovasc Magn R*. 2015;17.
49. Lang RM, Badano LP, Mor-Avi V, Afilalo J, Armstrong A, Ernande L, Flachskampf FA, Foster E, Goldstein SA, Kuznetsova T, Lancellotti P, Muraru D, Picard MH, Rietzschel ER, Rudski L, Spencer KT, Tsang W, Voigt JU. Recommendations for cardiac chamber quantification by echocardiography in adults: an update from the American Society of Echocardiography and the European Association of Cardiovascular Imaging. *Eur Heart J Cardiovasc Imaging*. 2015;16(3):233-70.
50. Erley J, Genovese D, Tapaskar N, Alvi N, Rashedi N, Besser SA, Kawaji K, Goyal N, Kelle S, Lang RM, Mor-Avi V, Patel AR. Echocardiography and cardiovascular magnetic resonance based evaluation of myocardial strain and relationship with late gadolinium enhancement. *J Cardiovasc Magn Reson*. 2019;21(1):46.
51. Riffel JH, Keller MGP, Aurich M, Sander Y, Andre F, Giusca S, Siepen FAD, Seitz S, Galuschky C, Korosoglou G, Mereles D, Katus HA, Buss SJ. Assessment of global longitudinal strain using standardized myocardial deformation imaging: a modality independent software approach. *Clinical Research in Cardiology*. 2015;104(7):591-602.
52. Bucius P, Erley J, Tanacli R, Zieschang V, Giusca S, Korosoglou G, Steen H, Stehning C, Pieske B, Pieske-Kraigher E, Schuster A, Lapinskas T, Kelle S. Comparison of feature tracking, fast-SENC, and myocardial tagging for global and segmental left ventricular strain. *ESC Heart Fail*. 2019.
53. Barbier P, Mirea O, Cefalu C, Maltagliati A, Savioli G, Guglielmo M. Reliability and feasibility of longitudinal AFI global and segmental strain compared with 2D left ventricular volumes and ejection fraction: intra- and inter-operator, test-retest, and inter-cycle reproducibility. *Eur Heart J Cardiovasc Imaging*. 2015;16(6):642-52.
54. Lapinskas T, Hireche-Chikaoui H, Zieschang V, Erley J, Stehning C, Gebker R, Giusca S, Korosoglou G, Zaliunas R, Backhaus SJ, Schuster A, Pieske B, Kelle S. Effect of comprehensive initial training on the variability of left ventricular measures using fast-SENC cardiac magnetic resonance imaging. *Sci Rep*. 2019;9(1):12223.
55. Armstrong AC, Ricketts EP, Cox C, Adler P, Arynchyn A, Liu K, Stengel E, Sidney S, Lewis CE, Schreiner PJ, Shikany JM, Keck K, Merlo J, Gidding SS, Lima JA. Quality Control and Reproducibility in M-Mode, Two-Dimensional, and Speckle Tracking

- Echocardiography Acquisition and Analysis: The CARDIA Study, Year 25 Examination Experience. *Echocardiography*. 2015;32(8):1233-40.
56. Maceira AM, Tuset-Sanchis L, Lopez-Garrido M, San Andres M, Lopez-Lereu MP, Monmeneu JV, Garcia-Gonzalez MP, Higuera L. Feasibility and reproducibility of feature-tracking-based strain and strain rate measures of the left ventricle in different diseases and genders. *J Magn Reson Imaging*. 2018;47(5):1415-25.
57. Khan JN, Singh A, Nazir SA, Kanagala P, Gershlick AH, McCann GP. Comparison of cardiovascular magnetic resonance feature tracking and tagging for the assessment of left ventricular systolic strain in acute myocardial infarction. *Eur J Radiol*. 2015;84(5):840-8.
58. Onishi T, Saha SK, Delgado-Montero A, Ludwig DR, Onishi T, Schelbert EB, Schwartzman D, Gorcsan J, 3rd. Global longitudinal strain and global circumferential strain by speckle-tracking echocardiography and feature-tracking cardiac magnetic resonance imaging: comparison with left ventricular ejection fraction. *J Am Soc Echocardiogr*. 2015;28(5):587-96.
59. Wang J, Li W, Sun J, Liu H, Kang Y, Yang D, Yu L, Greiser A, Zhou X, Han Y, Chen Y. Improved segmental myocardial strain reproducibility using deformable registration algorithms compared with feature tracking cardiac MRI and speckle tracking echocardiography. *J Magn Reson Imaging*. 2018;48(2):404-14.
60. Dobrovie M, Barreiro-Perez M, Curione D, Symons R, Claus P, Voigt JU, Bogaert J. Inter-vendor reproducibility and accuracy of segmental left ventricular strain measurements using CMR feature tracking. *European Radiology*. 2019;29(12):6846-57.
61. Mirea O, Pagourelas ED, Duchenne J, Bogaert J, Thomas JD, Badano LP, Voigt JU, Force EA-A-IST. Variability and Reproducibility of Segmental Longitudinal Strain Measurement: A Report From the EACVI-ASE Strain Standardization Task Force. *JACC Cardiovasc Imaging*. 2018;11(1):15-24.

Eidesstattliche Versicherung

„Ich, Jennifer Sigrid Myrtle Erley, versichere an Eides statt durch meine eigenhändige Unterschrift, dass ich die vorgelegte Dissertation mit dem Thema: „Myocardial strain: On agreement and reproducibility of a new parameter to determine ventricular function“/ „Strain des Herzmuskels: Über Vergleichbarkeit und Reproduzierbarkeit eines neuen Parameters zur Bestimmung der ventrikulären Funktion“ selbstständig und ohne nicht offengelegte Hilfe Dritter verfasst und keine anderen als die angegebenen Quellen und Hilfsmittel genutzt habe.

Alle Stellen, die wörtlich oder dem Sinne nach auf Publikationen oder Vorträgen anderer Autoren/innen beruhen, sind als solche in korrekter Zitierung kenntlich gemacht. Die Abschnitte zu Methodik (insbesondere praktische Arbeiten, Laborbestimmungen, statistische Aufarbeitung) und Resultaten (insbesondere Abbildungen, Graphiken und Tabellen) werden von mir verantwortet.

Ich versichere ferner, dass ich die in Zusammenarbeit mit anderen Personen generierten Daten, Datenauswertungen und Schlussfolgerungen korrekt gekennzeichnet und meinen eigenen Beitrag sowie die Beiträge anderer Personen korrekt kenntlich gemacht habe (siehe Anteilserklärung). Texte oder Textteile, die gemeinsam mit anderen erstellt oder verwendet wurden, habe ich korrekt kenntlich gemacht.

Meine Anteile an etwaigen Publikationen zu dieser Dissertation entsprechen denen, die in der untenstehenden gemeinsamen Erklärung mit dem/der Erstbetreuer/in, angegeben sind. Für sämtliche im Rahmen der Dissertation entstandenen Publikationen wurden die Richtlinien des ICMJE (International Committee of Medical Journal Editors; www.icmje.org) zur Autorenschaft eingehalten. Ich erkläre ferner, dass ich mich zur Einhaltung der Satzung der Charité – Universitätsmedizin Berlin zur Sicherung Guter Wissenschaftlicher Praxis verpflichte.

Weiterhin versichere ich, dass ich diese Dissertation weder in gleicher noch in ähnlicher Form bereits an einer anderen Fakultät eingereicht habe.

Die Bedeutung dieser eidesstattlichen Versicherung und die strafrechtlichen Folgen einer unwahren eidesstattlichen Versicherung (§§156, 161 des Strafgesetzbuches) sind mir bekannt und bewusst.“

Datum

Unterschrift

Anteilserklärung an den erfolgten Publikationen

Jennifer Sigrid Myrtle Erley hatte folgenden Anteil an den folgenden Publikationen:

Publikation 1: Erley J, Zieschang V, Lapinskas T, Demir A, Wiesemann S, Haass M, Osman NF, Simonetti OP, Liu Y, Patel AR, Mor-Avi V, Unal O, Johnson KM, Pieske B, Hansmann J, Schulz-Menger J, Kelle S. A multi-vendor, multi-center study on reproducibility and comparability of fast strain-encoded cardiovascular magnetic resonance imaging. *Int J Cardiovasc Imaging*. 2020.

Jennifer Erley (JE) rekrutierte die Probanden (mit Hilfe von AD); sie verfasste den Ethikantrag zusammen mit Hilfe von Prof. Dr. Sebastian Kelle (SK); sie organisierte die Untersuchungen an den drei verschiedenen Standorten (mit Hilfe von AD und SK); sie betreute alle Untersuchungen an den verschiedenen Standorten; sie analysierte die „SENC“-Dateien von allen Probanden, inklusive wiederholter Analysen um die Intraobserver-Reproduzierbarkeit zu bestimmen; sie organisierte die Auswertung bestimmter Daten durch eine erfahrene Kollegin um die Interobserver-Reproduzierbarkeit zu bestimmen; sie wertete alle Ergebnisse statistisch aus; sie verfasste das Manuskript für die Publikation (inklusive aller Tabellen und Figuren) und kümmerte sich um die Publikation des Manuskripts (inklusive der Revisionen).

Publikation 2: Erley J, Genovese D, Tapaskar N, Alvi N, Rashedi N, Besser SA, Kawaji K, Goyal N, Kelle S, Lang RM, Mor-Avi V, Patel AR. Echocardiography and cardiovascular magnetic resonance based evaluation of myocardial strain and relationship with late gadolinium enhancement. *J Cardiovasc Magn Reson*. 2019;21(1):46.:

JE war zuständig für den retrospektiven Einschluss der auf die Ein- und Ausschlusskriterien passenden Patienten (anhand Durchsichtung der MRT- und Echokardiografie-Datenbanken an der University of Chicago); sie führte die Analyse der „Feature Tracking“ und der „SENC“-Daten aller Patienten allein aus, inklusive wiederholter Analyse bestimmter Patienten um die Intraobserver-Reproduzierbarkeit zu bestimmen; sie organisierte die Auswertung der echokardiografischen Dateien und die wiederholte Auswertung der „SENC“ und „FT“ durch erfahrene Kollegen; sie wertete alle Ergebnisse statistisch aus (mit Hilfe von ARP, VM, SAB) und sie verfasste das Manuskript für die Publikation (inklusive aller Tabellen und Figuren) (mit Hilfe von ARP und VM).

Publikation 3: Bucius P, Erley J, Tanacli R, Zieschang V, Giusca S, Korosoglou G, Steen H, Stehning C, Pieske B, Pieske-Kraigher E, Schuster A, Lapinskas T, Kelle S. Comparison of feature tracking, fast-SENC, and myocardial tagging for global and segmental left ventricular strain. *ESC Heart Fail*. 2019.:

JE unterstützte SK, indem sie bei dem Kauf der Software für die „Tagging“-Analyse half und die Software installierte. Daraufhin half sie PB bei der Analyse der „Tagging“-Daten mittels dieser Software. Zudem unterstützte sie die Verfassung des Manuskriptes durch kritische Überprüfung.

Publikation 4: Lapinskas T, Hireche-Chikaoui H, Zieschang V, Erley J, Stehning C, Gebker R, Giusca S, Korosoglou G, Zaliunas R, Backhaus SJ, Schuster A, Pieske B, Kelle S. Effect of comprehensive

initial training on the variability of left ventricular measures using fast-SENC cardiac magnetic resonance imaging. Sci Rep. 2019;9(1):12223.:

JE unterstützte TL indem sie, TL, VZ und HH die fSENC-Daten analysierten. Darüber hinaus unterstützte JE die Verfassung des Manuskriptes durch kritische Überprüfung.

Unterschrift des Doktoranden/der Doktorandin

Liste ausgewählter Publikationen

1. **Erley J**, Zieschang V, Lapinskas T, Demir A, Wiesemann S, Haass M, Osman NF, Simonetti OP, Liu Y, Patel AR, Mor-Avi V, Unal O, Johnson KM, Pieske B, Hansmann J, Schulz-Menger J, Kelle S. A multi-vendor, multi-center study on reproducibility and comparability of fast strain-encoded cardiovascular magnetic resonance imaging. *Int J Cardiovasc Imaging*. 2020.
Journal Impact Factor (2018): 1.860
2. **Erley J**, Genovese D, Tapaskar N, Alvi N, Rashedi N, Besser SA, Kawaji K, Goyal N, Kelle S, Lang RM, Mor-Avi V, Patel AR. Echocardiography and cardiovascular magnetic resonance based evaluation of myocardial strain and relationship with late gadolinium enhancement. *J Cardiovasc Magn Reson*. 2019;21(1):46.
Journal Impact Factor (2018): 5.070
3. Bucius P, **Erley J**, Tanacli R, Zieschang V, Giusca S, Korosoglou G, Steen H, Stehning C, Pieske B, Pieske-Kraigher E, Schuster A, Lapinskas T, Kelle S. Comparison of feature tracking, fast-SENC, and myocardial tagging for global and segmental left ventricular strain. *ESC Heart Fail*. 2019.
Journal Impact Factor (2018): 3.407
4. Lapinskas T, Hireche-Chikaoui H, Zieschang V, **Erley J**, Stehning C, Gebker R, Giusca S, Korosoglou G, Zaliunas R, Backhaus SJ, Schuster A, Pieske B, Kelle S. Effect of comprehensive initial training on the variability of left ventricular measures using fast-SENC cardiac magnetic resonance imaging. *Sci Rep*. 2019;9(1):12223.
Journal Impact Factor (2018): 4.011



A multi-vendor, multi-center study on reproducibility and comparability of fast strain-encoded cardiovascular magnetic resonance imaging

Jennifer Erley¹ · Victoria Zieschang¹ · Tomas Lapinskas^{1,2} · Aylin Demir³ · Stephanie Wiesemann³ · Markus Haass⁴ · Nael F Osman^{5,6} · Orlando P Simonetti⁷ · Yingmin Liu⁸ · Amit R Patel⁹ · Victor Mor-Avi⁹ · Orhan Unal¹⁰ · Kevin M Johnson¹⁰ · Burkert Pieske^{1,11,12} · Jochen Hansmann¹³ · Jeanette Schulz-Menger^{3,12} · Sebastian Kelle^{1,11,12}

Received: 7 August 2019 / Accepted: 11 January 2020
© The Author(s) 2020

Abstract

Myocardial strain is a convenient parameter to quantify left ventricular (LV) function. Fast strain-encoding (fSENC) enables the acquisition of cardiovascular magnetic resonance images for strain-measurement within a few heartbeats during free-breathing. It is necessary to analyze inter-vendor agreement of techniques to determine strain, such as fSENC, in order to compare existing studies and plan multi-center studies. Therefore, the aim of this study was to investigate inter-vendor agreement and test-retest reproducibility of fSENC for three major MRI-vendors. fSENC-images were acquired three times in the same group of 15 healthy volunteers using 3 Tesla scanners from three different vendors: at the German Heart Institute Berlin, the Charité University Medicine Berlin-Campus Buch and the Theresien-Hospital Mannheim. Volunteers were scanned using the same imaging protocol composed of two fSENC-acquisitions, a 15-min break and another two fSENC-acquisitions. LV global longitudinal and circumferential strain (GLS, GCS) were analyzed by a trained observer (Myostrain 5.0, Myocardial Solutions) and for nine volunteers repeatedly by another observer. Inter-vendor agreement was determined using Bland-Altman analysis. Test-retest reproducibility and intra- and inter-observer reproducibility were analyzed using intraclass correlation coefficient (ICC) and coefficients of variation (CoV). Inter-vendor agreement between all three sites was good for GLS and GCS, with biases of 0.01–1.88%. Test-retest reproducibility of scans before and after the break was high, shown by ICC- and CoV values of 0.63–0.97 and 3–9% for GLS and 0.69–0.82 and 4–7% for GCS, respectively. Intra- and inter-observer reproducibility were excellent for both parameters (ICC of 0.77–0.99, CoV of 2–5%). This trial demonstrates good inter-vendor agreement and test-retest reproducibility of GLS and GCS measurements, acquired at three different scanners from three different vendors using fSENC. The results indicate that it is necessary to account for a possible bias (< 2%) when comparing strain measurements of different scanners. Technical differences between scanners, which impact inter-vendor agreement, should be further analyzed and minimized.

DRKS Registration Number: 00013253.

Universal Trial Number (UTN): U1111-1207-5874.

Keywords Strain · fSENC · Agreement · Reproducibility · CMR · Cardiac · Magnetic resonance

Abbreviations

CMR	Cardiovascular magnetic resonance	GLS	Global longitudinal strain
EF	Ejection fraction	IQR	Interquartile range
EPI	Echo planar imaging	LV	Left ventricular
fSENC	Fast strain-encoded magnetic resonance imaging	LOA	Limits of agreement
GCS	Global circumferential strain	MRI	Magnetic resonance imaging
		SAX	Short-axis
		SENC	Strain-encoded magnetic resonance imaging
		STE	Speckle tracking echocardiography
		2-Ch	2-Chamber
		3-Ch	3-Chamber
		4-Ch	4-Chamber

✉ Sebastian Kelle
kelle@dhzb.de

Extended author information available on the last page of the article

Introduction

Myocardial strain has proven to be an important parameter for further investigation of myocardial performance in addition to conventionally used volumetric measures, such as ejection fraction (EF) [1–3]. Strain can be determined using echocardiography and cardiovascular magnetic resonance (CMR) imaging. A common technique to measure strain in echocardiography is using speckle tracking (STE). STE is routinely used, for example to identify systolic dysfunction in heart failure patients with preserved EF [4] or as a marker for cardiotoxicity in patients undergoing chemotherapy [5]. An important step towards standardization of STE in preparation for broad clinical use was the recent publication of a consensus document on how strain measurements should be performed [6]. However, strain is not only influenced by measurement methods, but also by image quality, intra- and inter-observer reproducibility, the image acquisition system [7] and the post-processing software used [8, 9]. As the impact of these various factors on strain results remains unclear, guidelines recommend STE to be performed using the same vendor's acquisition system and software for individual patients [9].

As CMR emerged as the reference standard of cardiac morphology and function [10], various acquisition- and post-processing techniques to determine strain using CMR have been explored and validated [11]. Long acquisition times [12] and long breath-holds in patients with cardiac diseases, especially those who suffer from dyspnea, are some of the factors currently limiting use in clinical settings. Furthermore, no standardized approach to measure strain using CMR has been proposed yet, as was the case for STE. The lack of information on the influence of different magnetic resonance scanners and platforms on strain results is one challenge preventing standardization of CMR techniques. Nevertheless, this information is crucial since studies are conducted at different centers with varying scanners, at different field strengths and using different post-processing platforms. Without information on inter-vendor agreement, CMR-strain should only be determined using the same scanner and post-processing software for individual patients, as recommended for STE. Although this measure reduces possible bias on strain results, no comparison can be made between different studies and measurements performed at different centers, hampering the practicality of using strain routinely and the design of multi-center studies to further validate this method.

Strain-encoding (SENC), first described in 2001 by Osman et al. [13], is a novel imaging technique to measure strain. In comparison to myocardial tagging, SENC uses tag planes in which the sinusoidal phase is constant in parallel to the image plane [13]. Therefore, longitudinal

strain is determined using short-axis- and circumferential strain using long-axis views; radial strain is not measurable by SENC. Fast-SENC (fSENC) is a “real-time” scan that acquires all necessary data for one slice within one single heartbeat [14]. Hence, it is insensitive to breathing motion, resulting in a fast magnetic resonance imaging (MRI) exam for the patient at free breathing. Studies have shown that fSENC is equal or even superior to tagging [15] and highly reproducible concerning inter-study, as well as intra- and inter-observer reproducibility [2].

The aim of this study was to examine the inter-vendor agreement and reproducibility of CMR-derived strain, obtained with fSENC in the same group of volunteers at three different sites with individual MRI-platforms and sequences. In particular, our aims were to

1. investigate inter-vendor agreement of fSENC at 3 T using scanners from three major MRI vendors,
2. determine test-retest reproducibility of repeated scans at each scanner and
3. determine intra- and inter-observer reproducibility of the strain measurements.

Methods

Study population and design

Fifteen healthy volunteers with no history of cardiovascular diseases or contraindications against MRI [16] were prospectively identified and recruited for the study after obtaining a written informed consent. The study was approved by the Ethics Committee of the Charité-University-Medicine in Berlin and complied with the Declaration of Helsinki. It was registered at the German Register for Clinical Studies (DRKS) (registration number: 00013253) and the World Health Organization (WHO) (universal trial number (UTN): U1111-1207-5874).

Cardiovascular magnetic resonance imaging

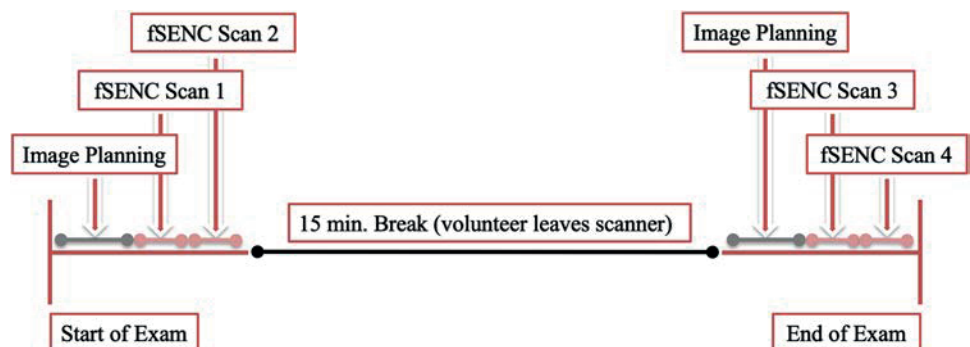
CMR images of all fifteen volunteers were acquired repeatedly at 3 T on three different scanners (names in alphabetical order and not according to site number: Ingenia, Philips, Best, The Netherlands; MAGNETOM Verio, Siemens Healthcare GmbH, Erlangen, Germany; SIGNA Architect, GE Healthcare, Milwaukee, WI, USA). CMR examinations took place within five months at: the German Heart Institute Berlin (site I), the Theresien-Hospital Mannheim (site II) and the Max-Delbrück Center for Molecular Medicine (MDC) in collaboration with Charité University Medicine

Berlin-Campus Buch (site III), each equipped with one of the above listed scanners.

Fast strain-encoding (fSENC)

The techniques applied to the pulse sequence (localized/reduced field-of-view fSENC, interleaved tuning, spiral imaging, ramped flip angle, etc.) to achieve image acquisition in a single heartbeat have been described previously [2, 14, 15]. Prior to in-vivo imaging, studies were performed in vitro with scanning platforms of the three different vendors using phantoms of very similar proportions, made of homogeneous MR-visible silicone gel with known mechanic properties [17]. Periodic non-flat compression and expansion was applied using an MR-compatible air cylinder as described by Osman et al. [17, 18]. Subsequently, scanning of the fifteen volunteers was performed at all three sites. All volunteers were scanned using the same imaging protocol, schematically depicted in Fig. 1. Each volunteer received four fSENC scans per site, adding up to 60 scans. The first two scans were performed consecutively using the same scanning parameters. Afterwards the volunteers left the scanner room for fifteen minutes, followed by two more fSENC acquisitions with the same parameters. Images were acquired in three long-axis views (2-chamber (2-ch), 3-chamber (3-ch), 4-chamber (4-ch)) to calculate left ventricular (LV) global circumferential strain (GCS) and in three short-axis views (SAX- basal, mid-ventricular (mid), apical) to calculate LV global longitudinal strain (GLS). Scanning was performed by the local team of one or two technicians at each site after being trained by the same representatives of the software provider on performing the fSENC acquisitions and completing a written test. Scanning parameters were allowed to be adjusted according to the different scanners, if needed. Heart rate (bpm) and blood pressure (mmHg) were monitored before, during and after the exam. Variables that might influence strain measurements, such as height, weight and smoking behavior, were determined before the scans at every site.

Fig. 1 Schematic outline showing the scan organization with a total of four fSENC scans per volunteer at every site



Technical parameters

Site I

At site I, images were acquired using a multi-element receive coil array, consisting of an anterior part on the patient's chest and a posterior part embedded in the patient table. A flexible number of up to 32 elements was employed, where the selection of coil elements was performed automatically by the MR software. Image acquisition was triggered on the R-wave using a 4-lead vector ECG. fSENC imaging parameters at site I were: field-of-view = $256 \times 256 \text{ mm}^2$, slice thickness = 10 mm, voxel size = $4 \times 4 \times 10 \text{ mm}^3$, reconstructed images at $1 \times 1 \times 10 \text{ mm}^3$ using zero-filled interpolation (in-plane ZIP 1024), spiral readout (3 interleaves) with acquisition time (TA) = 10 ms, flip angle = 30° , effective echo time (TE) = 0.7 ms, repetition time (TR) = 12 ms, temporal resolution = 36 ms, typical number of acquired heart phases = 22, spectrally selective fat suppression (SPIR), total acquisition time per slice < 1 s (1 heartbeat), total acquisition time per scan = 6 heartbeats.

Site II

At site II, a user-developed sequence was employed. Images were acquired using a multi-element receive coil array, as described for site I. fSENC spiral images were triggered on the R-wave using a 4-lead vector ECG. Field-of-view = $256 \times 256 \text{ mm}^2$, slice thickness = 7–8 mm, voxel size = $4 \times 4 \times 7 \text{ mm}^3$, reconstructed images at $1 \times 1 \times 7 \text{ mm}^3$, single-shot spiral readout (4 interleaves) with acquisition time (TA) = 7.5 ms, flip angle = 20° , effective echo time (TE) = 5.0 ms, repetition time (TR) = 9.1 ms, temporal resolution = 36.4 ms, typical number of acquired heart phases = 18, spectrally selective fat suppression (SPIR), total acquisition time per slice < 1 s (or one heartbeat), total acquisition time per scan = 6 heartbeats.

Site III

In comparison to the spiral pulse sequence at sites I and II, fSENC at site III is an Echo Planar Imaging (EPI) user-developed pulse sequence [19]. Volunteers were scanned using a 32-channel body coil and image acquisition was triggered on the R-wave using a 4-lead vector ECG. Epi-factor = 9, field-of-view = $450 \times 170 \text{ mm}^2$, slice thickness = 12 mm, voxel size = $4.7 \times 4.7 \times 12 \text{ mm}^3$, reconstructed resolution at $4.7 \times 4.7 \times 12 \text{ mm}^3$, flip angle = 12° , effective echo time (TE) = 1.18 ms, repetition time (TR) = 8.9 ms, temporal resolution = 35.6 ms, centric EPI recording, typical number of acquired heart phases = 22, spectrally selective fat suppression (SPIR). The acquisition happened in a single heartbeat, as for sites I and II. A separate heartbeat was used for EPI phase correction. The total acquisition time per slice was about 2 s (or two heartbeats) and per scan about 12 heartbeats.

Image analysis

All images were analyzed by one observer (JE) using dedicated software (Myostrain 5.0, Myocardial Solutions, Inc.,

Morrisville, North Carolina, USA), after being trained by a representative of the software company and completing a written test, as previously described [20]. Figure 2 demonstrates the process of image analysis, starting with the acquisition of the image on the scanner (1.), proceeding onto the color-coded image on the software, displaying the manually drawn endo- and epicardial contours at end-systole (2.) and onto the result of the strain analysis, represented by a color-coded map of the heart (3.). GCS was quantified in the three long-axis images by drawing epi- and endocardial contours manually at end-systole (as seen in Fig. 2), identified by the size of the heart and the color-coding of the images signaling contraction (blue). Papillary muscles and trabeculae were excluded from the endocardial contour. GLS was quantified using the short-axis images, again by drawing epi- and endocardial contours at end-systole (Fig. 2). The LV was automatically divided into 16 segments in the short-axis views and 21 segments in the long-axis views (according to the AHA model [21]) and segmental strain was calculated by applying an automated tracking algorithm. Peak systolic GCS and GLS were calculated as the average strain of all segments at end-systole in the long- and short-axis views, respectively. Scans were only excluded from the analysis if

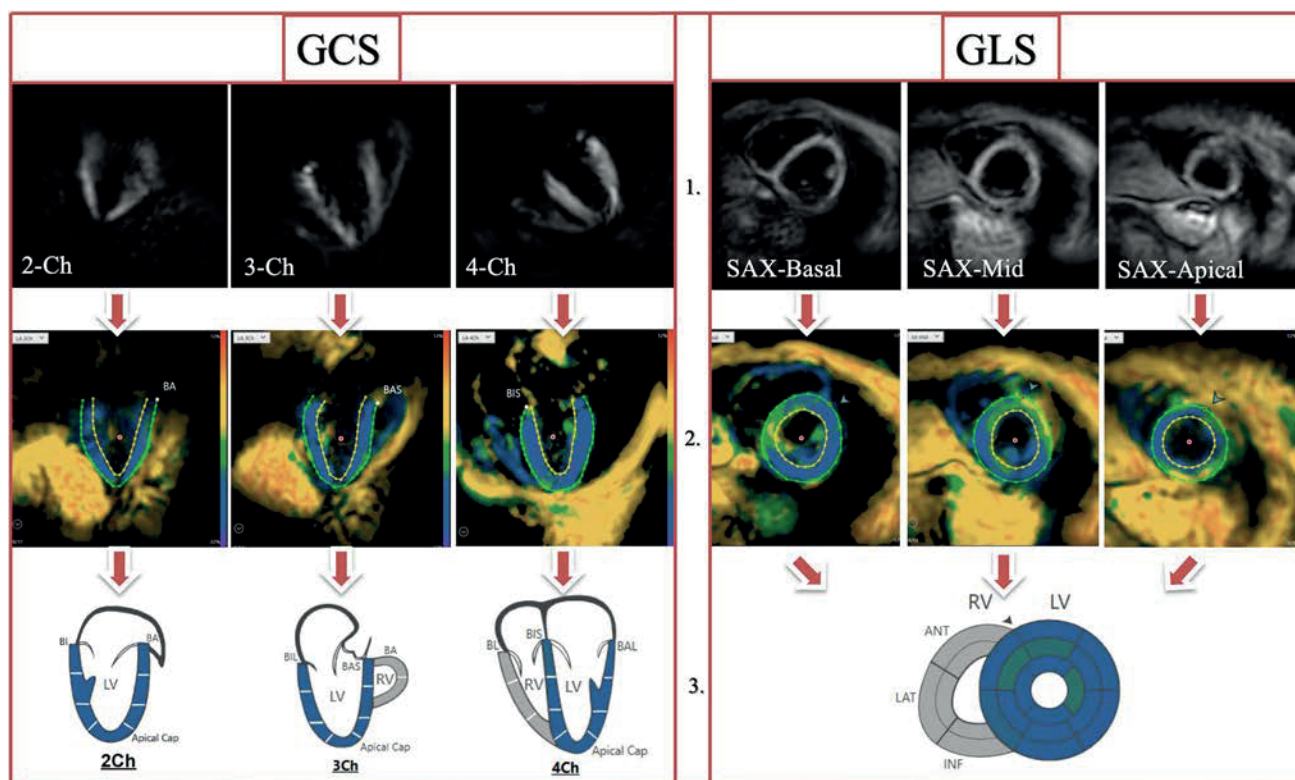


Fig. 2 fSENC- and corresponding color-coded images after post-processing at end-systole (blue representing strain in the normal range during contraction), as well as the myocardial segmentation as illustrated by the software. Legend: 1.=Images as shown on the scanner,

2.=Color-coded images on the software after post-processing, displaying manually drawn epi-and endocardial contours at end-systole, 3.=Results of the strain analysis, represented by a color-coded map of the heart

no view could be analyzed due to insufficient image quality (e.g. GCS could not be determined due to insufficient image quality of the 2-,3- and 4-chamber images). Figure 3 shows exemplary images of the same volunteer at the three sites, as displayed on the scanner and after post-processing.

Intra- and inter-observer reproducibility analysis

Measurements were repeated in a subset of three random volunteers per site (9 volunteers = 36 scans) by the first observer two months after the first analysis and by a second observer who received the same training by software representatives beforehand, blinded to all previous strain measurements. Before repeating the analysis, both observers came to a consensus of excluding volunteers, if both observers considered no view to have the sufficient image quality to determine either GCS or GLS reliably.

Statistical analysis

The distribution of all values was assessed for normality using the Shapiro-Wilks test. Normally distributed data is expressed as mean ± standard deviation, non-normally distributed data using median and interquartile range (IQR). Inter-vendor agreement between the three sites was

determined using Bland-Altman analysis. Test-retest reproducibility between averaged scans before (average strain of scan 1 and 2) and after the fifteen-minute break (average strain of scan 3 and 4) and between single scans was determined using intraclass correlation (ICC) and coefficients of variation (CoV). Wilcoxon test (for non-normally distributed strain parameters) and paired students t-test (for normally distributed strain parameters) were calculated to determine if differences in strain values between the sites and before and after the break were significant. Intra- and inter-observer reproducibility were analyzed using ICC and CoV. The following levels of agreement were used: excellent for ICC > 0.74, good for ICC 0.6–0.74, fair for ICC 0.4–0.59 and poor for ICC < 0.4 [2, 22]. All values are expressed using p-values and confidence intervals. A p-value of ≤ 0.05 was considered significant in two-tailed tests. Statistical analyses were conducted using SPSS (Version 25.0, IBM Corp., Armonk, NY, USA).

Results

fSENC-image acquisitions of the gel-phantoms were repeated several times. Mean strain and standard deviation were −28.1% (±0.3) for the system used at site I, −23.7

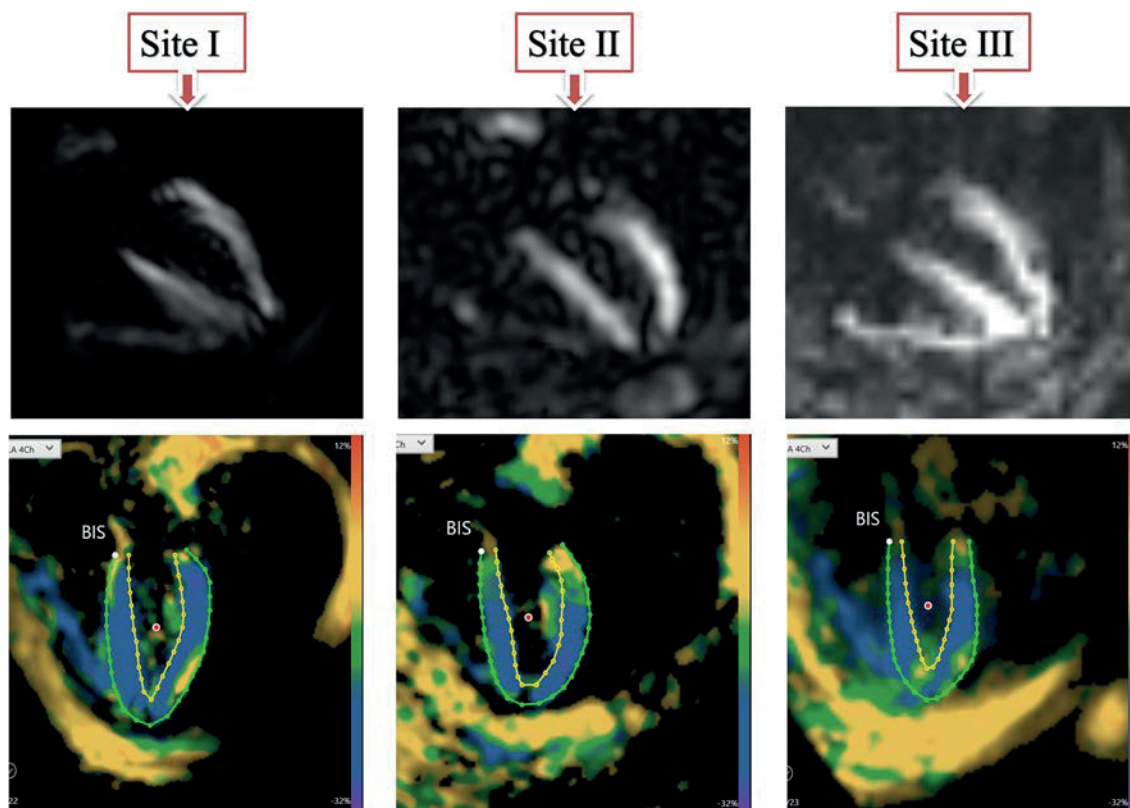


Fig. 3 4-chamber view images of the same volunteer scanned at the three different sites, as shown on the scanner and after post-processing

(± 0.9) for the system used at site II and $-26.8 (\pm 1.4)$ for the system used at site III. Table 1 portrays the baseline characteristics of the volunteers, vital signs and median (IQR) strain values. One complete fSENC-examination including all images was acquired in a median (IQR) scan time of two (1–4) min at all sites. Median image analysis time ranged from 10 to 14 min for one whole examination. A total of four scans were performed for each volunteer (twice before and twice after the break). At site I, one scan had to be excluded from GLS-analysis owing to motion artifacts during acquisition of the short-axis images. At site II, one volunteer could not be scanned due to unexpected technical difficulties. Further four scans were excluded from GLS- and nine from GCS-analysis because of artifacts that would not allow reliable contouring of the heart. At site III, no scan was excluded. A total of 51 scans (85.0%) were left for GLS- and 47 scans (78.3%) for GCS-analysis.

Inter-vendor agreement

Figure 4 shows box and whisker-plots to illustrate the range of strain values with regard to the different sites and the significance level of the differences, as calculated from the Bland-Altman analysis. The range of GLS-measurements was wider than of GCS-measurements. Differences in strain values were significant when comparing site I against either site II or III. Table 2 and Fig. 5 display the results of the Bland-Altman analysis. Inter-vendor agreement was good between all sites, shown by small biases (0.01–1.88% strain), but the limits of agreement (LOA) reflected a possible inconsistency regarding individual patients. Biases and limits of agreement were significant when comparing site I against either site II or III.

Table 1 Baseline characteristics of the volunteers (n = 15), median (IQR) scan time and median strain values (IQR) at the different sites

Volunteer characteristics	Site I	Site II	Site III
Female, n (%)	8 (53%)	8 (53%)	8 (53%)
Age (years)	25 (± 5)	25 (± 5)	25 (± 5)
Height (cm)	174 (± 9)	173 (± 8)	174 (± 9)
Weight (kg)	66 (± 11)	66 (± 11)	66 (± 11)
Smoking, n (%)	2 (13%)	3 (20%)	3 (20%)
Blood pressure before exam (mmHg)	123 (± 18)/68(± 11)	129 (± 18)/74 (± 9)	123 (± 16)/64 (± 9)
Blood pressure after exam (mmHg)	112 (± 17)/61(± 7)	127 (± 15)/70(± 7)	120 (± 16)/62(± 10)
Heart rate before exam (bpm)	74(± 12)	77 (± 15)	67 (± 12)
Heart rate after exam (bpm)	69(± 7)	75 (± 11)	76 (± 9)
Scan time (min.)	2 (1–2)	3 (2–6)	3 (1–4)
LV-GLS (%) (n = 51)	-19.2 (-20.5 to -18.0)	-17.8 (-20.0 to -16.4)	-17.9 (-20.0 to -16.0)
LV-GCS (%) (n = 47)	-19.7 (-21.1 to -18.3)	-18.9 (-20.0 to -17.1)	-18.2 (-19.2 to -16.8)

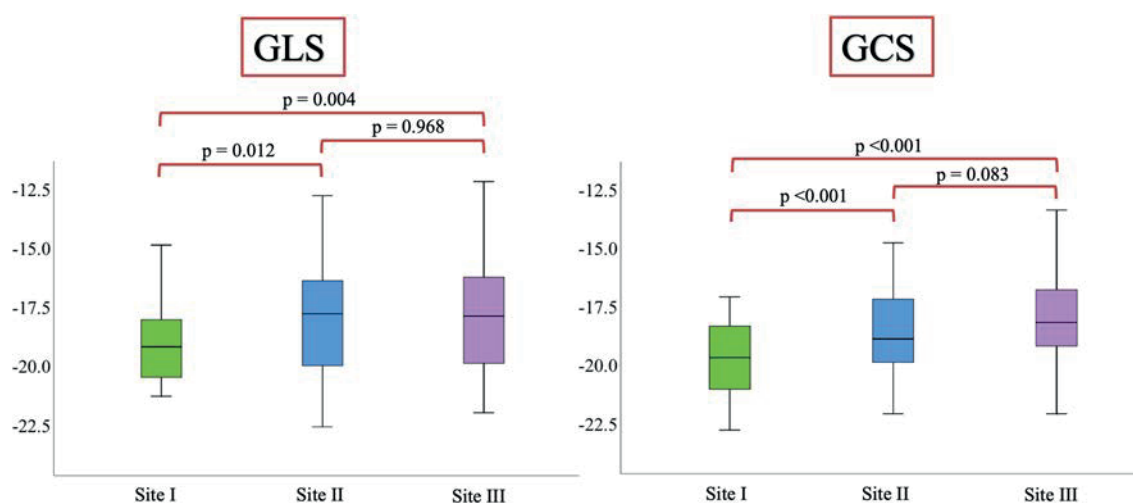


Fig. 4 Box and whisker-plots to illustrate the range of strain values with regard to the different sites and the significance level of the differences

Table 2 Results of the Bland-Altman analysis illustrating inter-vendor agreement

	Bias (%)	LOA (%)	p
LV-GLS (n=51)			
Site I vs. II	1.21	-5.25 to 7.68	0.012
Site I vs. III	1.24	-4.47 to 6.92	0.004
Site II vs. III	0.01	-4.78 to 4.81	0.968
LV-GCS (n=47)			
Site I vs. II	1.14	-2.34 to 4.64	<0.001
Site I vs. III	1.88	-3.02 to 6.79	<0.001
Site II vs. III	0.61	-3.99 to 5.20	0.083

Test-retest reproducibility

Table 3 displays the median (IQR) strain values of the averaged scans before and after the break and the corresponding p-value, as well as the ICC (95% CI) and CoV (\pm sd). As shown by the good- to excellent ICC- and CoV-values, test-retest reproducibility of averaged scans before and after the break was very high for all sites. The highest test-retest reproducibility was observed for LV-GLS at site II (ICC=0.97) and the lowest for LV-GLS at site I (ICC=0.63). At site I, test-retest reproducibility was higher for GCS-measures, whereas at site II and III, it was higher for GLS-measures. Nevertheless, differences in median strain between scans before and after the break were mostly insignificant (except for LV-GLS for site I). Table 4 shows the scan-rescan reproducibility between single scans. Overall, scan-rescan reproducibility was good, independent of

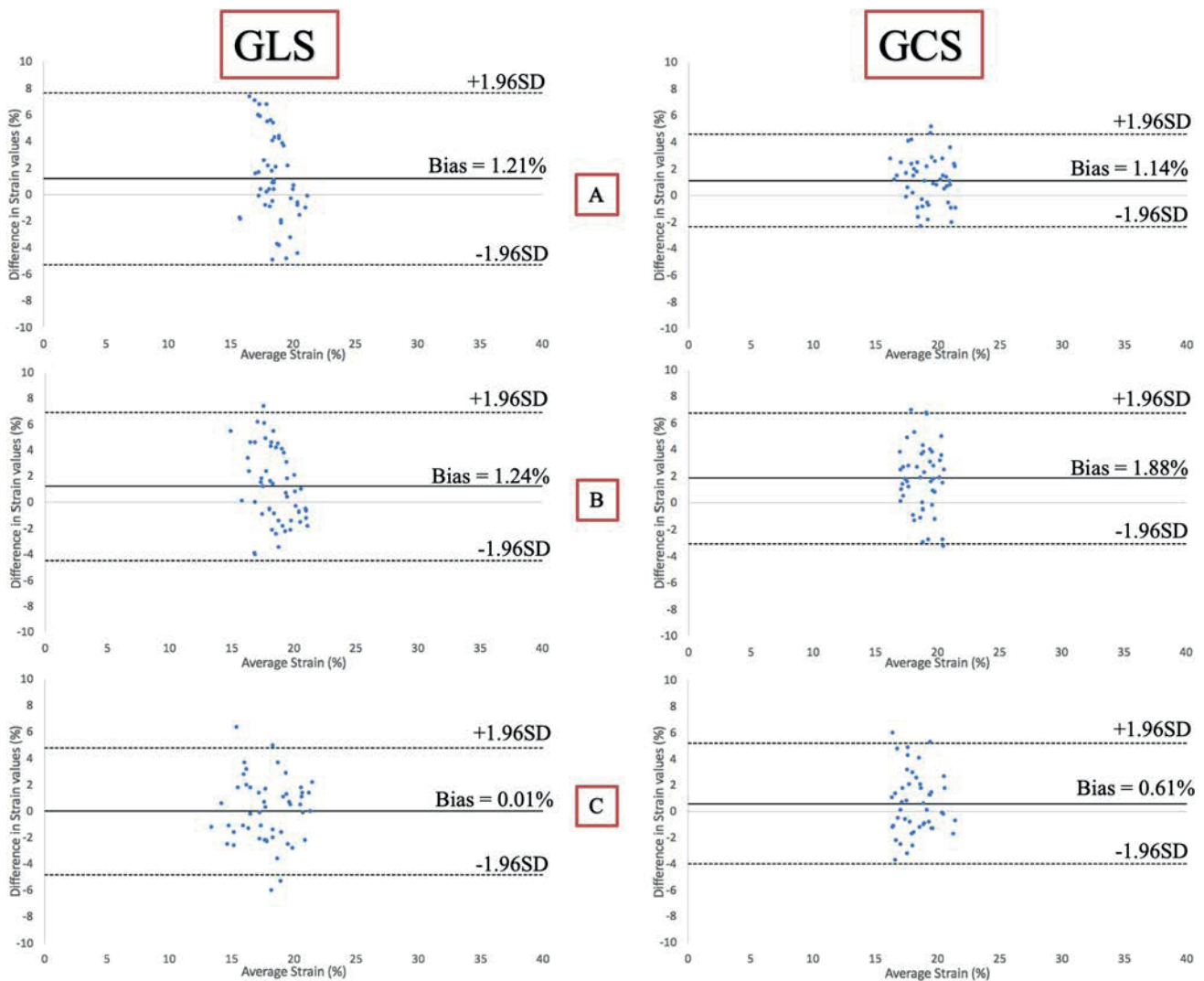


Fig. 5 Bland-Altman analysis comparing GLS and GCS between the different sites. Legend: **a** Site I vs. II, **b** Site I vs. III, **c** Site II vs. III

Table 3 Median (IQR) strain before and after the 15-min break at every site and results of the ICC (95% CI) and CoV (\pm sd) to display test-retest reproducibility

		Median (IQR) strain	p	ICC (95%CI)	p	CoV (\pm sd)
Site I	LV-GLS	-20.1 (-20.9 to -18.3) -19.4 (-20.6 to -17.8)	0.020	0.63 (0.21 to 0.86)	0.002	0.06 (\pm 0.05)
	LV-GCS	-19.0 (-21.1 to -18.3) -19.4 (-21.0 to -18.3)	0.950	0.82 (0.53 to 0.93)	<0.001	0.05 (\pm 0.03)
Site II	LV-GLS	-19.9 (-21.3 to -16.8) -20.1 (-21.2 to -17.0)	0.347	0.97 (0.90 to 0.99)	<0.001	0.03 (\pm 0.02)
	LV-GCS	-17.4 (-19.0 to -16.4) -17.3 (-18.6 to -16.7)	0.307	0.80 (0.47 to 0.94)	<0.001	0.04 (\pm 0.04)
Site III	LV-GLS	-18.8 (-20.2 to -15.1) -18.4 (-19.8 to -16.2)	0.977	0.82 (0.54 to 0.94)	<0.001	0.09 (\pm 0.07)
	LV-GCS	-17.2 (-18.6 to -16.3) -18.5 (-19.5 to -16.5)	0.056	0.69 (0.29 to 0.88)	0.001	0.07 (\pm 0.05)

scanner site (ICC = 0.97–0.70). The highest scan-rescan repeatability could be observed for site II between scans 3 and 4 and 1 and 3, the lowest regarding site I between scans 1 and 3.

Intra- and inter-observer reproducibility

Both observers independently excluded one volunteer out of nine from strain analysis, resulting in 32 scans. Intra- and inter-observer reproducibility were very high overall (Table 5), but even higher for GLS than for GCS.

Discussion

It has been shown that strain, determined using either echocardiography or CMR, is a valuable parameter to determine the impact of coronary artery disease on heart function [12], to detect LV dysfunction, especially in patients with heart failure when EF is still preserved [1, 4, 12, 23] and to reveal diffuse damage to the myocardium due to systemic diseases, such as cardiac amyloidosis [24, 25], sarcoidosis [26] or cardiotoxic effects of chemotherapy [5]. Despite these many possible indications, the use of strain in clinical routine is still challenging due to the impact of intra-, inter-observer- [7] and inter-vendor reproducibility of the different post-processing platforms [8, 9, 27] on strain results, which could also explain the lack of inter-technique agreement between echocardiography and CMR [28]. Therefore, before conducting studies to validate strain techniques in large patient cohorts, it is important to (1) identify the possible factors influencing strain results and to (2) minimize the impact of these factors. To address this issue, we compared GLS and GCS in healthy volunteers, who were all scanned using fSENC at three different sites with MRI scanners from major vendors.

Our results show:

- (1) good inter-vendor agreement of strain measurements using fSENC between all three vendors overall, reflected by small biases but substantial limits of agreement
- (2) very good test-retest reproducibility of fSENC when scanning volunteers again after a fifteen-minute break, regardless of vendor, and
- (3) good to excellent intra- and inter-observer reproducibility of fSENC strain measurements.

To our knowledge, no previous data on inter-vendor agreement of a CMR-technique to determine strain exists. Nevertheless, the influence of different ultrasound systems on 2D- and 3D-STE has been reported previously [7, 29–31]. As in our study, differences in STE-strain measurements between the different vendors were significant [7, 29, 30]. However, the bias between different ultrasound systems was similar or higher (0.1–3.7 [7], 1.1–7.0 [30], 1–1.55% [31]) than the bias between magnetic resonance scanners determined in our study group of fifteen volunteers (0.01–1.88%), with limits of agreement of a similar magnitude. The bias in our cohort of healthy volunteers was significant between site I and II or III. Moreover, the limits of agreement indicate that in some individuals the difference in strain values could be considerably higher than the bias. We believe that this study demonstrates the importance of further exploring inter-vendor agreement in larger cohorts to validate these results and to determine the agreement related to different scanners in patients. Our results indicate that it might possibly be helpful to implement scanner-related normal values and that one should be aware of this possible bias and limits of agreement when comparing strain results acquired at different scanners. This should also play a role when designing classifications based on strain, which determine diagnostic procedures and therapeutic decisions for patients.

An important factor that could influence inter-vendor agreement is the difference in technical characteristics of

Table 4 Scan-rescan reproducibility, represented using ICC (95% CI) and CoV

		ICC (95%CI)	p	CoV (\pm sd)
Site I	GLS			
	Scan 1 vs. 2	0.94 (0.81 to 0.98)	<0.001	0.03 (0.02)
	Scan 2 vs. 3	0.75 (0.16 to 0.92)	0.002	0.07 (0.04)
	Scan 3 vs. 4	0.97 (0.91 to 0.99)	<0.001	0.02 (0.02)
	Scan 1 vs. 3	0.70 (0.15 to 0.90)	0.013	0.06 (0.06)
	Scan 1 vs. 4	0.74 (0.27 to 0.91)	0.007	0.06 (0.06)
	Scan 2 vs. 4	0.79 (0.33 to 0.93)	0.002	0.07 (0.05)
	GCS			
	Scan 1 vs. 2	0.89 (0.68 to 0.96)	<0.001	0.05 (0.06)
	Scan 2 vs. 3	0.83 (0.47 to 0.94)	0.002	0.07 (0.06)
	Scan 3 vs. 4	0.86 (0.56 to 0.95)	0.001	0.05 (0.04)
	Scan 1 vs. 3	0.79 (0.37 to 0.93)	0.004	0.06 (0.04)
	Scan 1 vs. 4	0.86 (0.58 to 0.95)	<0.001	0.05 (0.04)
	Scan 2 vs. 4	0.88 (0.62 to 0.96)	<0.001	0.06 (0.05)
Site II	GLS			
	Scan 1 vs. 2	0.88 (0.61 to 0.96)	<0.001	0.07 (0.07)
	Scan 2 vs. 3	0.94 (0.80 to 0.98)	<0.001	0.04 (0.05)
	Scan 3 vs. 4	0.97 (0.91 to 0.99)	<0.001	0.03 (0.03)
	Scan 1 vs. 3	0.97 (0.89 to 0.99)	<0.001	0.04 (0.03)
	Scan 1 vs. 4	0.94 (0.81 to 0.98)	<0.001	0.06 (0.04)
	Scan 2 vs. 4	0.95 (0.77 to 0.99)	<0.001	0.05 (0.04)
	GCS			
	Scan 1 vs. 2	0.94 (0.79 to 0.98)	<0.001	0.04 (0.04)
	Scan 2 vs. 3	0.89 (0.61 to 0.97)	0.001	0.05 (0.03)
	Scan 3 vs. 4	0.85 (0.52 to 0.96)	0.001	0.05 (0.04)
	Scan 1 vs. 3	0.79 (0.20 to 0.95)	0.013	0.06 (0.04)
	Scan 1 vs. 4	0.85 (0.46 to 0.96)	0.002	0.04 (0.06)
	Scan 2 vs. 4	0.85 (0.50 to 1.00)	0.002	0.05 (0.05)
Site III	GLS			
	Scan 1 vs. 2	0.92 (0.77 to 0.97)	<0.001	0.08 (0.09)
	Scan 2 vs. 3	0.84 (0.51 to 0.95)	0.001	0.10 (0.11)
	Scan 3 vs. 4	0.96 (0.90 to 0.99)	<0.001	0.06 (0.05)
	Scan 1 vs. 3	0.89 (0.67 to 0.96)	<0.001	0.09 (0.09)
	Scan 1 vs. 4	0.89 (0.68 to 0.97)	<0.001	0.10 (0.08)
	Scan 2 vs. 4	0.85 (0.55 to 0.95)	0.001	0.10 (0.08)
	GCS			
	Scan 1 vs. 2	0.90 (0.70 to 0.97)	<0.001	0.06 (0.03)
	Scan 2 vs. 3	0.71 (0.18 to 0.90)	0.012	0.08 (0.06)
	Scan 3 vs. 4	0.85 (0.56 to 0.95)	0.001	0.06 (0.05)
	Scan 1 vs. 3	0.71 (0.12 to 0.90)	0.005	0.08 (0.06)
	Scan 1 vs. 4	0.79 (0.38 to 0.93)	<0.001	0.08 (0.05)
	Scan 2 vs. 4	0.83 (0.50 to 0.94)	0.001	0.07 (0.05)

the pulse sequence at the different scanners. A spiral read-out was used at sites I and II, whereas an EPI was used at site III, which may have different properties in terms of geometric distortion and susceptibility to off-resonant spins. Furthermore, the pulse sequence varied with regard to most

Table 5 Intra- and inter-observer reproducibility, reflected by ICC (95% CI) and CoV (\pm sd)

	ICC (95%CI)	p	CoV (\pm sd)
Intra-observer reproducibility			
LV-GLS	0.99 (0.98 to 1.00)	<0.001	0.02 \pm 0.02
LV-GCS	0.77 (0.47 to 0.90)	<0.001	0.05 \pm 0.04
Inter-observer reproducibility			
LV-GLS	0.96 (0.92 to 0.98)	<0.001	0.03 \pm 0.04
LV-GCS	0.82 (0.58 to 0.92)	<0.001	0.04 \pm 0.03

scanning parameters for each scanner. In order to determine the influence of the pulse sequence alone on strain measurements, phantoms were scanned at sites with the three different scanning systems before scanning the volunteers. Mean strain values of the phantoms were higher using the scanning systems at site II and III than using the system at site I, similar to the pattern of median GLS and GCS of the volunteers. This suggests that the pulse sequence itself could contribute to differences in strain values. Other possible variables with impact on inter-vendor agreement are the planning and training of different technicians, the experience and training of the observers and changes in the physiology of the volunteers. In order to minimize the effect of differences in knowledge and training of the technicians and observers in our study, all received training on image planning/analysis and completed written tests. Furthermore, a standardized imaging protocol was used at all three sites, but technicians were allowed to adjust the scanning parameters. Additionally, if two technicians performed the scanning, different levels of experience and planning styles resulted in different image planning at the same scanner. Due to the above listed reasons, the scans were of variable quality, which may have affected strain measurements. To monitor and reduce volunteer-related bias, volunteers were asked questions regarding their health, medications and smoking behavior before every scan and height, weight, blood pressure and heart frequency were monitored. Volunteers with new onset of disease or new intake of medication would have been excluded, but the impact of changes in factors such as weight and smoking behavior on strain measurements were not ruled out. In addition, it was not possible to keep the time difference between the scans at the three sites consistent, so we could not eliminate changes in myocardial function associated with timing of the scans. However, previous literature studying temporal variability of T₁- and T₂ mapping in volunteers after approximately 90 days [32]

and 4D flow in 10 volunteers with a difference of one year between scans [33] reported no significant differences or significant agreement of results, indicating that myocardial function in healthy volunteers should be stable over a certain time period up to 1 year. Furthermore, the volunteers were also scanned at different time-points during the day, allowing for short-term differences in loading conditions to possibly affect strain results. Nevertheless, we only observed minor changes in volunteer characteristics, vital parameters and CMR-parameters, so we assume that myocardial function was stable in our group of volunteers during the course of the study.

The good to excellent test-retest reproducibility of averaged scans before and after the break and between single scans observed in our group of volunteers, regardless of MRI scanner used, matches the excellent test-retest reproducibility Giusca et al. reported in fSENC scans of eleven healthy subjects and seven patients with heart failure repeated 63 days apart [2]. These results also suggest that effects of short-term differences in myocardial function relating to loading conditions, stroke volume and heart frequency are minimal in volunteers. Furthermore, the very good to excellent intra- and inter-observer reproducibility we reported agrees with previous studies investigating fSENC [2, 15] as well.

When comparing CMR techniques to measure strain, obstacles preventing broad clinical use are centered around the long acquisition and post-processing time, especially concerning myocardial tagging [15, 34]. Due to the fast image acquisition without the need for breath-holds, fSENC could be a potential alternative to tagging. Strain measurements using fSENC have already been shown to be valuable to detect hypertrophic cardiomyopathy when EF is preserved [35], right-ventricular dysfunction due to pulmonary hypertension [36] and diastolic dysfunction in patients with type II diabetes mellitus [37]. Furthermore, fSENC reliably identifies myocardial regions affected by coronary artery disease and infarction [38] and reliably estimates LV-volumes and EF in patients with coronary artery disease, as shown by a recent study from our group [39].

Clinical implications

Our results suggest that an average bias of 0.01% to 1.88% strain (< 1.24% for GLS and < 1.88% for GCS) should be taken into account when comparing fSENC results of healthy individuals acquired using different scanners. This implies that a strain difference of below 2% on average may represent normal variability in the measurement and not necessarily a decrease or increase in myocardial function, if scanning is performed using different scanners. The limits of agreement indicate that strain results from different scanners should not be used totally interchangeably. Larger studies

are needed for further validation in order to facilitate the planning and comparison of multi-center studies, which are needed for standardization of strain measurements and to determine inter-vendor agreement in patients. Furthermore, technical differences between different scanners and imaging sequences should be assessed.

Limitations

Our study group is composed of a relatively small sample size of healthy young volunteers, in order to eliminate the influence of pathologies on strain measurements. Hence, it is important to conduct further studies to assess inter-vendor agreement in a larger study cohort and in patients. Furthermore, in-vitro scanning was performed using different phantoms, at different sites than where the volunteers were scanned and with different number of repeats per site. Unfortunately, multiple scans at site II had to be excluded from further strain analysis due to technical complications that similarly occur in the clinical routine, such as a defect optical fiber cable (preventing one volunteer from being scanned) and a malfunctioning body coil, resulting in artifacts during four GLS and five GCS scans. Additionally, we only focused on fSENC in this study and did not include conventional tagging, the gold standard for strain measurements, since fSENC had previously been validated against tagging [15]. Similarly, we did not evaluate other techniques for measuring strain. Nevertheless, it would be interesting to examine the impact of different MRI scanners on other CMR techniques used to determine strain, including tagging.

Conclusion

We found good inter-vendor agreement of strain measurements acquired with the fSENC technique at 3 T using MRI scanners from three major vendors with small biases, but considerable limits of agreement and a significant difference in strain results. Test-retest reproducibility between repeated scans was very high, regardless of the scanner chosen. Moreover, reproducibility of strain measurements was good to excellent, independent of the employed MR-platform. fSENC can be considered a reliable technique and suitable for strain measurements at different centers and, with further development, has the potential to improve diagnostics and therapy in heart failure patients. Our results might help to interpret strain assessed by fSENC at different sites using MRI scanners from different vendors.

Acknowledgements Open Access funding provided by Projekt DEAL. We thank Corinna Else (RN), Monica Post (study nurse), Madeleine Solesch (RN), Petra Götz (RN), Denise Kleindienst (RN) and Kerstin Kretschel (RN) for the support regarding the planning of the study and

the scanning of the volunteers. We also want to thank people from the different vendors supporting the realization of the study at the various sites, namely Christian Stehning, PhD; Bernhard Schnackenburg, PhD; Martin Janich, PhD; Birgit Anders, PhD; Eman Ali, PhD; Erik Penner, PhD; Christian Geppert, PhD and Joachim Graessner.

Compliance with ethical standards

Conflict of interest SK and AP received funding and software support from Myocardial Solutions and Philips Healthcare. OS received research grants from Myocardial Solutions and Siemens. SK is on the Advisory Board of Myocardial Solutions and received an unrestricted research grant from Philips Healthcare and Siemens. SK, JSM and BP received support from the DZHK (German Center for Cardiovascular Research), Partner Site Berlin. The German Heart Institute Berlin is supported by Foundation German Heart Institute Berlin.

Open Access This article is licensed under a Creative Commons Attribution 4.0 International License, which permits use, sharing, adaptation, distribution and reproduction in any medium or format, as long as you give appropriate credit to the original author(s) and the source, provide a link to the Creative Commons licence, and indicate if changes were made. The images or other third party material in this article are included in the article's Creative Commons licence, unless indicated otherwise in a credit line to the material. If material is not included in the article's Creative Commons licence and your intended use is not permitted by statutory regulation or exceeds the permitted use, you will need to obtain permission directly from the copyright holder. To view a copy of this licence, visit <http://creativecommons.org/licenses/by/4.0/>.


References

1. Syeda B, Höfer P, Pichler P et al (2011) Two-dimensional speckle-tracking strain echocardiography in long-term heart transplant patients: a study comparing deformation parameters and ejection fraction derived from echocardiography and multislice computed tomography. *Eur J Echocardiogr* 12(7):490–496
2. Giusca S, Korosoglou G, Zieschang V et al (2018) Reproducibility study on myocardial strain assessment using fast-SENC cardiac magnetic resonance imaging. *Sci Rep* 8(1):14100
3. Onishi T, Saha SK, Delgado-Montero A et al (2015) Global longitudinal strain and global circumferential strain by speckle-tracking echocardiography and feature-tracking cardiac magnetic resonance imaging: comparison with left ventricular ejection fraction. *J Am Soc Echocardiogr* 28(5):587–596
4. Kraigher-Krainer E, Shah AM, Gupta DK et al (2014) Impaired systolic function by strain imaging in heart failure with preserved ejection fraction. *J Am Coll Cardiol* 63(5):447–456
5. Plana JC, Galderisi M, Barac A et al (2014) Expert consensus for multimodality imaging evaluation of adult patients during and after cancer therapy: a report from the American Society of Echocardiography and the European Association of Cardiovascular Imaging. *Eur Heart J Cardiovasc Imaging* 15(10):1063–1093
6. Voigt JU, Pedrizzetti G, Lysyansky P et al (2015) Definitions for a common standard for 2D speckle tracking echocardiography: consensus document of the EACVI/ASE/Industry Task Force to standardize deformation imaging. *Eur Heart J Cardiovasc Imaging* 16(1):1–11
7. Farsalinos KE, Daraban AM, Ünlü S, Thomas JD, Badano LP, Voigt JU (2015) Head-to-head comparison of global longitudinal strain measurements among nine different vendors: the EACVI/ASE inter-vendor comparison study. *J Am Soc Echocardiogr* 28(10):1171–1181 e1172
8. Collier P, Phelan D, Klein A (2017) A test in context: myocardial strain measured by speckle-tracking echocardiography. *J Am Coll Cardiol* 69(8):1043–1056
9. Lang RM, Badano LP, Mor-Avi V et al (2015) Recommendations for cardiac chamber quantification by echocardiography in adults: an update from the American Society of Echocardiography and the European Association of Cardiovascular Imaging. *Eur Heart J Cardiovasc Imaging* 16(3):233–270
10. Salerno M, Sharif B, Arheden H et al (2017) Recent advances in cardiovascular magnetic resonance: techniques and applications. *Circ Cardiovasc Imaging* 10(6):e0003951
11. Scatteia A, Baritussio A, Bucciarelli-Ducci C (2017) Strain imaging using cardiac magnetic resonance. *Heart Fail Rev* 22(4):465–476
12. Mangion K, McComb C, Auger DA, Epstein FH, Berry C (2017) Magnetic resonance imaging of myocardial strain after acute ST-segment-elevation myocardial infarction: a systematic review. *Circ Cardiovasc Imaging* 10(8):e006498
13. Osman NF, Sampath S, Atalar E, Prince JL (2001) Imaging longitudinal cardiac strain on short-axis images using strain-encoded MRI. *Magn Reson Med* 46(2):324–334
14. Pan L, Stuber M, Kraitchman DL, Fritzges DL, Gilson WD, Osman NF (2006) Real-time imaging of regional myocardial function using fast-SENC. *Magn Reson Med* 55(2):386–395
15. Korosoglou G, Youssef AA, Bilchick KC et al (2008) Real-time fast strain-encoded magnetic resonance imaging to evaluate regional myocardial function at 3.0 Tesla: comparison to conventional tagging. *J Magn Reson Imaging* 27(5):1012–1018
16. Dill T (2008) Contraindications to magnetic resonance imaging: non-invasive imaging. *Heart* 94(7):943–948
17. Mitchell MD, Kundel HL, Axel L, Joseph PM (1986) Agarose as a tissue equivalent phantom material for NMR imaging. *Magn Reson Imaging* 4(3):263–266
18. Osman NF (2003) Detecting stiff masses using strain-encoded (SENC) imaging. *Magn Reson Med* 49(3):605–608
19. Liu Y, Ahmad R, Jin N, et al (2019) Strain encoding (SENC) using EPI readout. Proceedings of CMR 2018—a joint EuroCMR/SCMR meeting. Vol ID#:371903. Euro CMR/SCMR, Barcelona
20. Lapinskas T, Hireche-Chikaoui H, Zieschang V et al (2019) Effect of comprehensive initial training on the variability of left ventricular measures using fast-SENC cardiac magnetic resonance imaging. *Sci Rep* 9(1):12223
21. Cerqueira MD, Weissman NJ, Dilsizian V et al (2002) Standardized myocardial segmentation and nomenclature for tomographic imaging of the heart. A statement for healthcare professionals from the Cardiac Imaging Committee of the Council on Clinical Cardiology of the American Heart Association. *Circulation* 105(4):539–542
22. Oppo K, Leen E, Angerson WJ, Cooke TG, McArdle CS (1998) Doppler perfusion index: an interobserver and intraobserver reproducibility study. *Radiology* 208(2):453–457
23. Buss SJ, Breuninger K, Lehrke S et al (2015) Assessment of myocardial deformation with cardiac magnetic resonance strain imaging improves risk stratification in patients with dilated cardiomyopathy. *Eur Heart J Cardiovasc Imaging* 16(3):307–315
24. Oda S, Utsunomiya D, Nakaura T et al (2017) Identification and assessment of cardiac amyloidosis by myocardial strain analysis of cardiac magnetic resonance imaging. *Circ J* 81(7):1014–1021
25. Urbano-Moral JA, Gangadharamurthy D, Comenzo RL, Pandian NG, Patel AR (2015) Three-dimensional speckle tracking echocardiography in light chain cardiac amyloidosis: examination of left and right ventricular myocardial mechanics parameters. *Rev Esp Cardiol* 68(8):657–664

26. Orii M, Hirata K, Tanimoto T et al (2015) Myocardial damage detected by two-dimensional speckle-tracking echocardiography in patients with extracardiac sarcoidosis: comparison with magnetic resonance imaging. *J Am Soc Echocardiogr* 28(6):683–691
27. Schuster A, Stahnke VC, Unterberg-Buchwald C et al (2015) Cardiovascular magnetic resonance feature-tracking assessment of myocardial mechanics: intervendor agreement and considerations regarding reproducibility. *Clin Radiol* 70(9):989–998
28. Amzulescu MS, Langet H, Saloux E et al (2017) Head-to-head comparison of global and regional two-dimensional speckle tracking strain versus cardiac magnetic resonance tagging in a multicenter validation study. *Circ Cardiovasc Imaging* 10(11):e006530
29. Mirea O, Pagourelas ED, Duchenne J et al (2018) Intervendor differences in the accuracy of detecting regional functional abnormalities: a report from the EACVI-ASE strain standardization task force. *JACC Cardiovasc Imaging* 11(1):25–34
30. Badano LP, Cucchini U, Muraru D, Al Nono O, Sarais C, Iliceto S (2013) Use of three-dimensional speckle tracking to assess left ventricular myocardial mechanics: inter-vendor consistency and reproducibility of strain measurements. *Eur Heart J Cardiovasc Imaging* 14(3):285–293
31. Gayat E, Ahmad H, Weinert L, Lang RM, Mor-Avi V (2011) Reproducibility and inter-vendor variability of left ventricular deformation measurements by three-dimensional speckle-tracking echocardiography. *J Am Soc Echocardiogr* 24(8):878–885
32. Altaba MA, Nolan MT, Connelly KA, Michalowska M, Wintersperger BJ, Thavendiranathan P. Temporal Variability of Native T1 and T2 Mapping in Healthy Volunteers 2018:Suppl_1. Located at: Circulation, Circulation.
33. Lorenz R, Bock J, Barker AJ et al (2014) 4D flow magnetic resonance imaging in bicuspid aortic valve disease demonstrates altered distribution of aortic blood flow helicity. *Magn Reson Med* 71(4):1542–1553
34. Ibrahim E-S (2011) Myocardial tagging by cardiovascular magnetic resonance: evolution of techniques—pulse sequences, analysis algorithms, and applications. *J Cardiovasc Magn Reson* 13:36
35. Sakamoto K, Oyama-Manabe N, Manabe O et al (2018) Heterogeneity of longitudinal and circumferential contraction in relation to late gadolinium enhancement in hypertrophic cardiomyopathy patients with preserved left ventricular ejection fraction. *Jpn J Radiol* 36(2):103–112
36. Freed BH, Tsang W, Bhawe NM et al (2015) Right ventricular strain in pulmonary arterial hypertension: a 2D echocardiography and cardiac magnetic resonance study. *Echocardiography* 32(2):257–263
37. Korosoglou G, Humpert PM, Ahrens J et al (2012) Left ventricular diastolic function in type 2 diabetes mellitus is associated with myocardial triglyceride content but not with impaired myocardial perfusion reserve. *J Magn Reson Imaging* 35(4):804–811
38. Korosoglou G, Lossnitzer D, Schellberg D et al (2009) Strain-encoded cardiac MRI as an adjunct for dobutamine stress testing: incremental value to conventional wall motion analysis. *Circ Cardiovasc Imaging* 2(2):132–140
39. Lapinskas T, Zieschang V, Erley J et al (2019) Strain-encoded cardiac magnetic resonance imaging: a new approach for fast estimation of left ventricular function. *BMC Cardiovasc Disord* 19(1):52

Publisher's Note Springer Nature remains neutral with regard to jurisdictional claims in published maps and institutional affiliations.

Affiliations

Jennifer Erley¹  · Victoria Zieschang¹ · Tomas Lapinskas^{1,2} · Aylin Demir³ · Stephanie Wiesemann³ · Markus Haass⁴ · Nael F Osman^{5,6} · Orlando P Simonetti⁷ · Yingmin Liu⁸ · Amit R Patel⁹ · Victor Mor-Avi⁹ · Orhan Unal¹⁰ · Kevin M Johnson¹⁰ · Burkert Pieske^{1,11,12} · Jochen Hansmann¹³ · Jeanette Schulz-Menger^{3,12} · Sebastian Kelle^{1,11,12}

Jennifer Erley
Jennifer.erley@charite.de

Victoria Zieschang
zieschang@dhzb.de

Tomas Lapinskas
tomas.lapinskas@lsmuni.lt

Aylin Demir
aylin.demir@charite.de

Stephanie Wiesemann
stephanie.wiesemann@charite.de

Markus Haass
M.Haass@theresienkrankenhaus.de

Nael F Osman
nael.osman@myocardialsolutions.com

Orlando P Simonetti
Orlando.Simonetti@osumc.edu

Yingmin Liu
Yingmin.Liu@osumc.edu

Amit R Patel
apatel2@medicine.bsd.uchicago.edu

Victor Mor-Avi
vmoravi@medicine.bsd.uchicago.edu

Orhan Unal
unal@wisc.edu

Kevin M Johnson
kmjohnson3@wisc.edu

Burkert Pieske
pieske@dhzb.de

Jochen Hansmann
J.Hansmann@theresienkrankenhaus.de

Jeanette Schulz-Menger
Jeanette.schulz-menger@charite.de

¹ Department of Internal Medicine/Cardiology, German Heart Institute Berlin, Augustenburger Platz 1, 13353 Berlin, Germany

² Department of Cardiology, Medical Academy, Lithuanian University of Health Sciences, Kaunas, Lithuania

³ Working Group Cardiovascular Magnetic Resonance, Experimental and Clinical Research Center, Max-Delbrueck Center for Molecular Medicine, Department of Cardiology

- and Nephrology, Charité Medical Faculty, HELIOS
Klinikum Berlin Buch, Berlin, Germany
- ⁴ Department of Internal Medicine/Cardiology/Angiology,
Theresienkrankenhaus Und St. Hedwig-Klinik, Mannheim,
Germany
- ⁵ Department of Radiology and Radiological Science, School
of Medicine, John Hopkins University, Baltimore, MD, USA
- ⁶ Myocardial Solutions, Inc, Morrisville, NC, USA
- ⁷ Departments of Internal Medicine and Radiology, The Ohio
State University, Columbus, OH, USA
- ⁸ Dorothy M. Davis Heart and Lung Research Institute,
Wexner Medical Center, The Ohio State University,
Columbus, OH, USA
- ⁹ Department of Cardiology, University of Chicago Medicine,
Chicago, IL, USA
- ¹⁰ Departments of Radiology and Medical Physics, University
of Wisconsin-Madison, Madison, WI, USA
- ¹¹ Department of Internal Medicine/Cardiology, Charité
Campus Virchow Klinikum, Berlin, Germany
- ¹² DZHK (German Center for Cardiovascular Research),
Partner Site Berlin, Berlin, Germany
- ¹³ Department of Radiology, Theresienkrankenhaus Und
St. Hedwig-Klinik, Mannheim, Germany

RESEARCH

Open Access



Echocardiography and cardiovascular magnetic resonance based evaluation of myocardial strain and relationship with late gadolinium enhancement

Jennifer Erley¹, Davide Genovese^{2,3}, Natalie Tapaskar², Nazia Alvi^{2,7}, Nina Rashedi², Stephanie A. Besser², Keigo Kawaji^{2,4}, Neha Goyal², Sebastian Kelle^{1,5,6}, Roberto M. Lang², Victor Mor-Avi² and Amit R. Patel^{2*}

Abstract

Objectives: We sought to: (1) determine the agreement in cardiovascular magnetic resonance (CMR) and speckle tracking echocardiography (STE) derived strain measurements, (2) compare their reproducibility, (3) determine which approach is best related to CMR late gadolinium enhancement (LGE).

Background: While STE-derived strain is routinely used to assess left ventricular (LV) function, CMR strain measurements are not yet standardized. Strain can be measured using dedicated pulse sequences (strain-encoding, SENC), or post-processing of cine images (feature tracking, FT). It is unclear whether these measurements are interchangeable, and whether strain can be used as an alternative to LGE.

Methods: Fifty patients underwent 2D echocardiography and 1.5 T CMR. Global longitudinal strain (GLS) was measured by STE (Epsilon), FT (NeoSoft) and SENC (Myocardial Solutions) and circumferential strain (GCS) by FT and SENC.

Results: GLS showed good inter-modality agreement (r -values: 0.71–0.75), small biases (< 1%) but considerable limits of agreement (– 7 to 8%). The agreement between the CMR techniques was better for GLS than GCS ($r = 0.81$ vs 0.67; smaller bias). Repeated measurements showed low intra- and inter-observer variability for both GLS and GCS (intraclass correlations 0.86–0.99; coefficients of variation 3–13%). LGE was present in 22 (44%) of patients. Both SENC- and FT-derived GLS and GCS were associated with LGE, while STE-GLS was not. Irrespective of CMR technique, this association was stronger for GCS (AUC 0.77–0.78) than GLS (AUC 0.67–0.72) and STE-GLS (AUC = 0.58).

Conclusion: There is good inter-technique agreement in strain measurements, which were highly reproducible, irrespective of modality or analysis technique. GCS may better reflect the presence of underlying LGE than GLS.

Keywords: Cardiac imaging, Left ventricular function, Myocardial deformation, Myocardial scar

* Correspondence: apatel2@medicine.bsd.uchicago.edu;
amitpatel@uchicago.edu

²Department of Medicine, University of Chicago Medical Center, 5758 S. Maryland Avenue, MC9067, Chicago, IL 60637, USA

Full list of author information is available at the end of the article



© The Author(s). 2019 **Open Access** This article is distributed under the terms of the Creative Commons Attribution 4.0 International License (<http://creativecommons.org/licenses/by/4.0/>), which permits unrestricted use, distribution, and reproduction in any medium, provided you give appropriate credit to the original author(s) and the source, provide a link to the Creative Commons license, and indicate if changes were made. The Creative Commons Public Domain Dedication waiver (<http://creativecommons.org/publicdomain/zero/1.0/>) applies to the data made available in this article, unless otherwise stated.

Introduction

Despite the important role left ventricular (LV) ejection fraction (EF) plays in clinical practice, it is influenced by heart rate and loading conditions. Given these limitations, there has been a considerable interest in myocardial strain as an alternative measure of myocardial performance. Depending on fiber direction in the different myocardial layers, longitudinal, circumferential and radial strain can be differentially impacted [1]. Studies have shown that myocardial strain is less dependent on loading conditions than EF [2, 3], and, as a result, better reflects subtle changes in the underlying myocardial substrate [4, 5]. Strain measurements using speckle tracking echocardiography (STE) have been widely reported, including evidence that strain is a better predictor of outcomes than EF [6]. Due to superior reproducibility of strain [7–9], it is recommended for clinical use to detect chemotherapy-related cardiotoxicity [10] and to evaluate cardiac involvement in infiltrative diseases, such as amyloidosis or sarcoidosis [11]. Several recent studies suggested STE strain as a potential surrogate for cardiovascular magnetic resonance (CMR) late gadolinium enhancement (LGE) imaging [9, 12], the current reference standard for detection of scar and infiltrative disease. This would be useful in cases where CMR is not available, gadolinium contrast is contraindicated, or in patients at greater risk of adverse long term events, such as children and pregnant women.

As CMR becomes more widely utilized, the need to incorporate strain assessment into the CMR exam is being increasingly recognized. Although several CMR techniques to assess strain have been recently described, this methodology is still not fully developed. One technique analyzes strain from cine-CMR images using feature tracking (FT) algorithms, similar to STE. FT-derived strain has been shown to detect ischemia during dobutamine stimulation [13] and to independently predict outcomes in patients with dilated cardiomyopathy [14]. Newer CMR techniques include dedicated pulse sequences that create images with strain information encoded into a color display to facilitate visual assessment of abnormalities. Although this strain-encoding (SENC) requires additional imaging, it does not significantly prolong the exam [15], and has higher spatial and temporal resolution even than myocardial tagging, the current reference standard for strain [16–18]. The ability of SENC to detect myocardial infarction and define its transmural extent has been reported [1, 17]. While echocardiographic studies showed that global longitudinal strain (GLS) is superior to global circumferential strain (GCS) in its ability to detect subtle myocardial abnormalities due to better reproducibility [11, 19], this has not been confirmed for CMR-derived strain.

Despite the growing number of strain related studies in the literature, the methodology of CMR strain has not been standardized, and it is not known to what extent these measurements are interchangeable with each other and with STE. Also, the reproducibility of these techniques is not well established. Furthermore, it is not clear whether the relationship of strain measurements (by either STE or CMR) with LGE is strong enough for strain to be considered as a surrogate. Finally, the differences between the strain components in this context are not well established. Accordingly, we sought to: 1) determine the inter-technique agreement between STE, FT and SENC strain measurements, 2) compare their reproducibility, and 3) determine which modality and technique shows the strongest association with LGE.

Methods

Study population and design

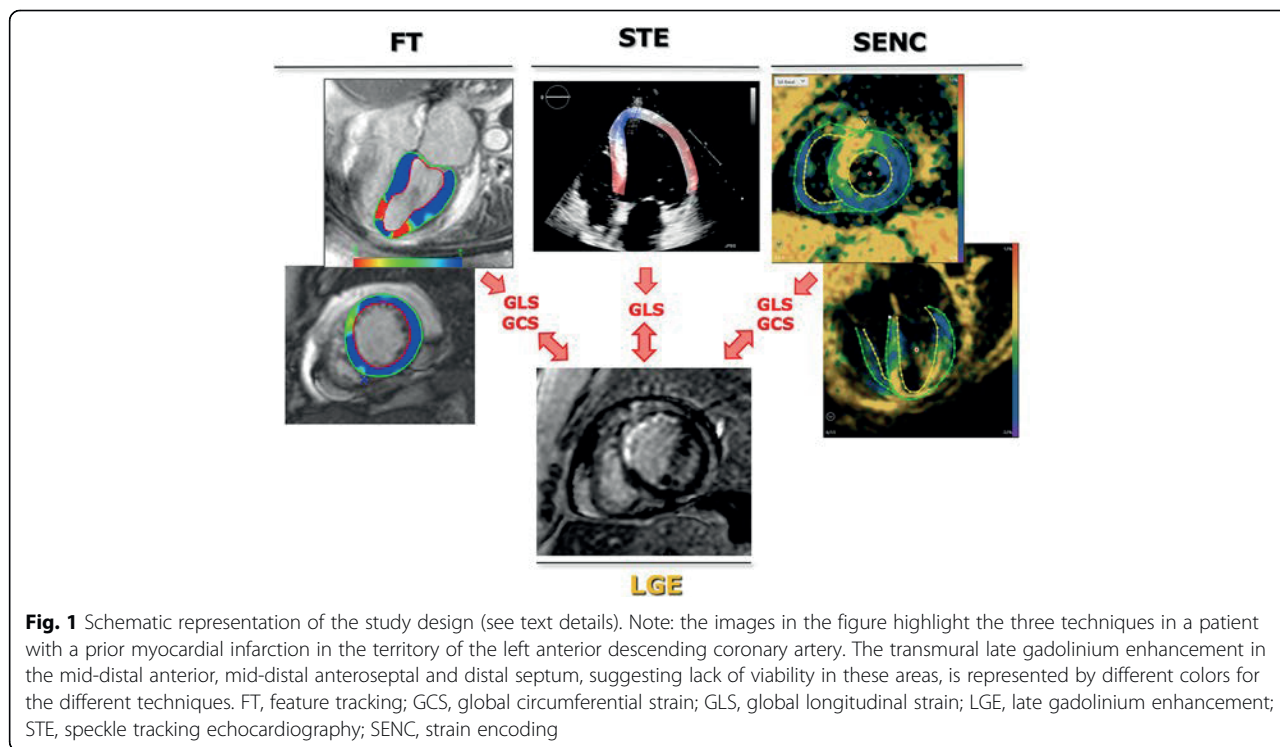
We retrospectively studied 50 patients who underwent CMR imaging (including SENC and LGE) and transthoracic 2D echocardiography at the University of Chicago, Chicago, Illinois, USA over a one-year period. Patients under 18 years of age and those who underwent a cardiac intervention between the two imaging tests were excluded. No patients were excluded on the basis of image quality of either modality. The Institutional Review Board approved this retrospective study with a waiver of consent.

Figure 1 schematically depicts the study design. The above three techniques were used to measure strain: feature tracking (FT) and strain encoding (SENC) images were analyzed to obtain both global longitudinal strain (GLS) and global circumferential strain (GCS), while speckle tracking echocardiography (STE) was used to obtain GLS. These measurements were compared between them and also correlated with presence of LGE.

Echocardiographic imaging and analysis

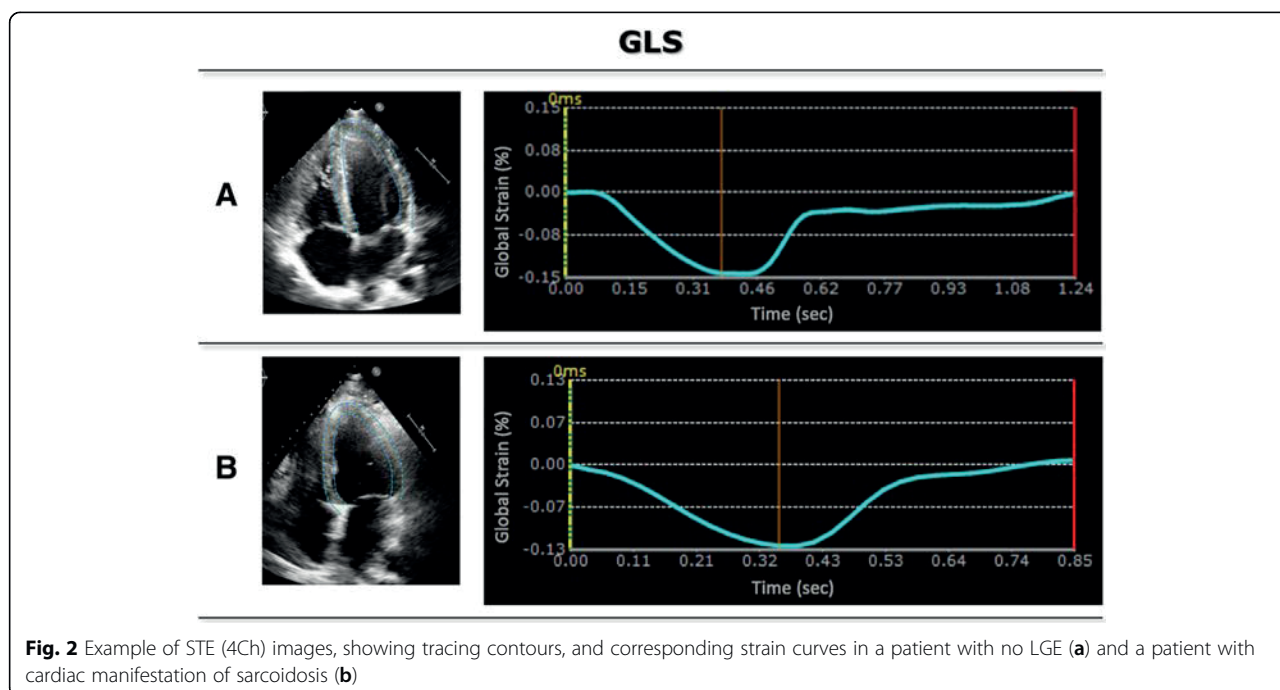
Transthoracic echocardiographic imaging was performed using the iE33 system with the X5–1 probe (Philips Healthcare, Best, the Netherlands). Apical long-axis, LV-focused two-, three- and four-chamber (2Ch, 3Ch and 4Ch) views were acquired, after optimizing the sector size, gain, depth, compress and time-gain compensation. Frame rate was maximized (73 ± 20 fps) by increasing the depth and decreasing the sector width.

The images were stored digitally and measured offline according to the guidelines [20] by an experienced reader, blinded to clinical data and all prior strain measurements and LGE findings. End-diastole (ED) was identified as the frame coinciding with the peak of the QRS complex, whereas end-systole (ES) was identified as the frame with the smallest LV cavity. LV GLS analysis was performed on the three long-axis views using vendor independent speckle-tracking software (Echo



Insight, Epsilon Imaging, Ann Arbor, Michigan, USA). This software is based on tracking ultrasound speckles frame-by-frame in order to quantify myocardial deformation. It has been previously validated by comparisons against other established techniques used to measure myocardial strain [3, 4, 7].

Specifically, for each view, strain analysis was performed by manually tracing at ED the region of interest along the endocardial border from the mitral valve annulus to the LV apex and back to the annulus (Fig. 2a). The software then automatically tracked the endocardial contours throughout the cardiac cycle. Manual adjustments were



made to the contours as needed to optimize tracking. All views were segmented according to the American Heart Association (AHA) guidelines and segmental strain was calculated automatically throughout the cardiac cycle. GLS was calculated throughout the cardiac cycle, resulting in a time-strain curve for each view (Fig. 2). Peak GLS values were averaged for the three views, resulting in a unique GLS value for each patient.

Cine CMR imaging and feature tracking analysis

CMR images were acquired on a 1.5 T scanner using a 5-channel surface coil (Achieva, Philips Healthcare). Retrospectively gated cine images were acquired using a balanced steady-state free precession pulse sequence in the standard long-axis views (2Ch, 3Ch, 4Ch) and short-axis slices (6 mm thickness, 4 mm gap), covering the LV from base to apex. Scanning parameter were: TR = 2.9 ms, TE = 1.5 ms, flip angle 60°, temporal resolution 30-40 ms.

FT was performed offline by an experienced observer, blinded to all prior strain measurements and LGE findings, using vendor independent software (SuiteHEART, Neosoft, Pewaukee, Wisconsin, USA). Similar to echocardiographic speckle tracking, the FT algorithm identifies image features in the myocardium that are consistently identifiable throughout the cardiac cycle, and tracks them frame-by-frame to quantify myocardial deformation. This is achieved by the following five steps:

(1) deformation models are created based on b-splines using contours and images; (2) position images are created by calculating how much each pixel within the myocardium is displaced over the cardiac cycle; (3) strain tensor is calculated; (4) tensor image is transformed from Cartesian coordinates to the radial/cross-radial coordinates; and (5) velocity and strain rate tensors are calculated using the central difference.

The long-axis cine images were used to determine GLS and short-axis slices covering the entire heart to determine GCS. First, ED and ES were determined automatically in each view and manually corrected as needed. The tracing of the region of interest in the long-axis images was performed by an automated machine-learning based process, tracking epi- and endocardial contours from the mitral valve annulus to the apex and back to the annulus. These contours were then reviewed on every frame throughout the cardiac cycle and manually corrected as needed to optimize endocardial detection and tracking while taking care to exclude papillary muscles and endocardial trabeculae from the LV cavity (Fig. 3a). All views were segmented according to the AHA guidelines and segmental strain was calculated automatically throughout the cardiac cycle. If segments were inadequately tracked, tracing was repeated until optimal tracking was achieved. Peak systolic GLS and GCS were calculated as a mean value of all segments (Fig. 3).

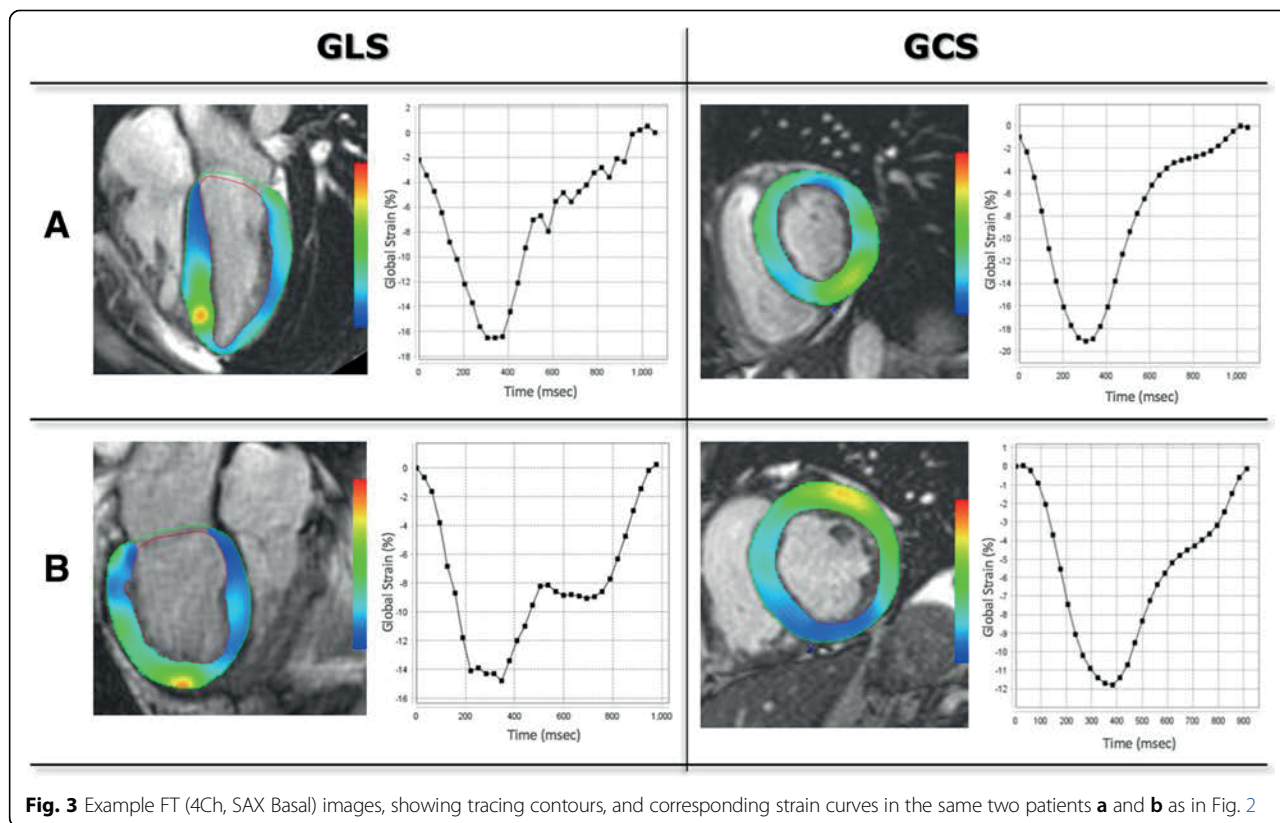


Fig. 3 Example FT (4Ch, SAX Basal) images, showing tracing contours, and corresponding strain curves in the same two patients **a** and **b** as in Fig. 2

CMR strain encoding and analysis

SENC images were acquired in three long-axis (2Ch, 3Ch, 4Ch) and three short-axis views (basal, mid, apical) with the following settings: TR = 13 ms; TE = 0.7 ms; FA = 30°; 256x256mm²; slice thickness = 10 mm; 24 ms SENC magnetization preparation prior to continuous acquisition of 40 ms (3 spiral interleaves) per temporal frame over 1 R-R cycle.

GLS was quantified using the three short-axis slices and GCS using the long-axis slices by the same observer three weeks after the analysis of the FT images to prevent bias, using vendor independent software (Myostrain 5.0, Myocardial Solutions, Morrisville, North Carolina, USA). Unlike STE and FT, SENC measures strain in the direction perpendicular to the imaging plane: circumferential from the long-axis and longitudinal from the short-axis images. Radial strain is not usually assessed using SENC. This is achieved by using specialized pulse sequences designed to measure strain and generate color-encoded strain maps superimposed on a static anatomic image of the heart [18].

ED and end-systole (ES) were selected manually in all slices according to the size of the myocardial cavity and the color-coding of the images, representing the state of contraction (blue = contracting- yellow = relaxing). Epi- and endocardial contours were drawn manually at ES, again using the mitral valve annulus and apex as landmarks in

the long-axis views and excluding the papillary muscles and trabeculae from the LV cavity (Fig. 4). GLS and GCS were automatically calculated for each view and then averaged. No segments were excluded from analysis.

Late gadolinium enhancement

LGE images were acquired in the same long-axis planes as the cine images and also in the short-axis slices covering the entire LV, 5–10 min after the infusion of gadolinium contrast (OmniscanTM or MultiHance TM, 0.05–0.1 mmol/kg, injected at 4 ml/s, IV), using a T1-weighted gradient echo pulse sequence with a phase sensitive inversion recovery reconstruction (TR = 4.5 ms; TE = 2.2 ms; TI = 250–300 ms, flip angle 30°, flip angle 5°, voxel size = 2x2x10 mm, SENSE factor = 1–2, no gaps). An inversion time scout sequence was used to select an inversion time between 200 and 300 ms for optimal nulling of normal myocardium. The presence of LGE was qualitatively evaluated by a clinical expert (Level II or III certified [21]) blinded to all strain results, but with access to patients’ clinical data, to identify areas of hyper-enhancement in the myocardium consistent with either post-infarct scar or cardiac involvement in infiltrative disease [22].

Reproducibility analysis

In a subset of 10 randomly selected patients, measurements were repeated by the same observer, two weeks

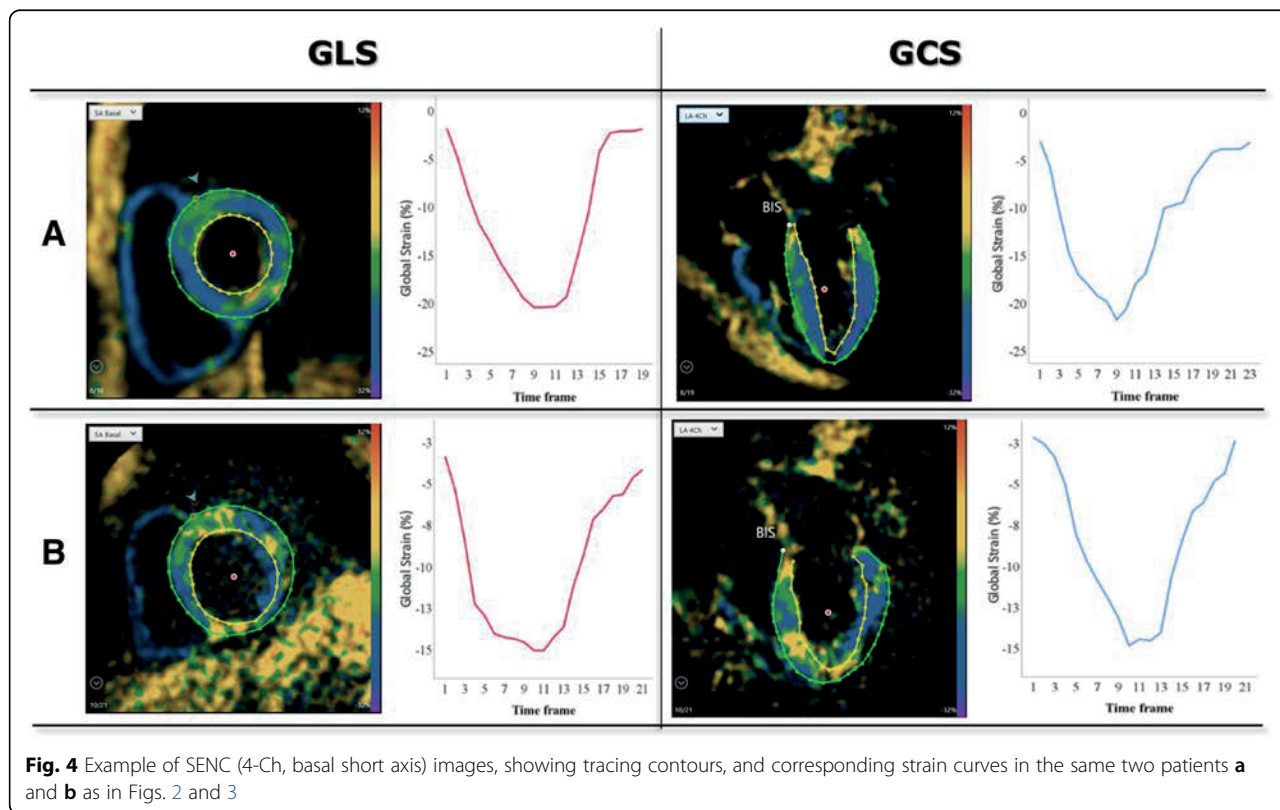


Fig. 4 Example of SENC (4-Ch, basal short axis) images, showing tracing contours, and corresponding strain curves in the same two patients **a** and **b** as in Figs. 2 and 3

after the first analysis (to prevent recall bias) and by a second independent observer for every modality and technique, all blinded to prior measurements and LGE findings.

Statistical analysis

All values were assessed for normality using the Shapiro-Wilk test. Normally distributed data is expressed as mean \pm SD, non-normally distributed data using median and interquartile range (IQR). Linear regression and Bland-Altman analyses were used to determine inter-technique agreement between STE, FT and SENC for GLS and between FT and SENC for GCS. Intra- and inter-observer variability was expressed in terms of intraclass correlations (ICC) and coefficients of variation (CoV). Receiver operating characteristics (ROC) - curves were generated to establish the relationship of each strain parameter (STE-GLS, FT-GLS, FT-GCS, SENC-GLS, SENC-GCS) to the presence of LGE and the area under curve (AUC) was calculated. A Mann-Whitney test was conducted to determine if strain values measured using each technique, differed significantly between the patient groups with and without LGE. Binary logistic regression analyses were performed to determine the associations between strain measurements and the presence of LGE, which was expressed in terms of odds ratios (OR). A *p*-value of ≤ 0.05 was considered significant in two-tailed tests. Variables that were significantly associated with LGE presence were checked for collinearity by Spearman rank correlations and entered into separate multivariate logistic regression models for each technique to avoid overfitting and identify strain parameters that were independently associated with LGE. Statistical analyses were conducted using SPSS (Version 25.0, Statistical Package for the Social Sciences (SSPS), International Business Machines, Inc., Armonk, New York, USA).

Results

The patient cohort included 15 patients with ischemic heart disease, 33 patients with non-ischemic heart disease and two patients with clinical indications for CMR but no cardiac diagnosis. The average time between echocardiogram and CMR-exam was 8.5 ± 9.8 days, with 35 patients (68.6%) scanned within the same week, and the remaining 15 patients with 30 days. Strain was evaluable using all techniques in 44/50 (88%) patients. In four patients, echocardiographic GLS could not be measured for technical reasons related to image transfer, in one patient FT-GLS and in another patient SENC-GLS could not be determined due to insufficient image quality. Table 1 shows the baseline characteristics, as well as CMR and echocardiographic measurements. Analysis time ranged from 3 to 5 min for STE, 8–44 min for FT (majority of time needed for GLS measurement), and 4–

Table 1 Baseline Characteristics of the Patient Population (*n* = 50)

Age (years)	51 \pm 9
Female, <i>n</i> (%)	26 (52%)
Median (IQR) BSA (m ²)	1.91 (1.71–2.06)
Ischemic heart disease, <i>n</i> (%)	15 (30%)
Non-ischemic heart disease, <i>n</i> (%)	33 (66%)
No cardiac diagnosis, <i>n</i> (%)	2 (4%)
LVEF (from CMR) (%)	56 (38–61)
Median (IQR) LVEDV Index (ml/m ²)	87 (69–113)
Median (IQR) LVESV Index (ml/m ²)	37 (30–56)
Average LV Mass Index (g/m ²)	61.16 \pm 24.95
LGE present, <i>n</i> (%)	22 (44%)
Median (IQR) GLS for Echo (<i>n</i> = 46)	–15.8 (–18.9 to –12.1)
Median (IQR) GLS for FT (<i>n</i> = 50)	–15.4 (–18.4 to –10.6)
Median (IQR) GLS for SENC (<i>n</i> = 50)	–14.9 (–19.3 to –11.1)
Median (IQR) GCS for FT (<i>n</i> = 50)	–14.3 (–18.3 to –11.1)
Median (IQR) GCS for SENC (<i>n</i> = 50)	–13.7 (–15.5 to –10.8)

Abbreviations: BSA Body surface area, LVEF left ventricular ejection fraction, LVEDV, LVESV left ventricular end diastolic/end systolic volume, LGE late gadolinium enhancement, GLS global longitudinal strain

7 min for SENC. Both GLS and GCS values were similar among the techniques used.

Figures 2, 3, 4 and 5 show examples of STE, FT, SENC and LGE analyses of two patients: one patient with no cardiac diagnosis (Figs. 2a, 3a, 4a and 5a) and another with a cardiac manifestation of sarcoidosis (Figs. 2b, 3b, 4b and 5b). Compared to the former case (Figs. 2a, 3a and 4a), the sarcoidosis patient had a peak GLS/GCS magnitude that was lower, as depicted by the strain curves obtained by all 3 imaging modalities/techniques (Figs. 2b, 3b and 4b). Figure 5 shows the corresponding LGE images of these two patients, depicting diffuse, patchy enhancement in most myocardial segments in the sarcoidosis patient (Fig. 5b), while the ventricle of the other patient (Fig. 5a) appears uniformly unenhanced.

Inter-technique agreement

Table 2 summarizes the results of inter-technique agreement, including linear regression and Bland-Altman analysis. GLS measurements showed high levels of inter-modality agreement, reflected by good correlations: *r*-values of 0.71 and 0.75 between STE and FT and SENC, respectively. The biases were small (all $< 1\%$ in strain units, corresponding to approximately 5% of the mean measured value; NS) with limits of agreement of -7 to 8% in strain units (corresponding to approximately 30–40% of the mean measured value), reflecting good inter-technique agreement but possible discordance in some individual patients. The agreement between the CMR techniques (FT and SENC) was better for GLS than GCS (*r* = 0.81 vs 0.67) and a smaller bias (-0.2 vs 1.0%).

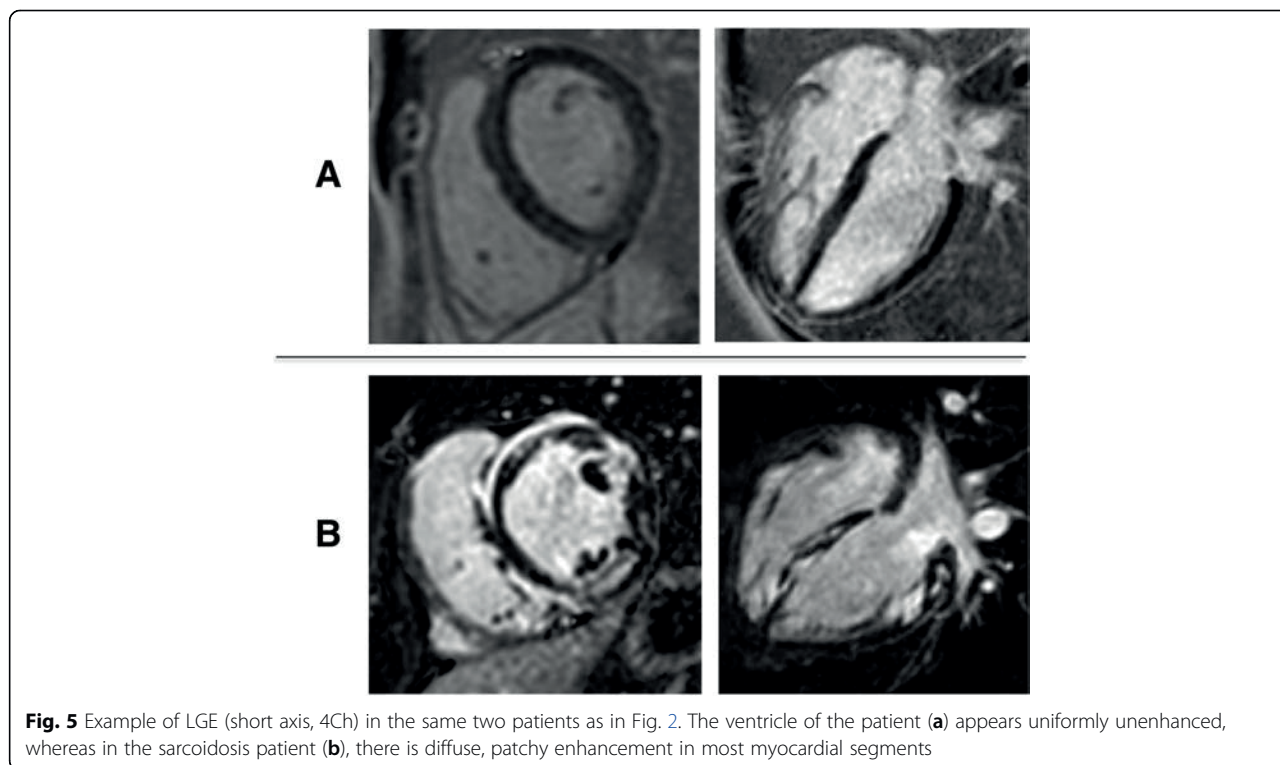


Fig. 5 Example of LGE (short axis, 4Ch) in the same two patients as in Fig. 2. The ventricle of the patient (a) appears uniformly unenhanced, whereas in the sarcoidosis patient (b), there is diffuse, patchy enhancement in most myocardial segments

Reproducibility analysis

Intra- and inter-observer variability, for both GLS and GCS, was very low for all modalities and techniques tested, reflecting excellent reliability based on ICC values of 0.86–0.99 and CoV 3–13% (Table 3). Regarding both modalities and techniques, intra- and inter-observer variability for GLS measurements were the lowest for SENC, represented by the highest ICC and the lowest CoV values. Concerning CMR-derived GCS, the intra-observer variability between FT and SENC was similar, while the inter-observer variability was lower for FT.

Association between strain and LGE

LGE was present in 22 (44%) patients. In 9/22 (41%) patients, LGE pattern was consistent with prior myocardial infarction, in 13/22 (59%) patients, LGE pattern suggested an underlying fibrosing, infiltrative (e.g. cardiac

amyloidosis) or inflammatory process (e.g. myocarditis), recognized by the location (not matching with vessel territories) and pattern (diffuse, patchy) of LGE.

Table 4 and Fig. 6 summarize median strain values of patients with and without LGE and the results of the Mann-Whitney test. Table 5 displays the results of the ROC-analysis and the logistic regression. There was a significant difference in strain between patients with and without LGE when measured using FT or SENC, but not with STE. Both SENC- and FT-derived GLS and GCS were significantly associated with LGE, while STE GLS was not. Irrespective of CMR-technique, the association with LGE was stronger for GCS than for GLS and STE GLS. Interestingly, CMR-derived GCS showed

Table 2 Results of the linear- regression and Bland-Altman analyses to determine inter-technique agreement between the different modalities and techniques

	r	p	Bias (%)	LOA (%)	p
LV-GLS					
Echo vs. FT	0.71	< 0.001	0.9	-5.8 to 7.6	0.07
Echo vs. SENC	0.75	< 0.001	0.6	-5.9 to 7.2	0.21
FT vs. SENC	0.81	< 0.001	-0.2	-6.6 to 6.3	0.72
LV-GCS					
FT vs. SENC	0.67	< 0.001	1.0	-5.8 to 7.8	0.05

Table 3 Results of the Reproducibility Analysis

			ICC	CoV
Intra-Observer Variability	GLS	STE	0.94	0.07 ± 0.05
		FT	0.89	0.13 ± 0.12
	SENC	0.99	0.04 ± 0.02	
		GCS	0.98	0.03 ± 0.03
Inter-Observer Variability	GLS	STE	0.91	0.07 ± 0.08
		FT	0.86	0.11 ± 0.19
	SENC	0.99	0.03 ± 0.03	
		GCS	0.99	0.03 ± 0.03
		SENC	0.94	0.08 ± 0.04

Table 4 Median strain values, measured using each technique, in patients without and with LGE and results of the Mann-Whitney test

	Patients without LGE	Patient group with LGE	p
Echo - GLS	-16.0 (-19.1 to -12.7)	-15.6 (-17.9 to -11.6)	0.212
FT - GLS	-17.3 (-18.8 to -13.1)	-12.5 (15.7 to -10.0)	0.003
FT - GCS	-17.8 (-19.1 to -13.5)	-12.0 (-14.3 to -9.10)	<0.001
SENC - GLS	-17.3 (-20.2 to -14.0)	-13.5 (-14.9 to -10.2)	0.010
SENC - GCS	-14.8 (-17.5 to -12.9)	-12.4 (-13.8 to -8.90)	<0.001

Data presented as median (interquartile range)

higher odds ratios than GLS, with SENC-derived GCS having the highest OR value. The two separate multivariate logistic regression models accounting for GLS and GCS derived by FT and SENC (Table 6) showed that GCS from either technique was a significant independent factor associated with presence of LGE over GLS.

Discussion

Echocardiography is typically the first imaging modality used to assess LV function in clinical routine, due to its low cost and widespread availability. In recent years, GLS using STE has been increasingly considered as an important parameter beyond the conventional measure of EF. An important step to make STE-derived GLS part of the clinical routine was the recent publication of a consensus document to standardize strain measurements [20]. Although several CMR-based strain measurement techniques have been described, this methodology has yet to be widely adopted into the clinical realm, and there is no consensus on what the optimal approach is. Similar to echocardiographic strain

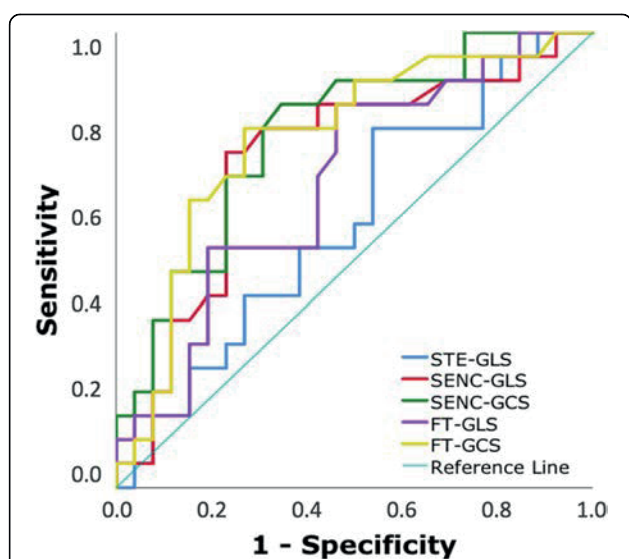


Fig. 6 Receiver operating characteristic (ROC)- curves depicting the relationship between strain parameters and the presence of LGE

Table 5 Results of ROC analysis and the univariate logistic regression analysis, demonstrating the association between strain measurements and LGE

	ROC analysis			Univariate logistic regression		
	AUC	95% CI	p	OR	95% CI	p
Echo - GLS	0.58	0.42-0.75	0.346	1.09	0.95-1.24	0.213
FT - GLS	0.67	0.52-0.83	0.048	1.19	1.04-1.36	0.013
FT - GCS	0.77	0.62-0.91	0.003	1.30	1.11-1.53	0.001
SENC - GLS	0.72	0.57-0.88	0.011	1.18	1.04-1.34	0.010
SENC - GCS	0.78	0.64-0.91	0.002	1.41	1.14-1.74	0.002

measurements, CMR strain also needs standardization prior to widespread clinical use.

Our study was designed as a step in this direction by comparing strain measurements obtained using the different modalities and techniques. In our study group: 1) on the average, there was a good inter-modality agreement between GLS from STE and CMR (both FT and SENC) and the agreement between CMR techniques was better for GLS than GCS; 2) in all comparisons, the limits of agreement were rather wide, indicating possible discordance in individual patients, 3) strain analyses, irrespective of modality or technique, were highly reproducible; and 4) STE-GLS was not significantly associated with LGE, whereas CMR-derived strain was, and the relationship was stronger for GCS than for GLS.

The good inter-modality agreement between GLS measured using CMR- and STE-derived strain is in line with most previous studies [23-26], although there is no consensus on this, as poor correlations have also been described [27]. Of note, previous authors have reported limits of agreement for both modalities and techniques that were similar or wider than in our study, indicating that inter-technique differences may be considerable in individual patients [23, 25, 26]. We also observed inter-technique agreement being higher for GLS than for GCS. One factor that may be affecting inter-modality and inter-technique agreement is the variability in strain measurements between vendors, even when using the same technique [28-31]. Also, intrinsic methodological

Table 6 Results of the multivariate logistic regression analysis for FT (Model 1)- and SENC (Model 2)-derived GLS and GCS, showing the strength of the association between strain measurements and LGE

	OR	95% CI	p
Model 1			
FT - GLS	0.95	0.75-1.22	0.696
FT - GCS	1.35	1.01-1.81	0.041
Model 2			
SENC - GLS	1.02	0.86-1.22	0.828
SENC - GCS	1.38	1.04-1.82	0.025

differences may be an additional contributing factor. Importantly, however, the low inter- and intra-observer variability found in our study for both modalities and techniques, is similar to previous studies [17, 23, 26, 27, 32, 33], confirming that myocardial strain derived by both STE and CMR-techniques is highly reproducible. From a clinical perspective, the high reproducibility implies that strain techniques may be particularly valuable in the follow-up of the course of a patient's disease. Nevertheless, it would be important to adhere to the same technique and to refrain from using different modalities interchangeably. Although no variation in clinical characteristics of the patients were noted between the two exams, we could not rule out changes in strain related to different loading conditions during the CMR and echocardiographic imaging, which were not performed on the same day.

In our study group, CMR-derived strain was significantly and independently associated with LGE, whereas STE-GLS was not. This relationship was stronger for GCS than for GLS. To our knowledge, this is the first study to establish the association between strain parameters and LGE for more than two modalities or techniques in the same patient cohort. Although echocardiography and CMR examinations were not performed on the same day, it is unlikely that differences in loading conditions alone could explain why CMR-derived strain was more closely associated with presence of scar than echocardiographic strain, because scar is not load dependent and was most likely consistently present during both examinations.

Moreover, our study group was composed of patients with heart disease of ischemic and non-ischemic etiology, unlike previous studies that focused on one specific diagnosis. Siegel et al. compared STE and FT in patients with Duchenne muscular dystrophy, and reported that, similar to our observation, FT was able to demonstrate presence of LGE, whereas STE was not [33]. However, their study used a small number of patients with a rare diagnosis. Altiok et al. only investigated GCS by STE and SENC in a group of patients with ischemic heart disease and concluded that both modalities were significantly associated with LGE [12]. Several previous studies of STE-GLS reported an association with LGE [11, 34, 35], which is contrary to our findings. This is probably due to the differences in patient populations (e.g. percentage of patients with LGE of ischemic origin) and the potential underlying differences in the prevalence, severity and specific patterns of strain abnormalities, as well as differences in measurement methodologies used.

When comparing the relationship with LGE for the CMR-techniques, we found that they performed similarly and that the relationship with LGE was stronger for

GCS than for GLS, irrespective of the technique. Previous studies that investigated the association of CMR-derived strain with LGE in patients with acute ischemic heart disease also reported superior association for GCS compared to GLS when using both SENC [1, 17] and FT [14]. Up to this point, only a limited number of studies with small patient cohorts focused on either non-ischemic heart diseases [36–38] or chronic infarctions [17, 39]. Further studies are needed to investigate the differences in strain behavior and the association between strain and LGE in different patient populations.

Clinical implications

Our results show that abnormal GCS measured by CMR-derived techniques indicates that LGE may be present. This may be clinically important when contrast use is problematic. Therefore, CMR may be useful in patients with suspected scar or other forms of myocardial damage, even when LGE imaging cannot be performed. Additionally, larger prospective studies to validate our results, and standardization of CMR-derived strain techniques are needed in order to facilitate the integration of this approach into clinical routine.

Limitations

This is a retrospective study with the intrinsic limitations of no fully standardized protocol of image acquisition, resulting in variable image quality that may have affected strain measurements. Also, this was a single-center study with a relatively small sample size, which requires further validation for the conclusions to be generalized. One of the consequences of the small sample size was that it did not allow us to include more than two variables in the multivariate logistic regression analysis. Also, it would be interesting to compare patients with ischemic heart disease (focal LGE) and those with non-ischemic etiology (diffuse LGE). However, our retrospective study was designed to include all patients who underwent CMR with SENC and echocardiography (within a month of each other) over a 1-year period, resulting in a total of 50 studies suitable for analysis. Unfortunately, the number of patients in each of the above two categories was too small to allow statistically meaningful comparisons.

Because segmental strain is not a commonly used parameter due to inferior reproducibility and inter-technique agreement compared to global strain [40, 41], we focused only on global strain, which does not provide information on the location of scar. Moreover, this aspect of our study was motivated by the fact that our study included comparisons between two different CMR techniques used in the same setting and same imaging planes against echocardiography, which is a completely independent imaging modality. Because spatial

registration between modalities is a well-known problem, we felt that segmental comparisons would be unfairly stacked against echocardiography because potential segment misalignment would affect these comparisons more than comparisons of global strain. Furthermore, intra-modality comparisons between SENC and FT would not be feasible in all patients because images of the scar may not have been acquired in both the long- and short-axis planes, which are utilized differently by the two CMR techniques. Nevertheless, it would be valuable to conduct analysis of regional strain in order to determine whether strain can reliably detect the location of scar, rather than its presence alone. In addition, the relationship between quantitative burden of LGE and strain was outside the scope of our study, which was designed to primarily investigate the inter-technique agreement and reproducibility of strain measurements.

Additionally, we did not include CMR-tagging in our study, although it is the current reference standard for strain measurements. Our study did not include tagging because various studies have already reported FT and SENC to be accurate compared to this reference [17, 42, 43], although the FT algorithm we used has not yet been evaluated on a large scale and may differ from the algorithms implemented in other software packages. We also did not investigate displacement encoding with stimulated echo (DENSE) strain imaging, although it would be interesting to include this modality as well, because there is no consensus in the literature regarding the level of inter-technique agreement between FT, SENC, and DENSE [41, 42].

Conclusion

We found good inter-technique agreement in strain measurements between STE and CMR techniques and among CMR techniques, with small biases but considerable limits of agreement, indicating possible discordance in individual patients. Importantly, all strain measurements were highly reproducible, irrespective of modality or analysis technique. When measured by any technique, CMR-GCS was the strain parameter most related with LGE in our cohort and may potentially be considered as a surrogate for LGE when contrast administration is contraindicated.

Abbreviations

AHA: American Heart Association; AUC: Area under the curve; CMR: Cardiovascular magnetic resonance; DENSE: Displacement encoding with stimulated echoes; ED: End-diastole; EF: Ejection fraction; ES: End-systole; FT: Feature tracking; GCS: Global circumferential strain; GLS: Global longitudinal strain; LGE: Late gadolinium enhancement; LV: Left ventricle/left ventricular; OR: Odds ratio; ROC: Receiver operator curve; SENC: Strain encoding; STE: Speckle tracking echocardiography

Acknowledgements

Not applicable.

Authors' contributions

JE: analyzed images, drafted the manuscript, DG: acquired data, analyzed images, critically reviewed the manuscript, NT: acquired data, analyzed images, critically reviewed the manuscript, NA: acquired data, analyzed images, critically reviewed the manuscript, SAB: performed statistical analysis, KK: coordinated imaging and analysis software installation and use, critically reviewed the manuscript, NG: acquired data, analyzed images, critically reviewed the manuscript, SK: concept development and critical review of the manuscript, RML: concept development and critical review of the manuscript, VMA: concept development and drafting the manuscript, ARP: all aspects of study. All authors read and approved the final manuscript.

Funding

No direct funding was received for this study; however, investigators have received research support (either funding or software support) for other studies from Myocardial Solutions (JE, SK, KK, ARP), Philips (KK, ARP, RML, SK), Neosoft (AP), and Epsilon (RML). SK is on the Advisory Board for Myocardial Solutions.

Availability of data and materials

Data supporting the results reported in the manuscript can be found in a computer workstation in the Cardiac Imaging Laboratory at the University of Chicago.

Ethics approval and consent to participate

The study was approved by the Institutional Review Board of the University of Chicago with a waiver of consent.

Consent for publication

Not applicable.

Competing interests

The authors declare that they have no competing interests.

Author details

¹Department of Internal Medicine / Cardiology, German Heart Center, Berlin, Germany. ²Department of Medicine, University of Chicago Medical Center, 5758 S. Maryland Avenue, MC9067, Chicago, IL 60637, USA. ³Department of Cardiac, Thoracic and Vascular Sciences, University of Padua, Padua, Italy. ⁴Department of Biomedical Engineering, Illinois Institute of Technology, Chicago, IL, USA. ⁵Department of Internal Medicine/Cardiology, Charité Campus Virchow Klinikum, Berlin, Germany. ⁶DZHK (German Center for Cardiovascular Research), Partner Site Berlin, Berlin, Germany. ⁷Department of Cardiology, Riverside Medical Center, Kankakee, IL, USA.

Received: 4 January 2019 Accepted: 1 July 2019

Published online: 08 August 2019

References


- Oyama-Manabe N, Ishimori N, Sugimori H, et al. Identification and further differentiation of subendocardial and transmural myocardial infarction by fast strain-encoded (SENC) magnetic resonance imaging at 3.0 tesla. *Eur Radiol.* 2011;21(11):2362–8.
- Knappe D, Pouleur AC, Shah AM, et al. Dyssynchrony, contractile function, and response to cardiac resynchronization therapy. *Circ Heart Fail.* 2011;4(4):433–40.
- Smedsrud MK, Pettersen E, Gjesdal O, et al. Detection of left ventricular dysfunction by global longitudinal systolic strain in patients with chronic aortic regurgitation. *J Am Soc Echocardiogr.* 2011;24(11):1253–9.
- Syeda B, Höfer P, Pichler P, et al. Two-dimensional speckle-tracking strain echocardiography in long-term heart transplant patients: a study comparing deformation parameters and ejection fraction derived from echocardiography and multislice computed tomography. *Eur J Echocardiogr.* 2011;12(7):490–6.
- Kutty S, Rangamani S, Venkataraman J, et al. Reduced global longitudinal and radial strain with normal left ventricular ejection fraction late after effective repair of aortic coarctation: a CMR feature tracking study. *Int J Cardiovasc Imaging.* 2013;29(1):141–50.
- Medvedofsky D, Maffessanti F, Weinert L, et al. 2D and 3D echocardiography-derived indices of left ventricular function and shape: relationship with mortality. *JACC Cardiovasc Imaging.* 2018;11:1569–79.

7. Sjøli B, Ørn S, Grenne B, et al. Comparison of left ventricular ejection fraction and left ventricular global strain as determinants of infarct size in patients with acute myocardial infarction. *J Am Soc Echocardiogr*. 2009;22(11):1232–8.
8. Giusca S, Korosoglou G, Zieschang V, et al. Reproducibility study on myocardial strain assessment using fast-SENC cardiac magnetic resonance imaging. *Sci Rep*. 2018;8(1):14100.
9. Altiok E, Neizel M, Tiemann S, et al. Layer-specific analysis of myocardial deformation for assessment of infarct transmural: comparison of strain-encoded cardiovascular magnetic resonance with 2D speckle tracking echocardiography. *Eur Heart J Cardiovasc Imaging*. 2013;14(6):570–8.
10. Plana JC, Galderisi M, Barac A, et al. Expert consensus for multimodality imaging evaluation of adult patients during and after cancer therapy: a report from the American Society of Echocardiography and the European Association of Cardiovascular Imaging. *J Am Soc Echocardiogr*. 2014;27(9):911–39.
11. Murtagh G, Laffin LJ, Patel KV, et al. Improved detection of myocardial damage in sarcoidosis using longitudinal strain in patients with preserved left ventricular ejection fraction. *Echocardiography*. 2016;33(9):1344–52.
12. Altiok E, Tiemann S, Becker M, et al. Myocardial deformation imaging by two-dimensional speckle-tracking echocardiography for prediction of global and segmental functional changes after acute myocardial infarction: a comparison with late gadolinium enhancement cardiac magnetic resonance. *J Am Soc Echocardiogr*. 2014;27(3):249–57.
13. Schneeweis C, Qiu J, Schnackenburg B, et al. Value of additional strain analysis with feature tracking in dobutamine stress cardiovascular magnetic resonance for detecting coronary artery disease. *J Cardiovasc Magn Reson*. 2014;16:72.
14. Buss SJ, Breuninger K, Lehrke S, et al. Assessment of myocardial deformation with cardiac magnetic resonance strain imaging improves risk stratification in patients with dilated cardiomyopathy. *Eur Heart J Cardiovasc Imaging*. 2015;16(3):307–15.
15. Korosoglou G, Lossnitzer D, Schellberg D, et al. Strain-encoded cardiac MRI as an adjunct for dobutamine stress testing: incremental value to conventional wall motion analysis. *Circ Cardiovasc Imaging*. 2009;2(2):132–40.
16. Youssef A, Ibrahim e-S, Korosoglou G, Abraham MR, Weiss RG, Osman NF. Strain-encoding cardiovascular magnetic resonance for assessment of right-ventricular regional function. *J Cardiovasc Magn Reson*. 2008;10:33.
17. Neizel M, Lossnitzer D, Korosoglou G, et al. Strain-encoded MRI for evaluation of left ventricular function and transmural in acute myocardial infarction. *Circ Cardiovasc Imaging*. 2009;2(2):116–22.
18. Osman NF, Sampath S, Atalar E, Prince JL. Imaging longitudinal cardiac strain on short-axis images using strain-encoded MRI. *Magn Reson Med*. 2001;46(2):324–34.
19. Kalam K, Otahal P, Marwick TH. Prognostic implications of global LV dysfunction: a systematic review and meta-analysis of global longitudinal strain and ejection fraction. *Heart*. 2014;100(21):1673–80.
20. Voigt JU, Pedrizzetti G, Lysyansky P, et al. Definitions for a common standard for 2D speckle tracking echocardiography: consensus document of the EACVI/ASE/industry task force to standardize deformation imaging. *Eur Heart J Cardiovasc Imaging*. 2015;16(1):1–11.
21. Kim RJ, Simonetti OP, Westwood M, et al. Guidelines for training in cardiovascular magnetic resonance (CMR). *J Cardiovasc Magn Reson*. 2018; 20(1):57.
22. Doesch C, Huck S, Böhm CK, et al. Visual estimation of the extent of myocardial hyperenhancement on late gadolinium-enhanced CMR in patients with hypertrophic cardiomyopathy. *Magn Reson Imaging*. 2010;28(6):812–9.
23. Obokata M, Nagata Y, Wu VC, et al. Direct comparison of cardiac magnetic resonance feature tracking and 2D/3D echocardiography speckle tracking for evaluation of global left ventricular strain. *Eur Heart J Cardiovasc Imaging*. 2016;17(5):525–32.
24. Onishi T, Saha SK, Delgado-Montero A, et al. Global longitudinal strain and global circumferential strain by speckle-tracking echocardiography and feature-tracking cardiac magnetic resonance imaging: comparison with left ventricular ejection fraction. *J Am Soc Echocardiogr*. 2015;28(5):587–96.
25. Lamacie MM, Thavendiranathan P, Hanneman K, et al. Quantification of global myocardial function by cine MRI deformable registration-based analysis: comparison with MR feature tracking and speckle-tracking echocardiography. *Eur Radiol*. 2017;27(4):1404–15.
26. Aurich M, Keller M, Greiner S, et al. Left ventricular mechanics assessed by two-dimensional echocardiography and cardiac magnetic resonance imaging: comparison of high-resolution speckle tracking and feature tracking. *Eur Heart J Cardiovasc Imaging*. 2016;17(12):1370–8.
27. Wang J, Li W, Sun J, et al. Improved segmental myocardial strain reproducibility using deformable registration algorithms compared with feature tracking cardiac MRI and speckle tracking echocardiography. *J Magn Reson Imaging*. 2018;48(2):404–14.
28. Badano LP, Cucchini U, Muraru D, Al Nono O, Sarais C, Iliceto S. Use of three-dimensional speckle tracking to assess left ventricular myocardial mechanics: inter-vendor consistency and reproducibility of strain measurements. *Eur Heart J Cardiovasc Imaging*. 2013;14(3):285–93.
29. Risum N, Ali S, Olsen NT, et al. Variability of global left ventricular deformation analysis using vendor dependent and independent two-dimensional speckle-tracking software in adults. *J Am Soc Echocardiogr*. 2012;25(11):1195–203.
30. Gayat E, Ahmad H, Weinert L, Lang RM, Mor-Avi V. Reproducibility and inter-vendor variability of left ventricular deformation measurements by three-dimensional speckle-tracking echocardiography. *J Am Soc Echocardiogr*. 2011;24(8):878–85.
31. Cao JJ, Ngai N, Duncanson L, Cheng J, Gliganic K, Chen Q. A comparison of both DENSE and feature tracking techniques with tagging for the cardiovascular magnetic resonance assessment of myocardial strain. *J Cardiovasc Magn Reson*. 2018;20(1):26.
32. Altiok E, Neizel M, Tiemann S, et al. Quantitative analysis of endocardial and epicardial left ventricular myocardial deformation-comparison of strain-encoded cardiac magnetic resonance imaging with two-dimensional speckle-tracking echocardiography. *J Am Soc Echocardiogr*. 2012;25(11):1179–88.
33. Siegel B, Olivieri L, Gordish-Dressman H, Spurney CF. Myocardial strain using cardiac MR feature tracking and speckle tracking echocardiography in Duchenne muscular dystrophy patients. *Pediatr Cardiol*. 2018;39(3):478–83.
34. Romano S, Judd RM, Kim RJ, et al. Feature-tracking global longitudinal strain predicts death in a multicenter population of patients with ischemic and nonischemic dilated cardiomyopathy incremental to ejection fraction and late gadolinium enhancement. *JACC Cardiovasc Imaging*. 2018;11(10):1419–29.
35. Huttin O, Marie PY, Benichou M, et al. Temporal deformation pattern in acute and late phases of ST-elevation myocardial infarction: incremental value of longitudinal post-systolic strain to assess myocardial viability. *Clin Res Cardiol*. 2016;105(10):815–26.
36. Kobayashi Y, Kobayashi H, T Giles J, et al. Detection of left ventricular regional dysfunction and myocardial abnormalities using complementary cardiac magnetic resonance imaging in patients with systemic sclerosis without cardiac symptoms: a pilot study. *Intern Med*. 2016;55(3):237–43.
37. Weigand J, Nielsen JC, Sengupta PP, Sanz J, Srivastava S, Uppu S. Feature tracking-derived peak systolic strain compared to late gadolinium enhancement in troponin-positive myocarditis: a case-control study. *Pediatr Cardiol*. 2016;37(4):696–703.
38. Sakamoto K, Oyama-Manabe N, Manabe O, et al. Heterogeneity of longitudinal and circumferential contraction in relation to late gadolinium enhancement in hypertrophic cardiomyopathy patients with preserved left ventricular ejection fraction. *Jpn J Radiol*. 2018;36(2):103–12.
39. McComb C, Carrick D, McClure JD, et al. Assessment of the relationships between myocardial contractility and infarct tissue revealed by serial magnetic resonance imaging in patients with acute myocardial infarction. *Int J Cardiovasc Imaging*. 2015;31(6):1201–9.
40. Khan JN, Singh A, Nazir SA, Kanagala P, Gershlick AH, McCann GP. Comparison of cardiovascular magnetic resonance feature tracking and tagging for the assessment of left ventricular systolic strain in acute myocardial infarction. *Eur J Radiol*. 2015;84(5):840–8.
41. Goto Y, Ishida M, Takase S, et al. Comparison of displacement encoding with stimulated echoes to magnetic resonance feature tracking for the assessment of myocardial strain in patients with acute myocardial infarction. *Am J Cardiol*. 2017;119(10):1542–7.
42. Wehner GJ, Jing L, Haggerty CM, et al. Comparison of left ventricular strains and torsion derived from feature tracking and DENSE CMR. *J Cardiovasc Magn Reson*. 2018;20(1):63.
43. Augustine D, Lewandowski AJ, Lazdam M, et al. Global and regional left ventricular myocardial deformation measures by magnetic resonance feature tracking in healthy volunteers: comparison with tagging and relevance of gender. *J Cardiovasc Magn Reson*. 2013;15:8.

Publisher's Note

Springer Nature remains neutral with regard to jurisdictional claims in published maps and institutional affiliations.

Comparison of feature tracking, fast-SENC, and myocardial tagging for global and segmental left ventricular strain

Paulius Bucius^{1,2} , Jennifer Erley¹, Radu Tanaciu¹, Victoria Zieschang¹, Sorin Giusca³, Grigorious Korosoglou³, Henning Steen⁴, Christian Stehning⁵, Burkert Pieske^{1,6,7}, Elisabeth Pieske-Kraigher^{6,7}, Andreas Schuster⁸, Tomas Lapinskas^{1,2,6} and Sebastian Kelle^{1,6,7*}

¹Department of Internal Medicine/Cardiology, German Heart Center Berlin, Berlin, Germany; ²Department of Cardiology, Medical Academy, Lithuanian University of Health Sciences, Kaunas, Lithuania; ³Department of Cardiology and Vascular Medicine, GRN Hospital Weinheim, Weinheim, Germany; ⁴Department of Internal Medicine/Cardiology, Marienkrankenhaus Hamburg, Hamburg, Germany; ⁵Philips Healthcare, Hamburg, Germany; ⁶DZHK (German Centre for Cardiovascular Research), Partner Site Berlin, Berlin, Germany; ⁷Department of Internal Medicine/Cardiology, Charité Campus Virchow Clinic, Berlin, Germany; ⁸Department of Cardiology and Pneumology, University Medical Center Göttingen, Georg-August University, Göttingen, Germany

Abstract

Aims A multitude of cardiac magnetic resonance (CMR) techniques are used for myocardial strain assessment; however, studies comparing them are limited. We sought to compare global longitudinal (GLS), circumferential (GCS), segmental longitudinal (SLS), and segmental circumferential (SCS) strain values, as well as reproducibility between CMR feature tracking (FT), tagging (TAG), and fast-strain-encoded (fast-SENC) CMR techniques.

Methods and results Eighteen subjects (11 healthy volunteers and seven patients with heart failure) underwent two CMR scans (1.5T, Philips) with identical parameters. Global and segmental strain values were measured using FT (Medis), TAG (Medviso), and fast-SENC (Myocardial Solutions). Friedman's test, linear regression, Pearson's correlation coefficient, and Bland–Altman analyses were used to assess differences and correlation in measured GLS and GCS between the techniques. Two-way mixed intra-class correlation coefficient (ICC), coefficient of variance (COV), and Bland–Altman analysis were used for reproducibility assessment.

All techniques correlated closely for GLS (Pearson's r : 0.86–0.92) and GCS (Pearson's r : 0.85–0.94). Intra-observer and inter-observer reproducibility was excellent in all techniques for both GLS (ICC 0.92–0.99, CoV 2.6–10.1%) and GCS (ICC 0.89–0.99, CoV 4.3–10.1%). Inter-study reproducibility was similar for all techniques for GLS (ICC 0.91–0.96, CoV 9.1–10.8%) and GCS (ICC 0.95–0.97, CoV 7.6–10.4%). Combined segmental intra-observer reproducibility was good in all techniques for SLS (ICC 0.914–0.953, CoV 12.35–24.73%) and SCS (ICC 0.885–0.978, CoV 10.76–19.66%). Combined inter-study SLS reproducibility was the worst in FT (ICC 0.329, CoV 42.99%), while fast-SENC performed the best (ICC 0.844, CoV 21.92%). TAG had the best reproducibility for combined inter-study SCS (ICC 0.902, CoV 19.08%), while FT performed the worst (ICC 0.766, CoV 32.35%). Bland–Altman analysis revealed considerable inter-technique biases for GLS (FT vs. fast-SENC 3.71%; FT vs. TAG 8.35%; and TAG vs. fast-SENC 4.54%) and GCS (FT vs. fast-SENC 2.15%; FT vs. TAG 6.92%; and TAG vs. fast-SENC 2.15%). Limits of agreement for GLS ranged from ± 3.1 (TAG vs. fast-SENC) to ± 4.85 (FT vs. TAG) for GLS and ± 2.98 (TAG vs. fast-SENC) to ± 5.85 (FT vs. TAG) for GCS.

Conclusions We found significant differences in measured GLS and GCS between FT, TAG, and fast-SENC. Global strain reproducibility was excellent for all techniques. Acquisition-based techniques had better reproducibility than FT for segmental strain.

Keywords Myocardial deformation; Strain; Cardiac magnetic resonance; SENC; Tagging; Feature tracking

Received: 3 July 2019; Revised: 10 October 2019; Accepted: 11 November 2019

*Correspondence to: Professor Sebastian Kelle, MD (FSCMR, FESC, FAHA), Department of Internal Medicine/Cardiology, German Heart Center Berlin and Charité University Medicine Berlin, Augustenburger Platz 1, 13353 Berlin, Germany. Tel: +49-30-4593 1182; Fax: +49-30-4593 2500. Email: kelle@dhzb.de

Introduction

Myocardial strain imaging has been shown to be useful in identification and risk stratification of a wide range of cardiac conditions.^{1,2} In certain conditions, its decline precedes that of the left ventricular ejection fraction (LVEF),^{3,4} which shows promise for it to become a supplementary tool for early diagnostics.

Since the inception of myocardial strain imaging in a form of cardiac magnetic resonance (CMR) myocardial tagging (TAG) in 1988 by Zerhouni *et al.*,⁵ it has rapidly spread inside the field of CMR. From 1990s to early 2000s, multiple acquisition-based CMR methods emerged as means to calculate myocardial deformation parameters. TAG has been extensively studied, validated, and shown to be a highly reproducible method for measurement of myocardial deformation.⁶ Despite its advantages, the usability of TAG is hampered by long acquisition and post-processing times.⁷ More recently, displacement encoding with stimulated echoes,⁸ strain-encoded CMR imaging (SENC),⁹ and fast-strain-encoded CMR imaging (fast-SENC)¹⁰ emerged as alternatives to TAG, offering faster acquisition and post-processing, as well as excellent reproducibility.^{11,12} Despite these advantages, all these techniques require acquisition of additional imaging sequences. In contrast, CMR feature tracking (FT) is a post-processing-based method that allows quantification of strain parameters from standard steady-state free precession (SSFP) cine images, clinically used for functional analysis of the heart. Given the fact that FT does not require additional imaging sequences and has a short post-processing time, it is now considered a preferred technique for myocardial deformation assessment.⁷ Each modality has its own advantages and disadvantages; however, given the acquisition and post-processing differences, variation in measured strain parameters is inevitable.

With this study, we sought to explore the differences in global left ventricular (LV) strain measurements derived using FT, fast-SENC, and TAG in a population of healthy subjects and heart failure (HF) patients. We also assessed the reproducibility and variability of the aforementioned modalities at intra-observer, inter-observer, and inter-study levels for global strain and intra-observer and inter-study levels for segmental strain.

Methods

Study population

In a period between March 2017 and September 2017, 11 healthy volunteers and seven HF patients [four with preserved LVEF (three of which with diastolic dysfunction and one with aortic stenosis) and three with reduced LVEF of

ischaemic origin] were included in the study; two CMR scans were performed on each participant, using an identical imaging protocol. Approval for the study was acquired from the Ethics Committee of Charité–Universitäts Medizin Berlin. The study complied with the declaration of Helsinki. Informed consent was given by all participants of the study.

Cardiovascular magnetic resonance acquisition

Cardiovascular magnetic resonance scans were performed on a 1.5 Tesla MRI scanner (Achieva, Philips Healthcare, Best, the Netherlands). A five-element-phased array cardiac coil was used for signal reception. Four-lead vector electrocardiogram was used for R-wave triggering. Images for FT, fast-SENC, and TAG were acquired in long-axis (LAX) 2-chamber, 3-chamber, and 4-chamber views, as well as a short-axis (SAX) stack. Balanced SSFP sequence with breath hold was used for FT analysis with the following acquisition parameters: repetition time (TR) = 3.3 ms, echo time (TE) = 1.6 ms, flip angle = 60°, acquisition voxel size = 1.8 × 1.7 × 8.0 mm³, and 30 phases per cardiac cycle. A single-breath hold, cardiac-triggered 2D TAG sequence was employed using an orthogonal saturation grid, with a grid spacing of 7 mm and a tag grid angle of 45°. Typical parameters of the subsequent imaging protocol were as follows: field of view = 340 × 340 mm², slice thickness = 8 mm, voxel size = 1.9 × 1.9 × 8 mm³, reconstructed resolution at 1.2 × 1.2 × 8 mm³, flip angle = 15°, TE = 1.8 ms, TR = 4.2 ms, temporal resolution = 55 ms, typical number of acquired heart phases = 16, and acquisition time per slice = 18 s. No parallel imaging was employed. A recently developed real-time free-breathing fast-SENC imaging technique (Myocardial Solutions, Inc., Morrisville, North Carolina, USA)¹⁰ was used for fast-SENC strain assessment. The following acquisition parameters were used: field of view = 256 × 256 mm², slice thickness 10 mm, voxel size 4 × 4 × 10 mm³, reconstructed resolution at 1 × 1 × 10 mm³ using zero-filled interpolation (in-plane ZIP 1024), single-shot spiral readout (three interleaves) with acquisition time = 10 ms, flip angle = 30°, TE = 0.7 ms, TR = 12 ms, temporal resolution = 36 ms, typical number of acquired heart phases = 22, spectrally selective fat suppression, and total acquisition time per slice <1 s.

Feature tracking analysis

Feature tracking analysis was performed offline using commercially available software (Medis Suite, version 3.1, Leiden, the Netherlands). Endocardial borders of the left ventricle were outlined in end-diastolic frame of the three LAX and three SAX (basal, mid-ventricular, and apical) images. Following an automatic propagation, adjustments were made to the contours where needed. Endocardial global longitudinal

strain (GLS) and circumferential strain (GCS) were derived by averaging the peak strain values of individual segments using 17 and 16 segment models.

Tagging analysis

Tagging-derived strain parameters were acquired using a commercially available software Segment version 2.2 R6960 (<http://segment.heiberg.se>).¹³ Endocardial and epicardial borders were outlined in end-systolic time frame of three LAX and SAX (basal, mid-ventricular, and apical) images. Automatic propagation algorithm was then applied, and necessary corrections were made by the observer. GLS and GCS parameters were derived by averaging the peak strain values of individual segments using 17 and 16 segments models.

Fast-strain-encoded cardiovascular magnetic resonance imaging analysis

Fast-SENC images were uploaded from the scanner into dedicated, commercially available MyoStrain software (Myocardial Solutions, Inc.). Endocardial and epicardial borders were outlined in three LAX and three SAX images at an end-systolic time frame. Necessary manual adjustments were made after automatic propagation by the software to ensure sufficient tracking throughout the cardiac cycle. LS values were extracted from the SAX images using a 16 segment model. Circumferential strain values were acquired from LAX images: GCS was calculated by averaging the peak strain values from a 17 segment model, while seven segments per slice (21 total segments), as provided by the software, were used for segmental comparison.

Given the counterintuitive nature of negative strain values becoming more positive in diseased subjects, absolute values of GCS and GLS are reported for easier interpretation of the results.

Intra-observer and inter-observer reproducibility

Every scan was analysed by two experienced raters in each modality for inter-observer variability testing. In order to determine the intra-observer variability, 10 randomly selected cases were analysed a second time by one of the observers after a minimum period of 4 weeks to ensure there was no recall bias. All observers were blinded to prior investigations and clinical data of the subjects.

Inter-study reproducibility

A second CMR scan with identical imaging parameters was performed in all of the individuals. Median time between

the two scans was 40 days. There was no change in medication or symptoms of the HF patients in between the scans. Additionally, we excluded new onset of cardiac disease in the healthy subjects. In order to prevent recall bias, the second scan was analysed after a minimum of 4 weeks by one of the observers, who was blinded to the results of the first scan and clinical data of the subjects.

Segmental comparison

Intra-observer and inter-study comparison was also performed on segmental basis for both segmental longitudinal (SLS) and segmental circumferential strain (SCS). Each technique was assessed by comparing the results of the first and the second measurement in individual segments first and then by pooling the data of all the segments to get a combined value.

Statistical analysis

Commercially available statistical analysis software (GraphPad Prism 8, GraphPad Software, San Diego, CA, USA) was used for statistical analysis. Continuous variables are expressed as either mean \pm standard deviation or median \pm interquartile range, according to normality of distribution, assessed by Shapiro–Wilk test. Strain measurements from three modalities were compared using Friedman’s test with Dunn’s post hoc test for pair-wise comparison. Linear regression analysis was used to assess the correlation between the imaging modalities, followed by Bland–Altman analysis of the mean bias and limits of agreement (LOA). Inter-observer and intra-observer, as well as inter-study variability, were assessed using the intra-class correlation coefficient (ICC) for absolute agreement and coefficient of variance (CoV), defined as standard deviation of the differences divided by the mean.¹⁴ Agreement levels were defined according to previous studies¹⁵: excellent for ICC > 0.74 , good for ICC $0.6–0.74$, fair for ICC $0.4–0.59$, and poor for ICC < 0.4 . Segmental intra-observer and inter-study variability and agreement was assessed using ICC and CoV. Alpha level of 0.05 and below was considered statistically significant.

Results

Global longitudinal strain

Global longitudinal strain measured by FT showed a trend towards being higher than that measured by fast-SENC (P value = 0.05), while fast-SENC-derived GLS was significantly higher than TAG (*Figure 1* and *Table 1*). Excellent correlation was observed between the three modalities.

Figure 1 Comparison of GLS (A) and GCS (B) measured using three CMR modalities. Results of Friedman's test with Dunn's post hoc analysis: ns— $P \geq 0.05$, *— $P < 0.05$, ***— $P < 0.001$. FT, feature tracking; GCS, global circumferential strain; GLS, global longitudinal strain; SENC, strain-encoded magnetic resonance imaging; TAG, myocardial tagging.

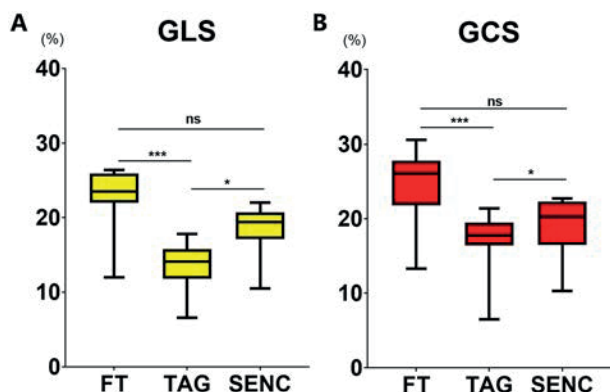


Table 1 Global strain values derived from different cardiovascular magnetic resonance techniques

	FT	TAG	SENC
GLS (%)	23.5 (22.0–25.9)	14.9 (11.8–16.9)	19.4 (17.1–20.7)
GCS (%)	26.1 (21.8–27.8)	17.8 (16.4–19.5)	20.3 (16.5–22.3)

Values are expressed as median (interquartile range). FT, feature tracking; GCS, global circumferential strain; GLS, global longitudinal strain; SENC, fast-strain-encoded cardiovascular magnetic resonance; TAG, myocardial tagging.

FT and fast-SENC had the closest correlation ($r = 0.924$, $P < 0.001$). Linear regression analyses and Bland–Altman comparisons for GLS are depicted in Figure 2. Visual

representation of differences in measured GLS between the techniques is depicted in Figure 3.

Global circumferential strain

Global circumferential strain measured by FT showed a trend towards being greater than fast-SENC ($P = 0.05$), while TAG-derived GCS was significantly lower than fast-SENC (Figure 1 and Table 1). All three modalities correlated closely with each other. TAG and fast-SENC had the closest correlation ($r = 0.938$, $P < 0.001$) and narrowest LOA (± 3.1), as depicted in Figure 4. Visual representation of differences in measured GLS between the techniques is depicted in Figure 5.

Feasibility

Feature tracking and fast-SENC analysis were successful in every scan, giving a feasibility of 100%. TAG analysis was not possible in 5/36 scans due to breathing artefacts, thus it was the method with the worst feasibility –86.1%. Direct comparison between all modalities was possible in 31 cases, and 36 cases were used for FT and fast-SENC comparison.

Intra-observer and inter-observer reproducibility

Intra-observer and inter-observer variability results are depicted in Table 2. Fast-SENC showed the least variability and highest reproducibility, followed by TAG and FT, respectively.

Figure 2 Linear regression and Bland–Altman analyses for global longitudinal strain comparison between FT vs. TAG, FT vs. FAST-SENC, and FAST-SENC vs. TAG. FT, feature tracking; SENC, strain-encoded magnetic resonance imaging; TAG, myocardial tagging.

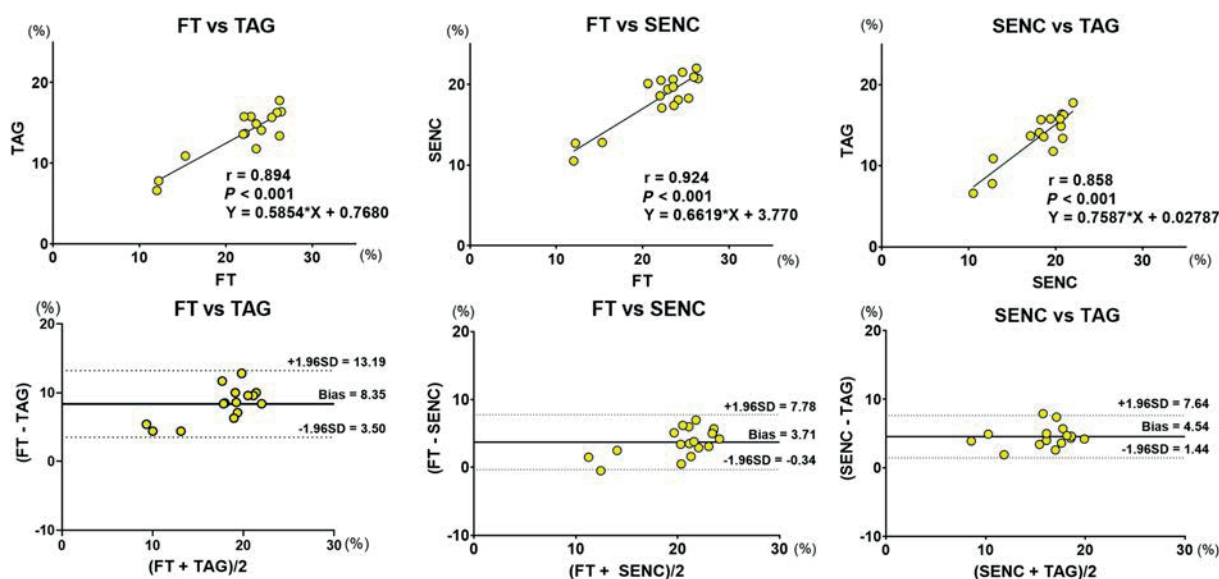
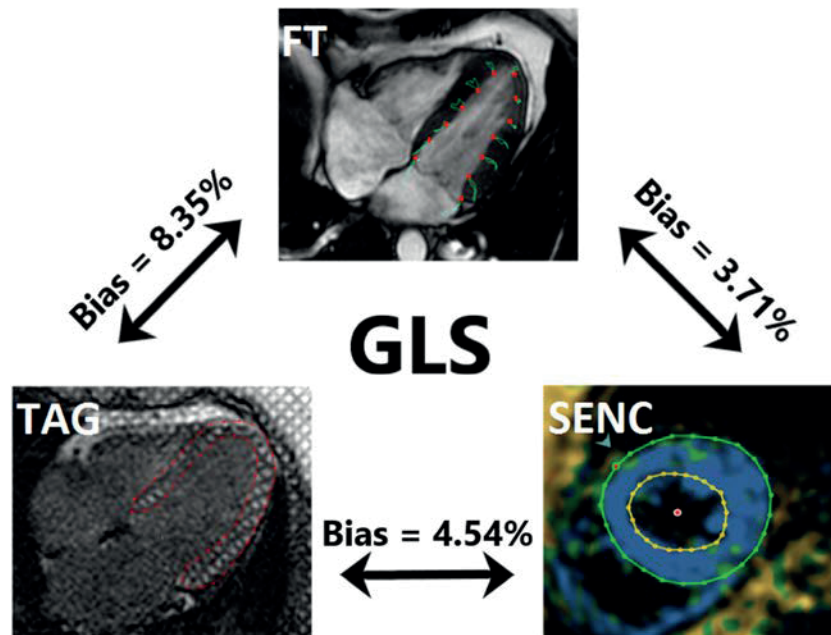


Figure 3 Visual representation of GLS assessment with the three different cardiovascular magnetic resonance techniques. TAG on the left, SENC on the right, and FT on the top picture. Mean difference (bias) between techniques, derived from Bland–Altman analyses, is shown. FT, feature tracking; GLS, global longitudinal strain; SENC, strain-encoded magnetic resonance imaging; TAG, myocardial tagging.



Inter-study reproducibility

We found excellent inter-study reproducibility in all of the techniques, as shown by measured ICCs (GLS: for FT = 0.91, $P < 0.001$; for TAG = 0.96, $P < 0.001$; and for fast-SENC = 0.94, $P < 0.001$; GCS: for FT = 0.97, $P < 0.001$; for TAG = 0.95, $P < 0.001$; and for fast-SENC = 0.96, $P <$

0.001). LOA, CoV, and inter-study biases are depicted in *Table 2*.

Segmental reproducibility

Values of combined segmental strain reproducibility comparison are depicted in *Table 3*, and values for individual

Figure 4 Linear regression and Bland–Altman analyses for global circumferential strain comparison between FT vs. TAG, FT vs. fast-SENC, and fast-SENC vs. TAG. FT, feature tracking; SENC, strain-encoded magnetic resonance imaging; TAG, myocardial tagging.

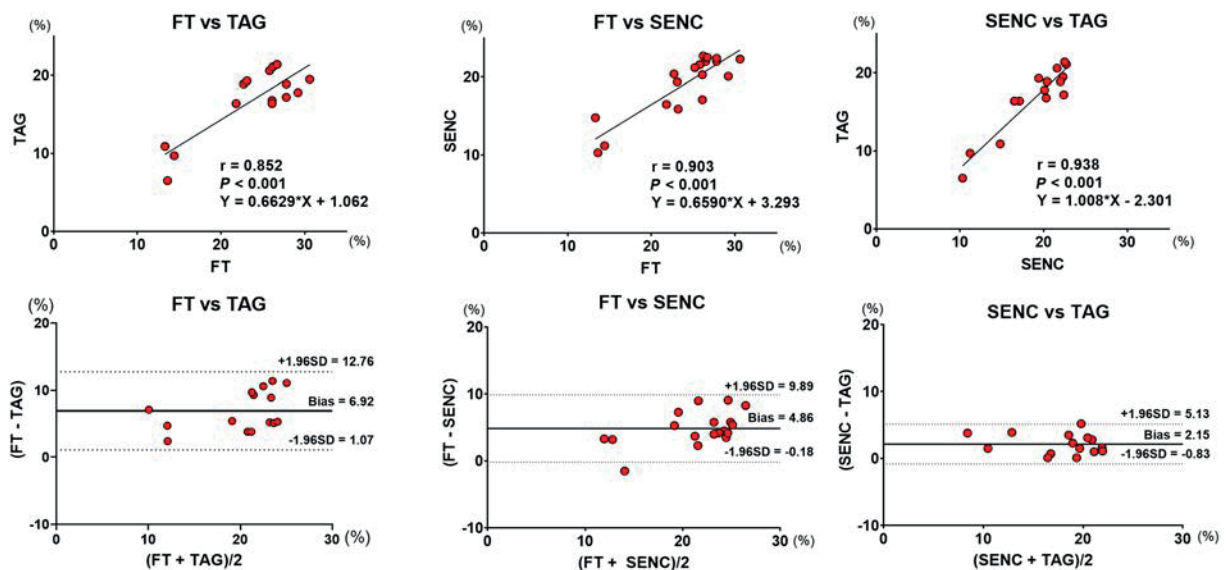


Figure 5 Visual representation of global longitudinal strain assessment with the three different cardiovascular magnetic resonance techniques. TAG on the left, SENC on the right, and FT on the top picture. Mean difference (bias) between techniques, derived from Bland–Altman analyses, is shown. FT, feature tracking; GCS, global circumferential strain; SENC, strain-encoded magnetic resonance imaging; TAG, myocardial tagging.

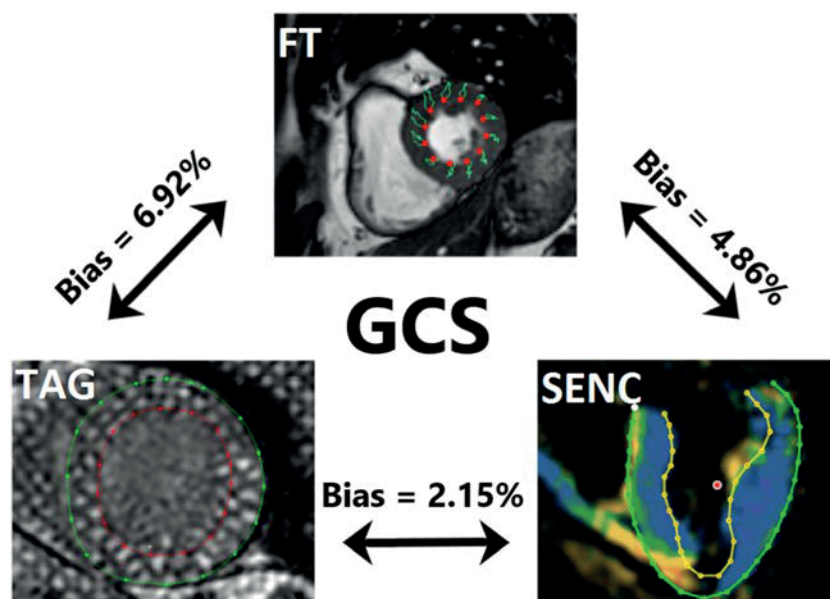


Table 2 Comparison of reproducibility of global strain parameters

	Bias (%)	Limits of agreement (\pm)	CoV (%)	ICC
Intra-observer reproducibility				
FT				
GLS	-0.32	1.6	3.8	0.95
GCS	0.94	3.45	6.2	0.89
TAG				
GLS	0.07	1.7	6.7	0.99
GCS	-0.2	1.6	5	0.99
SENC				
GLS	-0.03	0.6	1.5	0.99
GCS	0.14	1.15	3.11	0.99
Inter-observer reproducibility				
FT				
GLS	0.6	6.2	10.1	0.92
GCS	-3.3	5.0	10.1	0.86
TAG				
GLS	0.04	2.0	7.7	0.98
GCS	-0.5	2.7	8.2	0.97
SENC				
GLS	0.1	1.0	2.6	0.99
GCS	0.3	1.6	4.3	0.99
Inter-study reproducibility				
FT				
GLS	-0.69	4.7	10.8	0.91
GCS	0.37	3.5	7.6	0.97
TAG				
GLS	-0.42	2.5	9.4	0.96
GCS	-0.78	3.5	10.4	0.95
SENC				
GLS	-0.15	3.3	9.1	0.94
GCS	-0.27	3.3	8.9	0.96

CoV, coefficient of variance; FT, feature tracking; GCS, global circumferential strain; GLS, global longitudinal strain; ICC, intra-class correlation coefficient; SENC, fast-strain-encoded cardiovascular magnetic resonance imaging; TAG, myocardial tagging.

segments are presented in Supporting Information, *Tables S1–S6*. Combined intra-observer agreement was excellent in all of the techniques in both SLS (ICC: for FT = 0.914, $P < 0.001$; for TAG = 0.915, $P < 0.001$; and for fast-SENC = 0.953, $P < 0.001$) and SCS (ICC: for FT = 0.885, $P < 0.001$; for TAG = 0.978, $P < 0.001$; and for fast-SENC = 0.932, $P < 0.001$). SLS derived from fast-SENC had the lowest variation (CoV = 12.35%), followed by FT (CoV = 21.87%) and TAG (CoV = 24.73%). TAG showed the lowest variability for SCS (CoV = 10.76%), followed by fast-SENC (CoV = 17.59%) and FT (CoV = 19.66%). Inter-study agreement for SLS was poor for FT (ICC = 0.329, $P < 0.001$), while TAG and fast-SENC showed excellent agreement (ICC = 0.768, $P < 0.001$ and 0.844, $P < 0.001$, respectively). All of the modalities showed excellent inter-study agreement for SCS (ICC: for FT = 0.766, $P < 0.001$; for TAG = 0.902, $P < 0.001$; and for fast-SENC = 0.850, $P < 0.001$). Fast-SENC had the lowest variation for SLS (CoV = 21.92%), followed by TAG (CoV = 37.75%) and FT (CoV = 42.99%). As in intra-observer comparison, TAG performed the best for SCS (CoV = 19.08%), followed by fast-SENC (CoV = 23.52%) and FT (CoV = 32.35%).

Discussion

Speckle tracking echocardiography-derived strain values are recommended for clinical use by both European Society of Cardiology and American Heart Association,¹⁶ thus highlighting the current and future importance of strain imaging.

Table 3 Comparison of reproducibility of combined segmental strain parameters

		FT		TAG		SENC	
		Intra-observer	Inter-study	Intra-observer	Inter-study	Intra-observer	Inter-study
ICC	SLS	0.914	0.329	0.915	0.768	0.953	0.844
	SCS	0.885	0.766	0.978	0.902	0.932	0.850
COV (%)	SLS	21.87	42.99	24.73	37.75	12.35	21.92
	SCS	19.66	32.35	10.76	19.08	17.59	23.52

CoV, coefficient of variance; FT, feature tracking; ICC, intra-class correlation coefficient; SCS, segmental circumferential strain; SENC, fast-strain-encoded cardiovascular magnetic resonance imaging; SLS, segmental longitudinal strain; TAG, myocardial tagging.

Given the fact that CMR can overcome most of the echocardiography's inborn shortcomings, we expect CMR to become a more reliable tool for future deformation imaging. Indeed, CMR-derived strain has been shown to be more reproducible and to have better feasibility.¹⁷ However, despite CMR's advantages over echocardiography and promising studies regarding its possible usefulness in the clinical setting, the multitude of techniques for strain assessment, as well as inter-vendor differences within these techniques,^{18,19} hinder further clinical applicability of these measurements. In order for CMR-based strain measurements to become clinically useful, a standardization of available techniques is necessary.

The design of our study allowed for a direct comparison and exploration of differences between three widely used CMR-based strain measurement techniques. The main findings of our study are as follows:

- (1) There was significant bias between the three imaging techniques in measured GLS and GCS.
- (2) There was excellent correlation for both GLS and GCS between the three modalities tested.
- (3) Agreement and variability for intra-observer and inter-observer, as well as inter-study global strain measurements, was excellent in all three modalities.
- (4) Segmental strain comparison showed excellent intra-observer agreement in all three modalities. TAG and fast-SENC had better inter-study agreement than FT for segmental strain.

TAG has been historically considered the gold standard technique for strain assessment. It has been shown to be highly reproducible and used for validation of other strain assessment techniques.^{20,21} However, it requires long acquisition and post-processing times, in addition to suffering from low temporal and spatial resolutions, as well as tag fading during the diastole. Furthermore, in our cohort, TAG images could not be assessed in approximately 1/7th of all scans due to artefacts. In comparison, fast-SENC, despite also requiring acquisition of additional sequences, is a one heart-beat, free-breathing technique with quick post-processing.²² Our intra-observer and inter-observer comparisons show it to be more robust than TAG and to have comparable inter-

study reproducibility. Furthermore, a recent study by Lapinskas et al.²³ demonstrated feasibility of fast-SENC to assess LV volumes and LVEF, making it a convenient option for functional assessment of the heart. Such short acquisition and post-processing times make fast-SENC technique very attractive in daily routine, especially in severely ill patients and children.²² It must be noted that due to technical limitations, radial strain cannot be assessed from SENC acquisitions.⁷ Additionally, it has a worse spatial resolution than TAG and FT.²² On the other end of the spectrum, FT is a post-processing technique that does not require additional image acquisition. This gives FT an advantage for use in a clinical setting, as it can retrospectively be applied to SSFP images, acquired using a clinically standard CMR protocol. Furthermore, in our comparison, FT had excellent reproducibility and correlation with both TAG and fast-SENC. To sum up, both fast-SENC and FT possess certain advantages over the gold standard that make them more attractive for clinical use, while still maintaining robustness.

Although not apparent in global comparison, variability in segmental comparison was consistently higher in strain derived from LAX images, as compared with SAX images. It is in-line with previously published studies²⁴ and can be explained by poor tracking of basal segments in LAX images due to complex architecture of the mitral annulus.⁷ It would also explain why fast-SENC had by far the lowest variability in SLS comparison, although it was outperformed by TAG for SCS. Furthermore, fast-SENC was also the most robust modality in GLS comparisons. Given the fact that GLS is the most widely validated and the only clinically used strain measurement, fast-SENC could be a method of choice for future studies. Of note, FT performed worse than both acquisition-based techniques in segmental comparisons. It also had poor inter-study variability for both SCS (CoV 32.35%) and SLS (CoV 42.99%), supporting the opinions of previous authors that FT is not ready for use in segmental strain assessment.^{25,26} This may have significant implications especially in the detection of regional LV dysfunction, for example, in patients with suspected or known ischaemic heart disease. Additionally, by comparing intra-observer reproducibility of GCS between observers with different levels of experience, Feisst et al. demonstrated that reproducibility of FT is highly dependent on observer experience.²⁷ Since reproducibility

of the global measurements in our study closely matches that of an experienced observer from the aforementioned study, the results of our segmental comparison are indicative of a best-case scenario. Furthermore, a recent study by Backhaus *et al.* assessed the impact of observer training on reproducibility of FT strain measurements from three different vendors and found that the positive impact of observer experience is present independently of vendor choice.²⁸

It must also be highlighted that, despite excellent correlation and reproducibility of these techniques for global measurements, significant differences in measured strain between the modalities were detected in our study. The fact that our study design accounted for possible subject-related biases, such as different loading conditions, points towards a systematic difference between the techniques in question. Indeed, a recent meta-analysis by Vo *et al.*²⁹ sought to find normal values for CMR-derived strain parameters and reported similar albeit less pronounced differences in GLS and GCS between these modalities. The observed differences can at least in part be explained by looking at how the strain values are derived in each technique. FT is a post-processing method that uses SSFP images to identify certain features within these images and tries to track them throughout the successive frames of the cine loop. However, through-plane movement can cause some of the tracked features to move out of the imaging plane and be replaced by other regions of the myocardium, thus causing through-plane motion artefacts. Furthermore, for FT, we reported endocardial strain values, which are naturally higher.² On the other hand, both TAG and fast-SENC are acquisition-based techniques and, as such, are not affected by through-plane motion artefacts. However, the latter uses parallel tags as opposed to orthogonal ones used in the former. Therefore, SAX images are used to acquire longitudinal strain, while circumferential strain is derived from the LAX images, essentially meaning that these techniques acquire strain measurements at different spatial points. In the end, even though all of these techniques employ CMR for image acquisition, there are fundamental differences in imaging protocols and analysis algorithms that ultimately amount to substantial bias.

Our study supports the previously expressed opinion that before further standardization is brought forward, different CMR modalities cannot be used interchangeably for strain assessment.¹⁸ However, reproducibility analysis of global measurements showed excellent results for all three techniques, which is encouraging for a shift towards clinical use, as excellent inter-study reproducibility is paramount in follow-up scans for assessment of disease progression.

Limitations

The main limitation of this study was a relatively small sample size. However, our cohort included both healthy volunteers

and HF patients with reduced and preserved LVEF. Secondly, images were analysed using different software solutions dedicated for each modality, thus inter-vendor differences could not be explored. Nonetheless, all the software solutions used in our study are validated and commercially available.

Conclusions

Important differences in measured GLS and GCS exist between FT, TAG, and fast-SENC, thus care should be taken when comparing these values. There was excellent GLS and GCS reproducibility at intra-observer, inter-observer, and inter-study levels and close correlation between these modalities. Acquisition-based techniques had better reproducibility than FT for segmental strain. Fast-SENC had the lowest variability for SLS, while TAG performed the best for SCS.

Conflict of interest

Authors declare no competing interests.

Author contributions

P.B. performed image and statistical analysis and drafted the manuscript. J.E., R.T., V.Z., S.G., and T.L. performed image analysis. J.E., S.G., G.K., H.S., B.P., E.P.K., A.S., T.L., and S.K. provided critical revision of the manuscript. G.K., H.S., B.P., E.P.K., A.S., and S.K. designed the study. C.S. acquired images and helped with drafting the manuscript. S.K. provided the conception of the study.

Funding

S.K. received an unrestricted research grant by Philips Healthcare and a research grant from Myocardial Solutions. S.K., T.L., B.P., A.S., and E.P.K. are supported by the DZHK (German Centre for Cardiovascular Research) and by the BMBF (German Ministry of Education and Research).

Availability of data and material

The datasets used and/or analysed during the current study are available from the corresponding author on reasonable request.

Supporting information

Additional supporting information may be found online in the Supporting Information section at the end of the article.

Table S1. Segmental comparison of ICC for FT.

Table S2. Segmental comparison of ICC for TAG.

Table S3. Segmental comparison of ICC for SENC.

Table S4. Segmental comparison of CoV for FT.

Table S5. Segmental comparison of CoV for TAG.

Table S6. Segmental comparison of CoV for SENC.

Table S7. Haemodynamic status of study subjects during the first and second MRI scan.

References

- Choi E-Y, Rosen BD, Fernandes VRS, Yan RT, Yoneyama K, Donekal S, Opdahl A, Almeida ALC, Wu CO, Gomes AS, Bluemke DA, Lima JAC. Prognostic value of myocardial circumferential strain for incident heart failure and cardiovascular events in asymptomatic individuals: the Multi-Ethnic Study of Atherosclerosis. *Eur Heart J [Internet]*. 2013 Aug 7; **34**: 2354–2361.
- Smiseth OA, Torp H, Opdahl A, Haugaa KH, Urheim S. Myocardial strain imaging: how useful is it in clinical decision making? *Eur Heart J [Internet]*. 2016 Apr 14; **37**: 1196–1207.
- Negishi K, Negishi T, Haluska BA, Hare JL, Plana JC, Marwick TH. Use of speckle strain to assess left ventricular responses to cardiotoxic chemotherapy and cardioprotection. *Eur Heart J - Cardiovasc Imaging [Internet]*. 2014 Mar 1; **15**: 324–331.
- Urbano-Moral JA, Rowin EJ, Maron MS, Crean A, Pandian NG. Investigation of global and regional myocardial mechanics with 3-dimensional speckle tracking echocardiography and relations to hypertrophy and fibrosis in hypertrophic cardiomyopathy. *Circ Cardiovasc Imaging [Internet]*. 2014 Jan; **7**: 11–19.
- Zerhouni EA, Parish DM, Rogers WJ, Yang A, Shapiro EP. Human heart: tagging with MR imaging—a method for noninvasive assessment of myocardial motion. *Radiology [Internet]*. 1988 Oct; **169**: 59–63.
- Swoboda PP, Larghat A, Zaman A, Fairbairn TA, Motwani M, Greenwood JP, Plein S. Reproducibility of myocardial strain and left ventricular twist measured using complementary spatial modulation of magnetization. *J Magn Reson Imaging [Internet]*. 2014 Apr; **39**: 887–894.
- Scatteia A, Baritussio A, Bucciarelli-Ducci C. Strain imaging using cardiac magnetic resonance. *Heart Fail Rev [Internet]*. 2017 Jul 15; **22**: 465–476.
- Feng L, Donnino R, Babb J, Axel L, Kim D. Numerical and in vivo validation of fast cine displacement-encoded with stimulated echoes (DENSE) MRI for quantification of regional cardiac function. *Magn Reson Med [Internet]* 2009 Sep; **62**: 682–690. Available from: <http://www.ncbi.nlm.nih.gov/pubmed/19585609>.
- Osman NF, Sampath S, Atalar E, Prince JL. Imaging longitudinal cardiac strain on short-axis images using strain-encoded MRI. *Magn Reson Med [Internet]*. 2001 Aug; **46**: 324–334.
- Pan L, Stuber M, Kraitchman DL, Fritzsche DL, Gilson WD, Osman NF. Real-time imaging of regional myocardial function using fast-SENC. *Magn Reson Med [Internet]* 2006 Feb; **55**: 386–395. Available from: <http://www.ncbi.nlm.nih.gov/pubmed/16402379>.
- Lin K, Meng L, Collins JD, Chowdhary V, Markl M, Carr JC. Reproducibility of cine displacement encoding with stimulated echoes (DENSE) in human subjects. *Magn Reson Imaging [Internet]* 2017 Jan; **35**: 148–153. Available from: <https://linkinghub.elsevier.com/retrieve/pii/S0730725X1630114X>.
- Giusca S, Korosoglou G, Zieschang V, Stoiber L, Schnackenburg B, Stehning C, Gebker R, Pieske B, Schuster A, Backhaus S, Pieske-Kraigher E, Patel A, Kawaji K, Steen H, Lapinskas T, Kelle S. Reproducibility study on myocardial strain assessment using fast-SENC cardiac magnetic resonance imaging. *Sci Rep [Internet]* 2018 Dec; **20**: 14100. Available from: <http://www.nature.com/articles/s41598-018-32226-3>.
- Eds NS, Hutchison D. Functional imaging and modeling of the heart. *Proc 8th Int Conf FIMH 2015 [Internet]* 2015; **9126**: 69121–69121.
- Cicchetti DV. Guidelines, criteria, and rules of thumb for evaluating normed and standardized assessment instruments in psychology. *Psychol Assess [Internet]* 1994; **6**, 4: 284–290.
- Oppo K, Leen E, Angerson WJ, Cooke TG, McArdle CS. Doppler perfusion index: an interobserver and intraobserver reproducibility study. *Radiology [Internet]*. 1998 Aug; **208**: 453–457.
- Voigt J-U, Pedrizzetti G, Lysyansky P, Marwick TH, Houle H, Baumann R, Pedri S, Ito Y, Abe Y, Metz S, Song JH, Hamilton J, Sengupta PP, Kolias TJ, D'Hooge J, Aurigemma GP, Thomas JD, Badano LP. Definitions for a common standard for 2D speckle tracking echocardiography: consensus document of the EACVI/ASE/Industry Task Force to standardize deformation imaging. *Eur Heart J - Cardiovasc Imaging [Internet]*. 2015 Jan 1; **16**(1):1–11.
- Obokata M, Nagata Y, Wu VC-C, Kado Y, Kurabayashi M, Otsuji Y, Takeuchi M. Direct comparison of cardiac magnetic resonance feature tracking and 2D/3D echocardiography speckle tracking for evaluation of global left ventricular strain. *Eur Heart J - Cardiovasc Imaging [Internet]*. 2016 May; **17**: 525–532.
- Cao JJ, Ngai N, Duncanson L, Cheng J, Gliganic K, Chen Q. A comparison of both DENSE and feature tracking techniques with tagging for the cardiovascular magnetic resonance assessment of myocardial strain. *J Cardiovasc Magn Reson [Internet]*. 2018 Dec 19; **20**(12):26.
- Beerbaum P, Lotz J, Bigalke B, Fasshauer M, Kowallick JT, Steinmetz M, Hasenfuß G, Staab W, Lamata P, Ritter C, Sohns JM, Unterberg-Buchwald C, Stahnke V-C, Kutty S, Schuster A. Cardiovascular magnetic resonance feature-tracking assessment of myocardial mechanics: intervendor agreement and considerations regarding reproducibility. *Clin Radiol [Internet]*. 2015; **70**: 989–998.
- Aurich M, Keller M, Greiner S, Steen H, aus dem Siepen F, Riffel J, Katus HA, Buss SJ, Mereles D. Left ventricular mechanics assessed by two-dimensional echocardiography and cardiac magnetic resonance imaging: comparison of high-resolution speckle tracking and feature tracking. *Eur Heart J - Cardiovasc Imaging [Internet]* 2016 Dec; **17**: 1370–1378.
- Hor KN, Gottliebson WM, Carson C, Wash E, Cnota J, Fleck R, Wansapura J, Klimeczek P, Al-Khalidi HR, Chung ES, Benson DW, Mazur W. Comparison of magnetic resonance feature tracking for strain calculation with harmonic phase imaging analysis. *JACC Cardiovasc Imaging [Internet]*. 2010; **3**: 144–151.
- Korosoglou G, Giusca S, Hofmann NP, Patel AR, Lapinskas T, Pieske B, Steen H, Katus HA, Kelle S. Strain-encoded magnetic resonance: a method for the assessment of myocardial deformation. *ESC Heart Fail [Internet]* 2019 Apr 25; ehf2.12442.
- Lapinskas T, Zieschang V, Erley J, Stoiber L, Schnackenburg B, Stehning

- C, Gebker R, Patel AR, Kawaji K, Steen H, Zaliunas R, Backhaus SJ, Schuster A, Makowski M, Giusca S, Korosoglou G, Pieske B, Kelle S. Strain-encoded cardiac magnetic resonance imaging: a new approach for fast estimation of left ventricular function. *BMC Cardiovasc Disord [Internet]*. 2019 Mar 5; **19**():52. Available from: <http://www.ncbi.nlm.nih.gov/pubmed/30836942>
24. Claus P, Omar AMS, Pedrizzetti G, Sengupta PP, Nagel E. Tissue tracking technology for assessing cardiac mechanics. *JACC Cardiovasc Imaging [Internet]*. 2015 Dec; **8**: 1444–1460. Available from: <https://linkinghub.elsevier.com/retrieve/pii/S1936878X15008451>.
25. Wu L, Germans T, Güçlü A, Heymans MW, Allaart CP, van Rossum AC. Feature tracking compared with tissue tagging measurements of segmental strain by cardiovascular magnetic resonance. *J Cardiovasc Magn Reson [Internet]*. 2014 Dec 22; **16**():10.
26. Morton G, Schuster A, Jogiya R, Kutty S, Beerbaum P, Nagel E. Inter-study reproducibility of cardiovascular magnetic resonance myocardial feature tracking. *J Cardiovasc Magn Reson [Internet]* 2012; **14**: 43.
27. Feisst A, Kuetting DLR, Dabir D, Luetkens J, Homsy R, Schild HH, Thomas D. Influence of observer experience on cardiac magnetic resonance strain measurements using feature tracking and conventional tagging. *IJC Hear Vasc [Internet]*. 2018 Mar; **18**: 46–51. Available from: <https://linkinghub.elsevier.com/retrieve/pii/S2352906718300332>.
28. Backhaus SJ, Metschies G, Billing M, Kowallick JT, Gertz RJ, Lapinskas T, Pieske B, Lotz J, Bigalke B, Kutty S, Hasenfuß G, Beerbaum P, Kelle S, Schuster A. Cardiovascular magnetic resonance imaging feature tracking: impact of training on observer performance and reproducibility. Coelho-Filho OR, editor. *PLoS One [Internet]*. 2019 Jan 25; **14**():e0210127.
29. Vo HQ, Marwick TH, Negishi K. MRI-derived myocardial strain measures in normal subjects. *JACC Cardiovasc Imaging [Internet]*. 2018 Feb; **11**: 196–205. Available from: <https://linkinghub.elsevier.com/retrieve/pii/S1936878X1730253X>.

OPEN

Effect of comprehensive initial training on the variability of left ventricular measures using fast-SENC cardiac magnetic resonance imaging

Tomas Lapinskas^{1,2,7}, Hanane Hireche-Chikaoui¹, Victoria Zieschang¹, Jennifer Erley¹, Christian Stehning³, Rolf Gebker^{1,7}, Sorin Giusca⁴, Grigorios Korosoglou⁴, Remigijus Zaliunas², Sören Jan Backhaus^{5,8}, Andreas Schuster^{5,8,9}, Burkert Pieske^{1,7} & Sebastian Kelle^{1,6,7}

Cardiac magnetic resonance (CMR) is becoming the imaging modality of choice in multicenter studies where highly reproducible measurements are necessary. The purpose of this study was to assess the effect of comprehensive initial training on reproducibility of quantitative left ventricular (LV) parameters estimated using strain-encoded (SENC) imaging. Thirty participants (10 patients with heart failure (HF) and preserved LV ejection fraction (HFpEF), 10 patients with HF and reduced LV ejection fraction (HFrEF) and 10 healthy volunteers) were examined using fast-SENC imaging. Four observers with different experience in non-invasive cardiac imaging completed comprehensive initial training course and were invited to perform CMR data analysis. To assess agreement between observers, LV volumes, mass, ejection fraction (LVEF), global longitudinal strain (GLS) and global circumferential strain (GCS) were estimated using dedicated software (MyoStrain, USA). To test intraobserver agreement data analysis was repeated after 4 weeks. SENC imaging and analysis were fast and were completed in less than 5 minutes. LV end-diastolic volume index (LVEDVi), LVEF and strain were significantly lower in HFpEF patients than in healthy volunteers ($p = 0.019$ for LVEDVi; $p = 0.023$ for LVEF; $p = 0.004$ for GLS and $p < 0.001$ for GCS). All LV functional parameters were further reduced in HFrEF. Excellent interobserver agreement was found for all LV parameters independently of the level of experience. The reproducibility of LV mass was lower, especially at the intraobserver level (ICC 0.91; 95% CI 0.74–0.96). LV volumetric and functional parameters derived using fast-SENC imaging, are highly reproducible. The appropriate initial training is relevant and allows to achieve highest concordance in fast-SENC measurements.

In addition to clinical signs and symptoms, a detailed assessment of structural and functional cardiac parameters is considered to be essential and provides important diagnostic information in patients with heart failure (HF)^{1,2}. Over the past decade cardiac magnetic resonance (CMR) has evolved into the reference standard to assess cardiac anatomy and function^{3,4}. Because of its excellent endocardial border definition, cine CMR imaging is the accepted gold standard for quantification of ventricular volumes, mass and ejection fraction^{5,6}. While important

¹Department of Internal Medicine/Cardiology, German Heart Center Berlin, Berlin, Germany. ²Department of Cardiology, Medical Academy, Lithuanian University of Health Sciences, Kaunas, Lithuania. ³Philips Healthcare, Hamburg, Germany. ⁴Department of Cardiology and Vascular Medicine, GRN Hospital Weinheim, Weinheim, Germany. ⁵Department of Cardiology and Pneumology, University Medical Center, Georg-August University, Göttingen, Germany. ⁶Department of Internal Medicine/Cardiology, Charité Campus Virchow Clinic, Berlin, Germany. ⁷DZHK (German Centre for Cardiovascular Research), Partner Site Berlin, Berlin, Germany. ⁸DZHK (German Centre for Cardiovascular Research), Partner Site Göttingen, Göttingen, Germany. ⁹Department of Cardiology, Royal North Shore Hospital, The Kolling Institute, Northern Clinical School, University of Sydney, Sydney, Australia. Correspondence and requests for materials should be addressed to T.L. (email: tomas.lapinskas@ismuni.lt)

Fast-SENC Training Flowchart

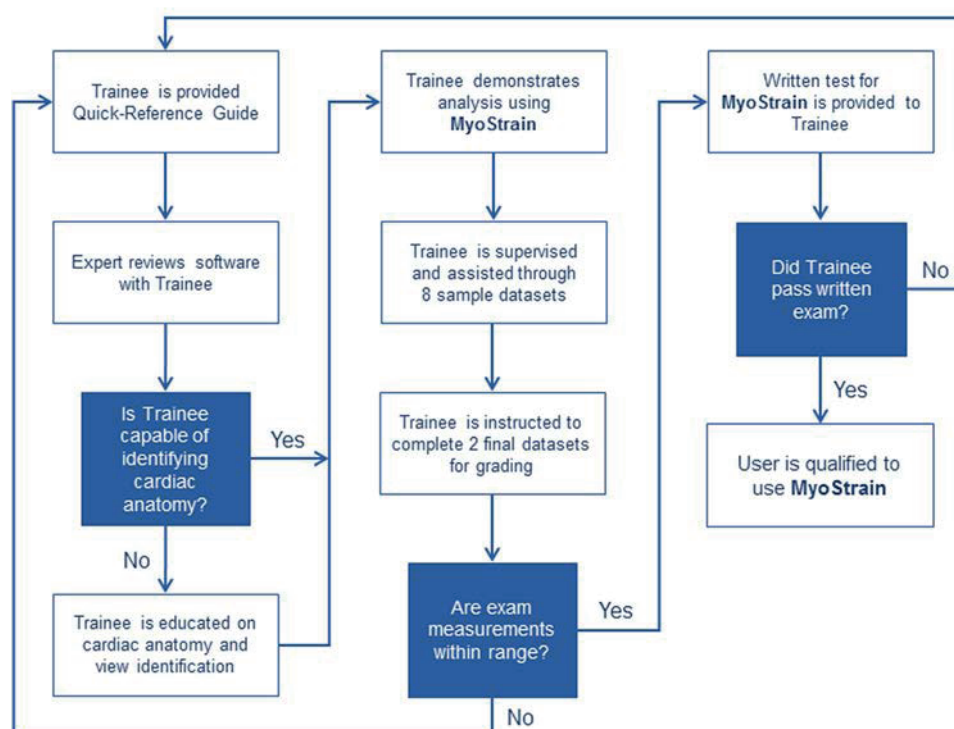


Figure 1. Fast-SENC training flowchart. Before starting the analysis of CMR data, observers acquired similar comprehensive expert-guided training. The training consisted of a 2 to 4-hour training course designed to provide the skills necessary to correctly use the software. After successful completion of the training course and examination observers were allowed to start study data analysis.

achievements in CMR techniques have reduced total scan time, quantitative volumetric analysis has not changed significantly and requires time and human resources^{7,8}.

Growing evidence suggests that conventional functional parameters such as left ventricular ejection fraction (LVEF) may not be sensitive enough to detect subtle changes in ventricular function⁹. Tissue-tracking techniques have enabled the non-invasive assessment of myocardial deformation and it appears that myocardial strain might be a more robust marker of the failing myocardium^{10–12}. Strain-encoded magnetic resonance (SENC) imaging was developed on the concepts of myocardial tagging and first described in 2001¹³. In line with other tissue tracking techniques, SENC provides quantitative information about myocardial mechanics and has been validated and applied in multiple experimental and clinical settings^{14–16}. Fast-SENC technique is a real-time version of SENC that has shortened the scan duration to a single heartbeat¹⁷. The absence of contrast agent and free breathing during data acquisition are important advantages that make the technique desirable in daily routine. Moreover, recent achievements in fast-SENC data analysis tools have enabled quantification of conventional left ventricular (LV) volumetric and functional parameters with excellent accuracy and minimal educational efforts¹⁸.

More and more clinical decision making relies on CMR derived data^{19–21}; hence, interobserver and intraobserver variability may become an important source of bias. Although recommendations exist for CMR acquisition²² and data post-processing^{23,24}, the lack of proper initial training of the observers may lead to significant measurement variance which becomes more apparent in multicenter studies. Indeed, appropriate education^{25,26} as well as repeated measurements²⁷ might improve interobserver reproducibility for volumetric and functional measures of the left ventricle.

We set up this study to investigate the effect of comprehensive initial training on reproducibility of LV volumes, mass, ejection fraction and strain derived using fast-SENC imaging. The main hypothesis was that appropriate initial training has an important impact in terms of cardiac imaging of the readers on the concordance of measurements.

Materials and Methods

Study population. The study population comprised patients with heart failure and preserved LVEF (HFpEF, n = 10), reduced LVEF (HFrfEF, n = 10) and healthy volunteers (n = 10). The study complies with the Declaration of Helsinki and was approved by the ethics committee board of the Charité-Universitätsmedizin Berlin. All participants provided written informed consent before entering the study.

Left ventricular volumetric and functional analysis performed by 4 different observers:

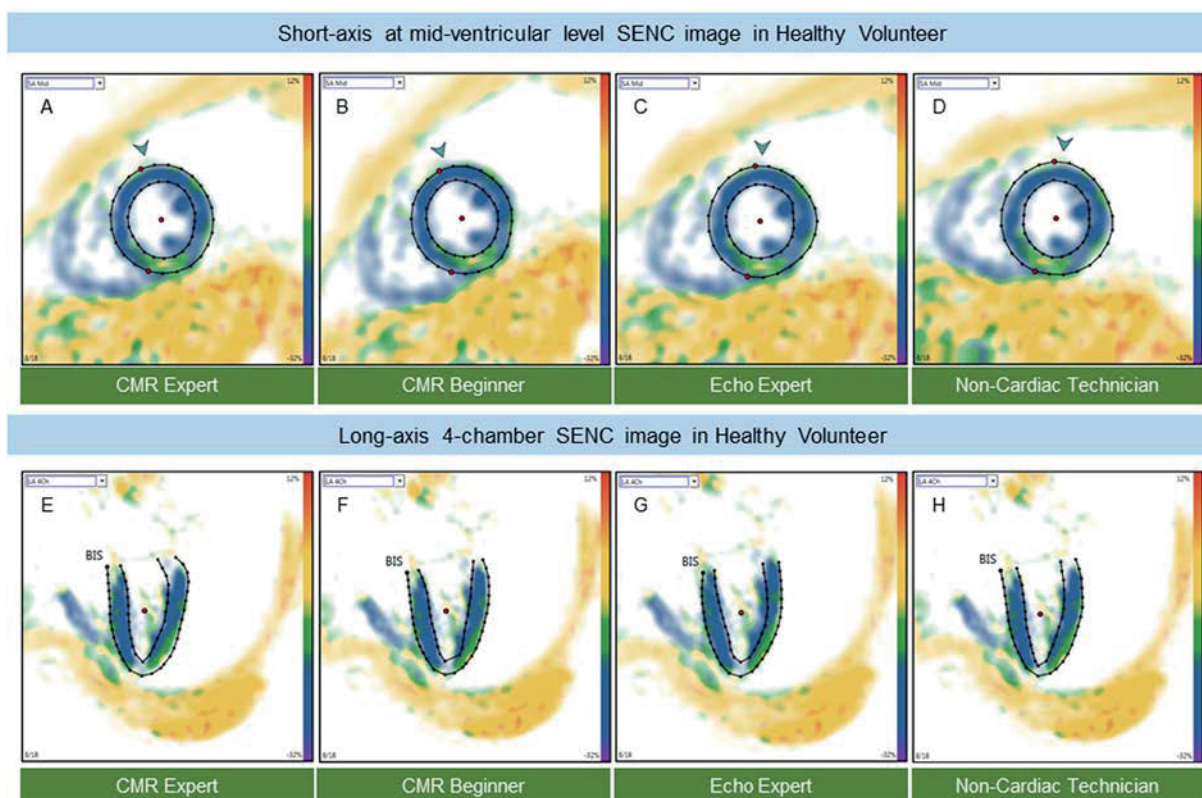


Figure 2. Example of fast-SENC images acquired in a healthy volunteer and uploaded into a dedicated MyoStrain software. CMR images were derived in three long-axis and three short-axis views. Endocardial and epicardial borders were traced at end-diastolic and end-systolic cardiac phases by four observers: CMR expert (A,E) CMR beginner (B,F) echocardiography expert (C,G) and non-cardiac technician (D,H). CMR = cardiac magnetic resonance; SENC = strain-encoded imaging.

CMR acquisition. All CMR studies were performed on a 1.5 T MRI scanner (Achieva, Philips Healthcare, Best, The Netherlands) using a five-element phased array cardiac coil in supine position.

A previously described¹⁷ real-time free breathing SENC imaging technique (Myocardial Solutions, Inc., Morrisville, North Carolina, USA) based on the acquisition of two images with different frequency modulation was employed. Images were taken in three different LV long-axis (two-, three- and four-chamber) and three LV short-axis (at basal, mid-ventricular and apical level) views. The slices of different LV short-axis levels were identified as follows: basal level slice was considered and used for quantitative analysis if complete LV myocardium was visible throughout the entire cardiac cycle; mid-ventricular level slice was selected at the level of both papillary muscles; and apical level slice was considered if blood pool was still visible throughout the entire cardiac cycle (no obliteration of the LV cavity at end-systolic phase). Typical fast-SENC parameters were as follows: field-of-view = $256 \times 256 \text{ mm}^2$, slice thickness = 10 mm, voxel size = $4.0 \times 4.0 \times 10 \text{ mm}^3$, single-shot spiral read-out (3 interleaves) with acquisition time (TA) = 10 ms, flip angle = 30° , effective echo time (TE) = 0.7 ms, repetition time (TR) = 12 ms, temporal resolution = 36 ms, typical number of acquired phases = 22, spectrally selective fat suppression (SPIR), total acquisition time per slice < 1 s.

Study observers. The four observers with different knowledge and experience in CMR imaging were invited to perform analysis of acquired CMR data: (1) CMR expert (TL) (level 3 certified, performing routine clinical CMR scanning and data post-processing for >5 years); (2) CMR beginner (VZ) (with basic knowledge and <3 months of experience in CMR imaging); (3) Echo expert (HHC) (level 3 certified, performing advanced echocardiography studies including speckle tracking echocardiography in high-volume cardiovascular unit) and (4) Non-cardiac technician (JE) (fully-trained radiographer without any experience in data post-processing).

Training protocol. Before starting the CMR data analysis, all observers were trained similarly by a representative of the software company with an emphasis on possible sources of error. A Quick-Reference Guide was given to each trainee before starting the training. The training consisted of a 2 to 4-hour training course designed to provide observers with the skills necessary to correctly use the dedicated MyoStrain software (Fig. 1). A set of 8 cases was used during the training including different cardiac conditions (healthy, cardiomyopathies, ischemic heart disease) and possible image quality issues (suboptimal field-of-view, patient movement or image artifacts)

Left ventricular volumetric and functional analysis performed by 4 different observers:

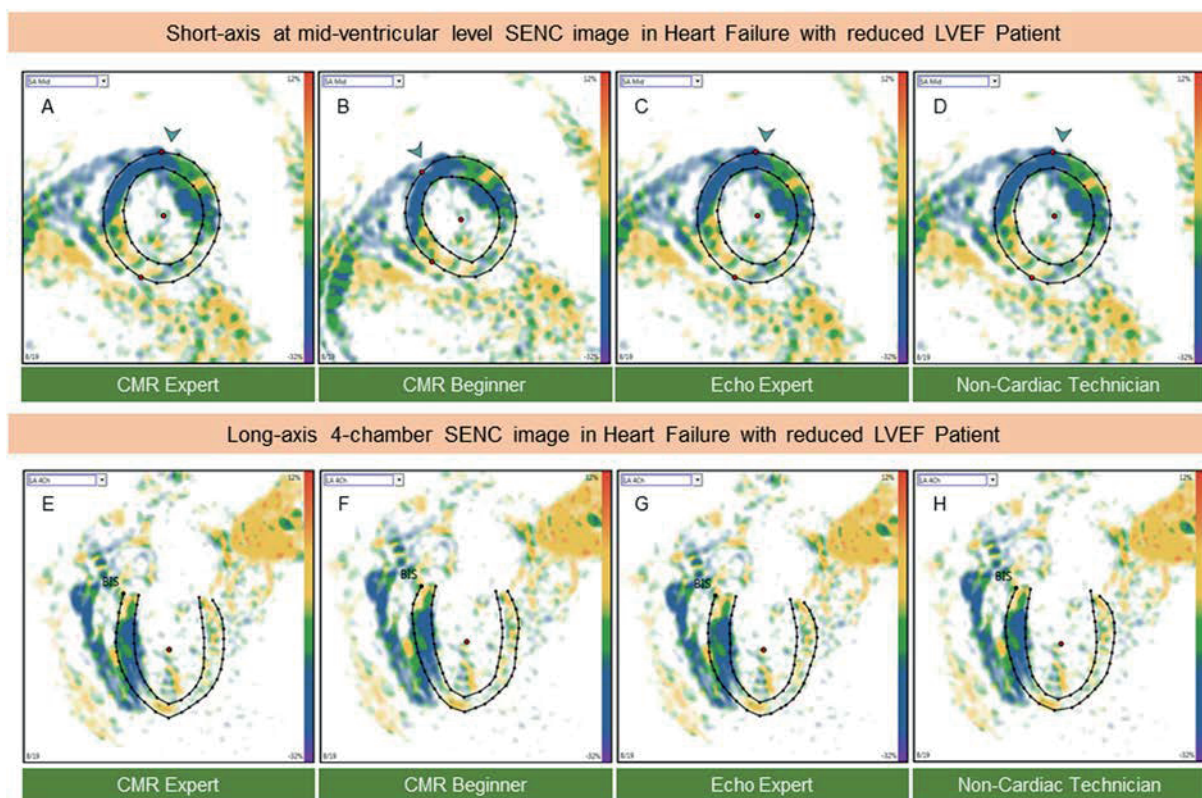


Figure 3. Example of fast-SENC images acquired in HFrEF patients and uploaded into a dedicated MyoStrain software. Endocardial and epicardial borders were traced at end-diastolic and end-systolic cardiac phases by four observers: CMR expert (A,E) CMR beginner (B,F) echocardiography expert (C,G) and non-cardiac technician (D,H). CMR = cardiac magnetic resonance; SENC = strain-encoded imaging; HFrEF = heart failure with reduced left ventricular ejection fraction.

Parameter	Volunteers (n = 10)	HFpEF (n = 10)	HFrEF (n = 10)	P value		
				Volunteers vs. HFpEF	Volunteers vs. HFrEF	HFpEF vs. HFrEF
LVEDVi (ml/m ²)	87.80 ± 7.65	75.20 ± 11.66	133.74 ± 22.00	0.019	<0.001	<0.001
LVESVi (ml/m ²)	34.71 ± 5.35	33.42 ± 7.38	100.31 ± 26.51	0.579	<0.001	<0.001
LVEF (%)	60.41 ± 5.57	55.96 ± 3.40	25.64 ± 10.45	0.023	<0.001	<0.001
LVMi (g/m ²)	55.36 ± 7.35	59.89 ± 9.25	88.60 ± 17.22	0.315	<0.001	<0.001
GLS (%)	-20.45 ± 1.46	-18.92 ± 0.84	-10.92 ± 4.33	0.004	<0.001	<0.001
GCS (%)	-21.25 ± 1.19	-17.35 ± 1.89	-11.89 ± 3.07	<0.001	<0.001	<0.001

Table 1. Comparison of LV volumes, mass, ejection fraction and strain parameters among healthy volunteers and patients with heart failure with preserved (HFpEF) and reduced LV ejection fraction (HFrEF). Results are reported as mean ± standard deviation. LV = left ventricular; LVEDVi – left ventricular end-diastolic volume index; LVESVi = left ventricular end-systolic volume index; LVEF = left ventricular ejection fraction; LVMi = left ventricular mass index; GLS = global longitudinal strain; GCS = global circumferential strain; HFpEF = heart failure with preserved ejection fraction; HFrEF = heart failure with reduced ejection fraction.

which may arise when using the software. Each trainee had a hands-on analysis session in a blinded manner with personal feedback from the expert. Observers were instructed not to analyze if they thought image quality was inadequate. After completion of the 8 cases, 2 additional datasets were provided and analyzed independently from the expert. The analyses were collected and reviewed by the training site to ensure that measurements were performed correctly. Estimates collected from these analyses had to fall within acceptable ranges. A written test was also mandatory and comprised 50 questions covering cardiac anatomy, view identification and image quality as well as identification of systolic and diastolic cardiac phases. A score of 80% or above on the written exam was considered “passed”. After completion of the training course and positive feedback from the training site, observers were allowed to start study data analysis.

Parameter	Mean difference \pm SD	Limits of agreement	ICC (95% CI)
	CMR Expert vs. CMR Beginner		
LVEDVi (ml/m ²)	1.07 \pm 5.86	−10.42 to 12.56	0.99 (0.98 to 1.00)
LVESVi (ml/m ²)	0.10 \pm 7.14	−13.89 to 14.09	0.99 (0.98 to 1.00)
LVMi (g/m ²)	−2.24 \pm 6.57	−15.13 to 10.64	0.97 (0.93 to 0.99)
LVEF (%)	0.76 \pm 5.64	−10.30 to 11.82	0.97 (0.94 to 0.99)
GLS (%)	−0.02 \pm 0.39	−0.78 to 0.73	1.00 (1.00 to 1.00)
GCS (%)	0.22 \pm 0.66	−1.07 to 1.52	0.99 (0.99 to 1.00)
CMR Expert vs. Echo Expert			
LVEDVi (ml/m ²)	3.29 \pm 5.89	−8.25 to 14.83	0.99 (0.96 to 1.00)
LVESVi (ml/m ²)	1.45 \pm 5.24	−8.81 to 11.72	0.99 (0.99 to 1.00)
LVMi (g/m ²)	−2.32 \pm 6.04	−14.16 to 9.51	0.98 (0.94 to 0.99)
LVEF (%)	0.07 \pm 4.23	−8.22 to 8.36	0.99 (0.97 to 0.99)
GLS (%)	−0.13 \pm 0.50	−1.11 to 0.85	1.00 (1.00 to 1.00)
GCS (%)	0.19 \pm 0.59	−0.96 to 1.33	1.00 (0.99 to 1.00)
CMR Expert vs. Non-Cardiac Technician			
LVEDVi (ml/m ²)	3.12 \pm 8.87	−14.27 to 20.51	0.98 (0.95 to 0.99)
LVESVi (ml/m ²)	1.51 \pm 4.79	−7.88 to 10.90	1.00 (0.99 to 1.00)
LVMi (g/m ²)	0.75 \pm 7.40	−13.76 to 15.25	0.97 (0.93 to 0.98)
LVEF (%)	0.38 \pm 5.60	−10.60 to 11.35	0.98 (0.95 to 0.99)
GLS (%)	0.25 \pm 0.43	−0.58 to 1.09	1.00 (0.99 to 1.00)
GCS (%)	0.19 \pm 0.85	−1.47 to 1.85	0.99 (0.98 to 1.00)

Table 2. Bland-Altman analysis and ICC of pairwise comparison between study observers for LV volumes, mass, ejection fraction and strain parameters (analysis of entire study population, $n = 30$). Results are reported as mean \pm standard deviation. ICC = intraclass correlation coefficient; CI = confidence interval; CMR = cardiac magnetic resonance. Other abbreviations as in Table 1.

Parameter	First measurement	Second measurement	Mean difference	Limits of agreement	ICC (95% CI)
LVEDVi (ml/m ²)	97.84 \pm 29.26	99.36 \pm 30.31	−1.52 \pm 9.42	−19.98 to 16.95	0.98 (0.95 to 0.99)
LVESVi (ml/m ²)	56.05 \pm 34.16	60.38 \pm 35.90	−4.33 \pm 8.13	−20.27 to 11.60	0.98 (0.95 to 0.99)
LVMi (g/m ²)	70.19 \pm 20.20	64.45 \pm 16.45	5.75 \pm 9.34	−12.57 to 24.06	0.91 (0.74 to 0.96)
LVEF (%)	46.58 \pm 17.02	43.10 \pm 17.01	3.48 \pm 4.76	−5.85 to 12.81	0.97 (0.88 to 0.99)
GLS (%)	−16.74 \pm 5.03	−16.60 \pm 4.87	−0.14 \pm 9.11	−1.93 to 1.65	0.99 (0.98 to 1.00)
GCS (%)	−16.61 \pm 4.47	−16.28 \pm 4.58	−0.33 \pm 0.95	−2.19 to 1.54	0.99 (0.97 to 0.99)

Table 3. Bland-Altman analysis and ICC of pairwise comparison to assess intraobserver agreement for LV volumes, mass, ejection fraction and strain parameters (analysis of entire study population, $n = 30$). Results are reported as mean \pm standard deviation. Abbreviations as in Table 1.

Image analysis. All fast-SENC images were uploaded from the MRI scanner and analyzed using dedicated MyoStrain, version 4.2 software (Morrisville, NC, USA). LV end-diastolic (LVEDV), LV end-systolic volumes (LVESV) and LV mass (LVM) were quantified using manual planimetry of the endocardial and epicardial surface from three long-axis fast-SENC images and LVEF was calculated (Figs 2 and 3). The quality of the contouring was evaluated by visually comparing the tracking process with the underlying myocardial motion. Papillary muscles were considered part of the blood pool. LV volumes and mass were adjusted to body surface area. The LV longitudinal and circumferential strain was extracted from three LV short-axis and three LV long-axis fast-SENC images, respectively. The global strain values were calculated by averaging measurements obtained from 16 segments for global longitudinal strain (GLS) and 17 segments for global circumferential strain (GCS).

Statistical analysis. Data were analyzed using IBM SPSS Statistics, version 21.0 software (SPSS Inc., Chicago, IL, USA) for Windows. Continuous variables were expressed as mean \pm standard deviation. The distribution of continuous variables was assessed using the Shapiro-Wilk test and comparisons between groups were performed with the 2-sample *t* test and the Mann-Whitney U test where appropriate. Interobserver and intraobserver variability was assessed by intraclass correlation (ICC) (2-way mixed model, absolute agreement between single measurements) and Bland-Altman analysis²⁸. Agreement was considered excellent for ICC >0.74, good for ICC 0.60–0.74, fair for ICC 0.40–0.59, and poor for ICC <0.40²⁹. A *p* value of <0.05 was considered statistically significant.

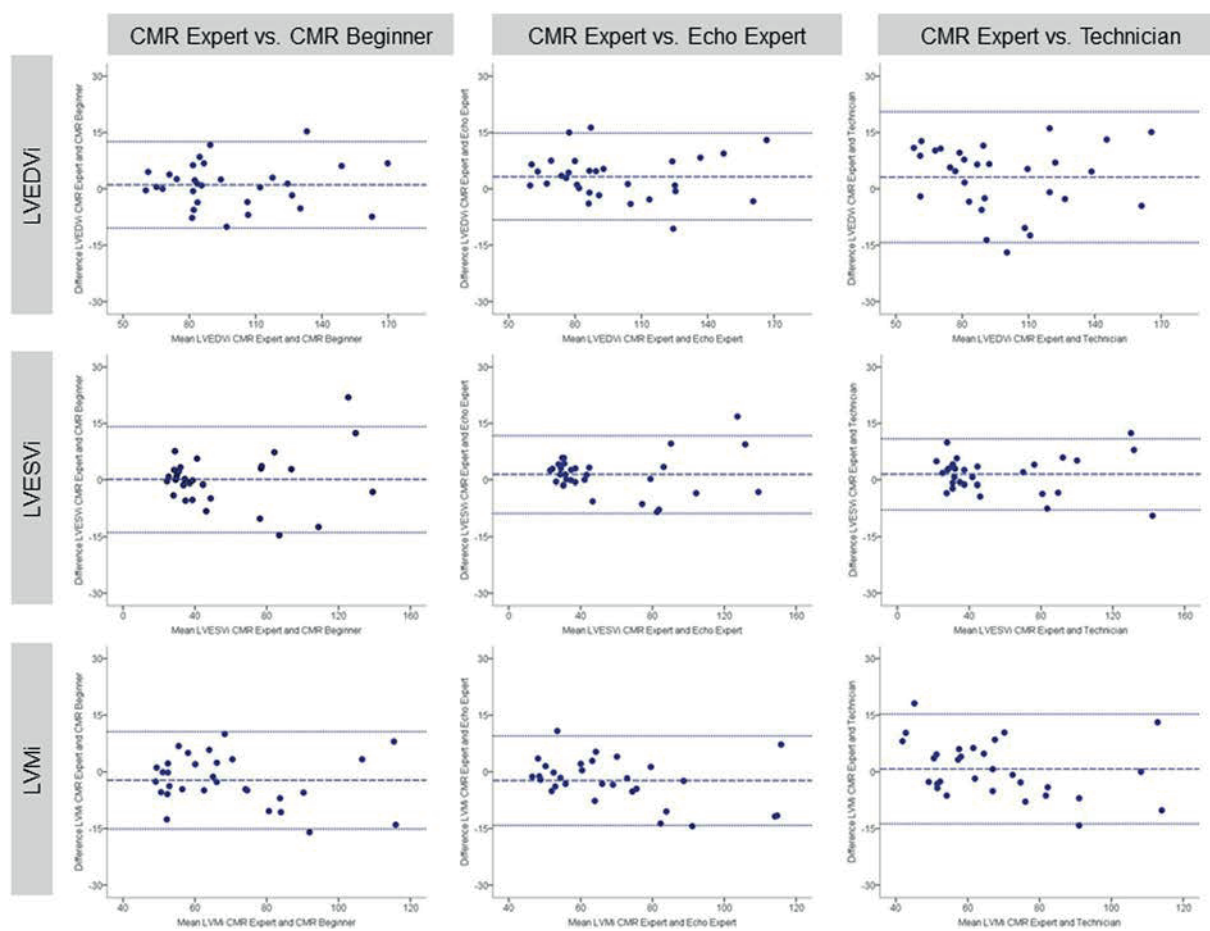


Figure 4. Bland-Altman plots with limits of agreement (1.96 standard deviations) demonstrate the interobserver agreement of fast-SENC for LVEDVi, LVESVi and LVMi. The middle-dashed line is the mean of difference of measures. The upper and lower dotted lines are ± 1.96 standard deviation. SENC = strain-encoded imaging; LVEDVi = left ventricular end-diastolic volume index; LVESVi = left ventricular end-systolic volume index; LVMi = left ventricular mass index.

Ethics approval and consent to participate. The local ethics committee (Charité-Universitätsmedizin Berlin) approved the research and consent was obtained for all study participants.

Results

All study participants were able to complete the entire study protocol. SENC imaging and analysis was fast with a 15 second scan time and a 3 to 5 minute post-processing time for complete quantitative assessment including LV volumes, mass, ejection fraction and global longitudinal and circumferential strain.

There was no significant difference in LVESV and LVM indices between healthy volunteers and HFpEF patients ($p = 0.579$ for LVESVi and $p = 0.315$ for LVMi), while LVEDVi, LVEF and strain values were significantly lower in HFpEF ($87.80 \pm 7.65 \text{ ml/m}^2$ vs. $75.20 \pm 11.66 \text{ ml/m}^2$, $p = 0.019$ for LVEDVi; $60.41 \pm 5.57\%$ vs. $55.96 \pm 3.40\%$, $p = 0.023$ for LVEF; $-20.45 \pm 1.46\%$ vs. $-18.92 \pm 0.84\%$, $p = 0.004$ for GLS and $-21.25 \pm 1.19\%$ vs. $-17.35 \pm 1.89\%$, $p < 0.001$ for GCS). All LV functional parameters were further reduced in HFpEF patients compared with healthy volunteers or HFpEF. LV volumes and mass were significantly larger in HFpEF than in other study subjects. Table 1 demonstrates fast-SENC derived parameters in the study population.

Excellent interobserver reproducibility was found for volumetric and functional LV parameters independently of the previous reader's experience. The least reproducible measure was LVMi with lowest agreement at intra-observer level (ICC 0.91; 95% confidence interval 0.74–0.96) (intraobserver analysis was performed by CMR beginner). Tables 2 and 3 summarize values for mean difference \pm SD, limit of agreement and ICC between study observers for LV volumes, mass and function. Correspondingly, Bland-Altman plots for LVEF and strain are displayed in Figs 4 and 5. Bland-Altman plots for intraobserver reproducibility are depicted in Fig. 6.

Discussion

The current study was designed to test whether comprehensive initial training has more relevant impact on the reproducibility of LV volumetric and functional parameters estimated using fast-SENC technique than observers experience. Our data analysis demonstrated that:

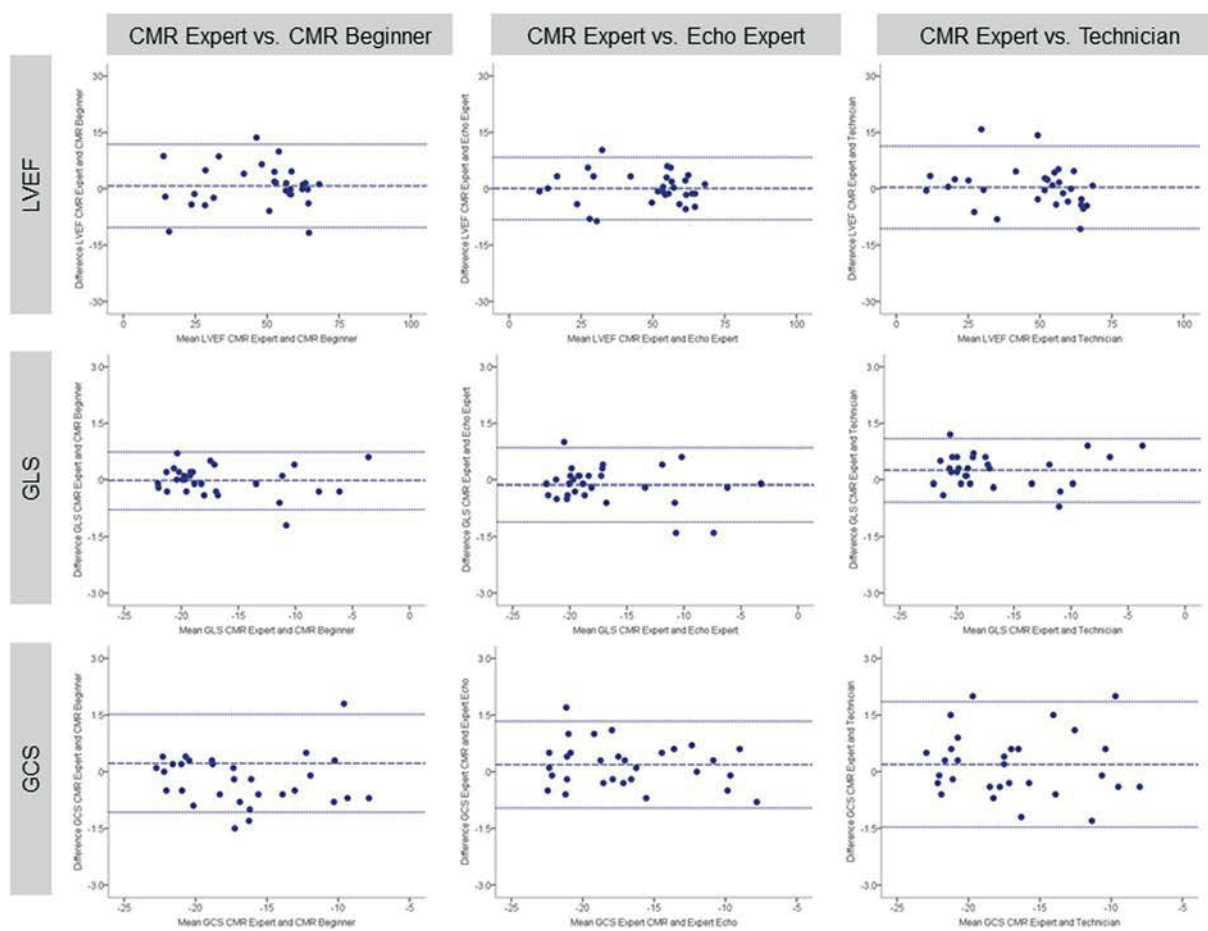


Figure 5. Bland-Altman plots with limits of agreement (1.96 standard deviations) demonstrate the interobserver agreement of fast-SENCR for LVEF, GLS and GCS. LVEF = left ventricular ejection fraction; GLS = global longitudinal strain; GCS = global circumferential strain.

- LV volumetric and functional parameters can be precisely derived from fast-SENCR images in a single short data analysis session.
- Appropriate initial training is important and has impact on the concordance in measurements among observers independently of their previous experience.
- Excellent interobserver and intraobserver agreement is present for all quantitative LV parameters, especially for GLS and GCS, whereas measures of LV mass appear less robust.

The assessment of LV function is probably the most important part of every cardiac imaging study. The majority of clinical decision making algorithms largely rely on quantitative variables such as LVEF^{30–32}. It has been shown that this single measure is critical for diagnosis of HF and selection of optimal medical or device therapy³³. However, there is evidence that advanced measures of myocardial performance, such as strain or torsion, are better predictors of outcome than LVEF or wall motion score index^{34,35}. Tissue-tracking techniques such as speckle tracking echocardiography, CMR tagging, displacement encoded with stimulated echoes (DENSE) imaging or feature tracking appear very promising and have shown the ability to detect early changes in myocardial motion³⁶. Historically, CMR tagging was the first technique implemented for the analysis of myocardial deformation³⁷. However, time-consuming data acquisition and analysis remain important limitations of this standard of reference technique^{38,39}.

In 2001 Osman *et al.*, proposed a new method for measuring the myocardial strain orthogonal to the imaging plane, called SENC-MRI¹³. The method required the acquisition of two images and allowed straightforward and fast computation of longitudinal strain. Recent achievements in SENC technique have shortened the scan duration to a single heartbeat and eliminated the demand of multiple breath-holds⁴⁰. Fast-SENCR was validated against the conventional CMR tagging and excellent correlation between the methods was shown^{41,42}. The ability to obtain accurate measurements in a short time is highly desirable, especially in severely ill patients and children. We successfully completed image acquisition and data analysis in less than five minutes, while participants were still in the MRI scanner. Such achievements make the implementation of this technique in the clinical realm very promising.

The reliability and reproducibility of LV functional measures are of great importance for patient management, therapy monitoring and outcome studies⁴³. A lower level of variability permits detection of smaller changes and

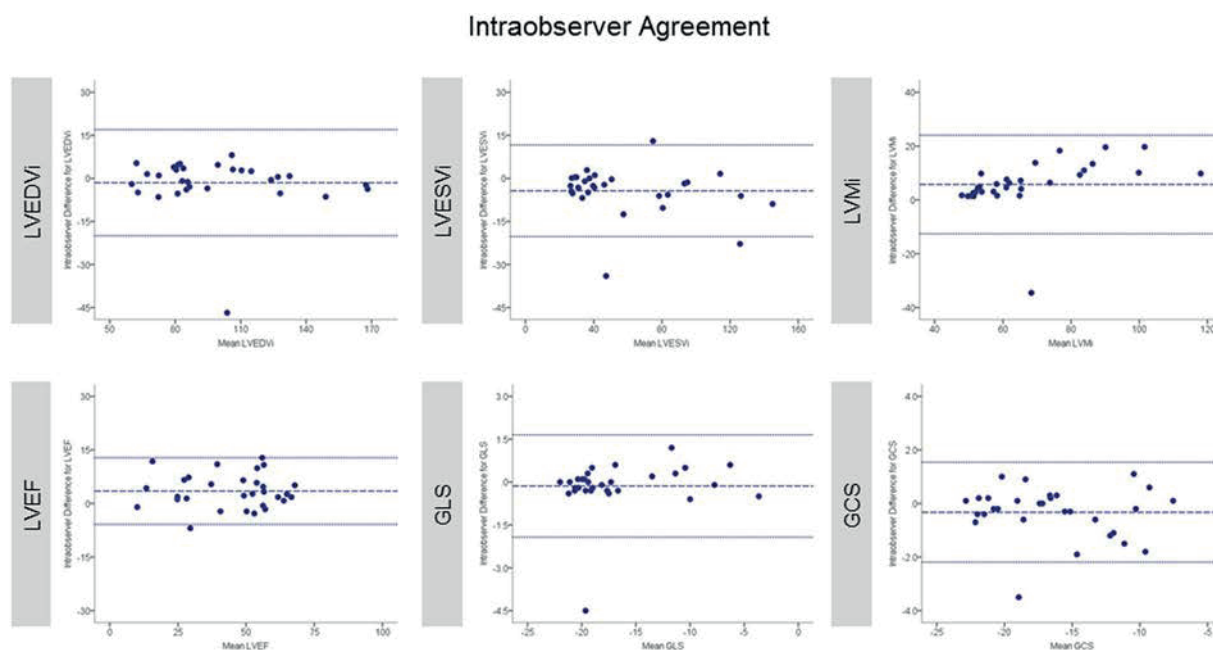


Figure 6. Bland-Altman plots with limits of agreement show the intraobserver agreement of fast-SENC for LVEDVi, LVESVi, LVMI, LVEF, GLS and GCS. The middle-dashed line is the mean of difference of measures. The upper and lower dotted lines are ± 1.96 standard deviation. SENC = strain-encoded imaging; LVEDVi = left ventricular end-diastolic volume index; LVESVi = left ventricular end-systolic volume index; LVMI = left ventricular mass index; LVEF = left ventricular ejection fraction; GLS = global longitudinal strain; GCS = global circumferential strain.

may reduce the necessary sample size for clinical trials^{44,45}. Neizel *et al.*, evaluated interobserver agreement in healthy volunteers and found very high reproducibility in SENC strain measurements ($r = 0.87$), which was superior to CMR tagging (0.81)⁴². Hamdan *et al.*, reported similar findings in healthy volunteers scanned on a 3.0 T MRI system with ICC between observers and repeated studies ranging from 0.92 to 0.98⁴⁶. Our findings are in line with the results of previous studies. We found excellent interobserver and intraobserver agreement of LV global longitudinal and circumferential strain. Moreover, for the first time we demonstrated excellent interobserver and intraobserver reproducibility of LV volumes and ejection fraction estimated using fast-SENC imaging. As reported previously, the agreement of LV mass measurements was lower, especially at the intraobserver level (ICC 0.91; 95% confidence interval 0.74–0.96).

At present, CMR is becoming the imaging modality of choice in multicentric cardiovascular trials⁴⁷; therefore, inter-institutional agreement of derived measures must be recognized as a relevant source of error. Sample size calculation is an important aspect of study design and depends on the concordance of measurements. Much attention has been attributed to CMR scanning and data analysis guidelines^{22–24}. However, little is known on whether knowledge, experience or appropriate initial training has more impact on the precision of measurements. Beerbaum *et al.*, investigated the impact of interobserver variance between the institutions for volumetric and flow CMR data. Images were analyzed by experienced readers only. Inter-institutional agreement was assessed before and after a dedicated training course. Interestingly, in patients, on transverse planes, variation coefficient for LV volumes was significantly decreased by training ($p < 0.007$). For short-axis volumetry training also resulted in narrower limits of agreement. The reproducibility did not improve significantly with training in healthy volunteers. However, the highest variability after training in volunteers was found for LV mass (transverse acquisition: 12–15%, short-axis acquisition: 9–12%)⁴⁸.

In a recent study, Negishi *et al.* evaluated the role of experience in the precision and validity of strain measurements derived using speckle tracking echocardiography. Their study revealed that although the group with the highest level of experience achieved better agreement than those with no experience, the ICC of the inexperienced observers was still very high (0.996 vs. 0.975; $p = 0.0002$)⁴⁹. To examine the importance of initial training we selected four study observers with different knowledge and experience background but provided comprehensive and expert-guided training. Data analysis demonstrated that interobserver agreement was excellent independently of readers' expertise. Nevertheless, it should be noted that LV mass measurements were more variable, especially at the intraobserver level (analysis performed by a CMR beginner), confirming that degree of experience might be also important and should not be underestimated. Despite higher variability, the concordance of LV mass measurements is still clinically acceptable (ICC 0.91).

Our very recent study was conducted to evaluate the impact of proper training on the variability of myocardial strain measurements derived using different commercially available CMR feature tracking software packages. Study results demonstrated that dedicated training of the observer significantly improves reproducibility of LV GLS and GCS⁵⁰. Findings of this study are in line with previous studies and confirm that appropriate initial

training might be more important to achieve highest concordance in CMR measurements. In the light of inadequate experience in CMR imaging fast-SENC technique would be highly desirable in non-expert CMR centers where precise quantitative LV analysis could be performed rapidly even by unexperienced readers.

Limitations

Several limitations of the current study should be noted. First, the population of this study was relatively small. Second, it was single center, single vendor, single software and single MRI lab protocol. Third, only fast-SENC imaging was used to investigate the performance of observers without reflection of other CMR tissue tracking techniques such as tagging, DENSE or feature tracking. We also did not compare fast-SENC images acquired by MRI scanners of different vendors. Lastly, we did not assess the variability of measurements before the training of the observers.

Conclusion

Excellent reproducibility of LV volumetric and functional parameters makes fast-SENC a reliable imaging modality for future studies. Although level of experience is important, it appears that appropriate initial training has much more impact on the agreement of derived measurements. However, larger multicenter studies using MRI scanners and software packages from different vendors are necessary to confirm our findings.

Data Availability

The datasets used and/or analyzed during the current study are available from the corresponding author on reasonable request.

References

- Pennell, D. J. Ventricular volume and mass by CMR. *J Cardiovasc Magn Reson.* **4**, 507–513 (2002).
- Solomon, S. D. *et al.* Influence of ejection fraction on cardiovascular outcomes in a broad spectrum of heart failure patients. *Circulation.* **112**, 3738–3744 (2005).
- Attili, A. K., Schuster, A., Nagel, E., Reiber, J. H. C. & Van Der Geest, R. J. Quantification in cardiac MRI: Advances in image acquisition and processing. *International Journal of Cardiovascular Imaging.* **26**, 27–40 (2010).
- Flachskampf, F. A. *et al.* Cardiac Imaging to Evaluate Left Ventricular Diastolic Function. *JACC Cardiovasc Imaging.* **8**, 1071–1093 (2015).
- Chuang, M. L. *et al.* Importance of imaging method over imaging modality in noninvasive determination of left ventricular volumes and ejection fraction: assessment by two- and three-dimensional echocardiography and magnetic resonance imaging. *J Am Coll Cardiol.* **35**, 477–484 (2000).
- Lapinskas, T. Ischemic heart disease: a comprehensive evaluation using cardiovascular magnetic resonance. *Medicina (Kaunas).* **49**, 97–110 (2013).
- Butler, S. P. *et al.* Reproducibility study of left ventricular measurements with breath-hold cine MRI using a semiautomated volumetric image analysis program. *J Magn Reson Imaging.* **8**, 467–472 (1998).
- Thiele, H. *et al.* Improved accuracy of quantitative assessment of left ventricular volume and ejection fraction by geometric models with steady-state free precession. *J Cardiovasc Magn Reson.* **4**, 327–339 (2002).
- Cikes, M. & Solomon, S. D. Beyond ejection fraction: An integrative approach for assessment of cardiac structure and function in heart failure. *Eur Heart J.* **37**, 1642–1650 (2016).
- Sachdev, V. *et al.* Myocardial strain decreases with increasing transmural extent of infarction: A doppler echocardiographic and magnetic resonance correlation study. *J Am Soc Echocardiogr.* **19**, 34–39 (2006).
- Pedrizetti, G., Mangual, J. & Tonti, G. On the geometrical relationship between global longitudinal strain and ejection fraction in the evaluation of cardiac contraction. *J Biomech.* **47**, 746–749 (2014).
- Buss, S. J. *et al.* Assessment of myocardial deformation with cardiac magnetic resonance strain imaging improves risk stratification in patients with dilated cardiomyopathy. *Eur Hear J Cardiovasc Imaging.* **16**, 307–315 (2015).
- Osman, N. F., Sampath, S., Atalar, E. & Prince, J. L. Imaging longitudinal cardiac strain on short-axis images using strain-encoded MRI. *Magn Reson Med.* **46**, 324–334 (2001).
- Tanaka, A. *et al.* *In situ* constructive myocardial remodeling of extracellular matrix patch enhanced with controlled growth factor release. *J Thorac Cardiovasc Surg.* **150**, 1280–1290 (2015).
- Ibrahim, E. S. H. *et al.* Real-time MR imaging of myocardial regional function using strain-encoding (SENC) with tissue through-plane motion tracking. *J Magn Reson Imaging.* **26**, 1461–1470 (2007).
- Korosoglou, G. *et al.* Strain-encoded magnetic resonance: a method for the assessment of myocardial deformation. *ESC Heart Fail.* **2**, 12442 (2019).
- Pan, L. *et al.* Real-time imaging of regional myocardial function using fast-SENC. *Magn Reson Med.* **55**, 386–395 (2006).
- Lapinskas, T. *et al.* Strain-encoded cardiac magnetic resonance imaging: a new approach for fast estimation of left ventricular function. *BMC Cardiovasc Disord.* **19**, 1–7 (2019).
- Mordi, I. R. *et al.* Comprehensive Echocardiographic and Cardiac Magnetic Resonance Evaluation Differentiates Among Heart Failure With Preserved Ejection Fraction Patients, Hypertensive Patients, and Healthy Control Subjects. *JACC Cardiovasc Imaging.* **11**, 577–585 (2018).
- Vincenti, G. *et al.* Stress Perfusion CMR in Patients With Known and Suspected CAD: Prognostic Value and Optimal Ischemic Threshold for Revascularization. *JACC Cardiovasc Imaging.* **10**, 526–537 (2017).
- Bucciarelli-Ducci, C. *et al.* CMR Guidance for Recanalization of Coronary Chronic Total Occlusion. *JACC Cardiovasc Imaging.* **9**, 547–556 (2016).
- Kramer, C. M., Barkhausen, J., Flamm, S. D., Kim, R. J. & Nagel, E. Standardized cardiovascular magnetic resonance (CMR) protocols 2013 update. *J Cardiovasc Magn Reson.* **15**, 91 (2013).
- Schulz-Menger, J. *et al.* Standardized image interpretation and post processing in cardiovascular magnetic resonance: Society for Cardiovascular Magnetic Resonance (SCMR) Board of Trustees Task Force on Standardized Post Processing. *J Cardiovasc Magn Reson.* **15**, 35 (2013).
- Valsangiacomo Buechel, E. R. *et al.* Indications for cardiovascular magnetic resonance in children with congenital and acquired heart disease: an expert consensus paper of the Imaging Working Group of the AEPIC and the Cardiovascular Magnetic Resonance Section of the EACVI. *Eur Hear J Cardiovasc Imaging.* **16**, 281–297 (2015).
- Hoffmann, R. *et al.* Refinements in stress echocardiographic techniques improve inter-institutional agreement in interpretation of dobutamine stress echocardiograms. *Eur Heart J.* **23**, 821–829 (2002).
- Hoffmann, R. *et al.* Standardized guidelines for the interpretation of dobutamine echocardiography reduce interinstitutional variance in interpretation. *Am J Cardiol.* **82**, 1520–1524 (1998).

27. Gertz, R. J. *et al.* Inter-vendor reproducibility of left and right ventricular cardiovascular magnetic resonance myocardial feature-tracking. *PLoS One*. **13**, e0193746 (2018).
28. Bland, J. M. & Altman, D. G. Statistical Methods for Assessing Agreement Between Two Methods of Clinical Measurement. *Lancet*. **327**, 307–310 (1986).
29. Oppo, K., Leen, E., Angerson, W. J., Cooke, T. G. & McArdle, C. S. Doppler perfusion index: an interobserver and intraobserver reproducibility study. *Radiology*. **208**, 453–457 (1998).
30. Harjola, V.-P. *et al.* Organ dysfunction, injury and failure in acute heart failure: from pathophysiology to diagnosis and management. A review on behalf of the Acute Heart Failure Committee of the Heart Failure Association (HFA) of the European Society of Cardiology (ESC). *Eur J Heart Fail*. **19**, 821–836 (2017).
31. Zamorano, J. L. *et al.* ESC position paper on cancer treatments and cardiovascular toxicity developed under the auspices of the ESC committee for practice guidelines: The task force for cancer treatments and cardiovascular toxicity of the European Society of Cardiology (ESC). *Eur Heart J*. **37**, 2768–2801 (2016).
32. Baumgartner, H. *et al.* ESC/EACTS Guidelines for the management of valvular heart disease. *Eur Heart J*. **38**, 2739–2791 (2017).
33. Ponikowski, P. *et al.* ESC Guidelines for the diagnosis and treatment of acute and chronic heart failure. *Eur Heart J*. **37**, 2129–2200 (2016).
34. Stanton, T., Leano, R. & Marwick, T. H. Prediction of all-cause mortality from global longitudinal speckle strain: Comparison with ejection fraction and wall motion scoring. *Circ Cardiovasc Imaging*. **2**, 356–364 (2009).
35. Gavara, J. *et al.* Prognostic Value of Strain by Tissue Tracking Cardiac Magnetic Resonance After ST-Segment Elevation Myocardial Infarction. *JACC Cardiovasc Imaging*. **11**, 1448–1457 (2017).
36. Pedrizzetti, G., Claus, P., Kilner, P. J. & Nagel, E. Principles of cardiovascular magnetic resonance feature tracking and echocardiographic speckle tracking for informed clinical use. *J Cardiovasc Magn Reson*. **18**, 51 (2016).
37. Zerhouni, E. A., Parish, D. M., Rogers, W. J., Yang, A. & Shapiro, E. P. Human heart: tagging with MR imaging—a method for noninvasive assessment of myocardial motion. *Radiology*. **169**, 59–63 (1988).
38. Yeon, S. B. *et al.* Validation of *in vivo* myocardial strain measurement by magnetic resonance tagging with sonomicrometry. *J Am Coll Cardiol*. **38**, 555–561 (2001).
39. Ibrahim, E.-S. H. Myocardial tagging by Cardiovascular Magnetic Resonance: evolution of techniques-pulse sequences, analysis algorithms, and applications. *J Cardiovasc Magn Reson*. **13**, 36 (2011).
40. Shehata, M. L. *et al.* Real-time single-heartbeat fast strain-encoded imaging of right ventricular regional function: Normal versus chronic pulmonary hypertension. *Magn Reson Med*. **64**, 98–106 (2010).
41. Korosoglou, G. *et al.* Real-time fast strain-encoded magnetic resonance imaging to evaluate regional myocardial function at 3.0 Tesla: Comparison to conventional tagging. *J Magn Reson Imaging*. **27**, 1012–1018 (2008).
42. Neizel, M. *et al.* Strain-encoded (SENC) magnetic resonance imaging to evaluate regional heterogeneity of myocardial strain in healthy volunteers: Comparison with conventional tagging. *J Magn Reson Imaging*. **29**, 99–105 (2009).
43. Mirea, O. *et al.* Variability and Reproducibility of Segmental Longitudinal Strain Measurement: A Report From the EACVI-ASE Strain Standardization Task Force. *JACC Cardiovasc Imaging*. **11**, 15–24 (2018).
44. Morton, G. *et al.* Inter-study reproducibility of cardiovascular magnetic resonance myocardial feature tracking. *J Cardiovasc Magn Reson*. **14**, 43 (2012).
45. Lapinskas, T. *et al.* Cardiovascular magnetic resonance feature tracking in small animals – a preliminary study on reproducibility and sample size calculation. *BMC Med Imaging*. **17**, 51 (2017).
46. Hamdan, A. *et al.* Strain-encoded MRI to evaluate normal left ventricular function and timing of contraction at 3.0 tesla. *J Magn Reson Imaging*. **29**, 799–808 (2009).
47. Symons, R. *et al.* Long-Term Incremental Prognostic Value of Cardiovascular Magnetic Resonance After ST-Segment Elevation Myocardial Infarction. A Study of the Collaborative Registry on CMR in STEMI. *JACC Cardiovasc Imaging*. **11**, 813–825 (2017).
48. Beerbaum, P. *et al.* Cardiac function by MRI in congenital heart disease: Impact of consensus training on interinstitutional variance. *J Magn Reson Imaging*. **30**, 956–966 (2009).
49. Negishi, T. *et al.* Effect of Experience and Training on the Concordance and Precision of Strain Measurements. *JACC Cardiovasc Imaging*. **10**, 518–522 (2017).
50. Backhaus, S. J. *et al.* Cardiovascular magnetic resonance imaging feature tracking: Impact of training on observer performance and reproducibility. *PLoS One*. **14**, e0210127 (2019).

Acknowledgements

We thank Anne Wölffel-Gale for editorial assistance. S.K. was supported by an unrestricted research grant from Philips Healthcare and Myocardial Solutions. C.S. is an employee of Philips Healthcare. The study was supported by the German Centre for Cardiovascular Research (DZHK).

Author Contributions

All authors made relevant contributions to the study and reviewed the manuscript. T.L., V.Z., J.E. and H.H. analyzed and interpreted data. T.L. performed statistical analysis and drafted the manuscript. C.S. participated in the design of the study and coordinated CMR data acquisition. R.G., S.G. and S.J.B. helped with the interpretation of data. R.Z., G.K., B.P. and A.S. made substantial contributions to the concept of the study and revised the manuscript for important intellectual content. S.K. designed and coordinated the study, helped to interpret the data and to draft the manuscript. All authors have read and approved the final manuscript.

Additional Information

Competing Interests: S.K. received an unrestricted research grant by Philips Healthcare and a research grant from Myocardial Solutions. C.S. is an employees of Philips Healthcare. T.L., S.K., A.S. and B.P. received support from the DZHK (German Centre for Cardiovascular Research). The remaining authors declare that they have no competing interests.

Publisher's note: Springer Nature remains neutral with regard to jurisdictional claims in published maps and institutional affiliations.



Open Access This article is licensed under a Creative Commons Attribution 4.0 International License, which permits use, sharing, adaptation, distribution and reproduction in any medium or format, as long as you give appropriate credit to the original author(s) and the source, provide a link to the Creative Commons license, and indicate if changes were made. The images or other third party material in this article are included in the article's Creative Commons license, unless indicated otherwise in a credit line to the material. If material is not included in the article's Creative Commons license and your intended use is not permitted by statutory regulation or exceeds the permitted use, you will need to obtain permission directly from the copyright holder. To view a copy of this license, visit <http://creativecommons.org/licenses/by/4.0/>.

© The Author(s) 2019

Lebenslauf

Mein Lebenslauf wird aus datenschutzrechtlichen Gründen in der elektronischen Version meiner Arbeit nicht veröffentlicht.

Publikationsliste

1. **Erley J**, Genovese D, Tapaskar N, Alvi N, Rashedi N, Besser SA, Kawaji K, Goyal N, Kelle S, Lang RM, Mor-Avi V, Patel AR. Echocardiography and cardiovascular magnetic resonance based evaluation of myocardial strain and relationship with late gadolinium enhancement. *J Cardiovasc Magn Reson.* 2019;21(1):46.
Journal Impact Factor (2018): 5.070
2. **Erley J**, Zieschang V, Lapinskas T, Demir A, Wiesemann S, Haass M, Osman NF, Simonetti OP, Liu Y, Patel AR, Mor-Avi V, Unal O, Johnson KM, Pieske B, Hansmann J, Schulz-Menger J, Kelle S. A multi-vendor, multi-center study on reproducibility and comparability of fast strain-encoded cardiovascular magnetic resonance imaging. *Int J Cardiovasc Imaging.* 2020.
Journal Impact Factor (2018): 1.860
3. Bucius P, **Erley J**, Tanacli R, Zieschang V, Giusca S, Korosoglou G, Steen H, Stehning C, Pieske B, Pieske-Kraigher E, Schuster A, Lapinskas T, Kelle S. Comparison of feature tracking, fast-SENC, and myocardial tagging for global and segmental left ventricular strain. *ESC Heart Fail.* 2019.
Journal Impact Factor (2018): 3.407
4. Lapinskas T, Zieschang V, **Erley J**, Stoiber L, Schnackenburg B, Stehning C, Gebker R, Patel AR, Kawaji K, Steen H, Zaliunas R, Backhaus SJ, Schuster A, Makowski M, Giusca S, Korosoglou G, Pieske B, Kelle S. Strain-encoded cardiac magnetic resonance imaging: a new approach for fast estimation of left ventricular function. *BMC Cardiovasc Disord.* 2019;19(1):52.
Journal Impact Factor (2018): 1.947
5. Miskinyte E, Bucius P, **Erley J**, Zamani SM, Tanacli R, Stehning C, Schneeweis C, Lapinskas T, Pieske B, Falk V, Gebker R, Pedrizzetti G, Solowjowa N, Kelle S. Assessment of Global Longitudinal and Circumferential Strain Using Computed Tomography Feature Tracking: Intra-Individual Comparison with CMR Feature Tracking and Myocardial Tagging in Patients with Severe Aortic Stenosis. *J Clin Med.* 2019;8(9).
Journal Impact Factor (2018): 5.688
6. Lapinskas T, Hireche-Chikaoui H, Zieschang V, **Erley J**, Stehning C, Gebker R, Giusca S, Korosoglou G, Zaliunas R, Backhaus SJ, Schuster A, Pieske B, Kelle S. Effect of comprehensive initial training on the variability of left ventricular measures using fast-SENC cardiac magnetic resonance imaging. *Sci Rep.* 2019;9(1):12223.

Journal Impact Factor (2018): 4.011

Danksagung

Zuerst möchte ich gerne die Gelegenheit nutzen, mich von ganzem Herzen bei Herrn Professor Dr. Sebastian Kelle, dem Betreuer dieser Promotion und meinem Mentor, zu bedanken. Es wäre mir ohne seine Koordination, Hilfestellung und Expertise nicht möglich gewesen, diese Forschungsprojekte zu vollenden. Durch die Zusammenarbeit mit ihm habe ich ein großes Interesse an der Forschung in der nicht-invasiven Bildgebung entwickelt. Zudem möchte ich Herrn Professor Kelle für die Möglichkeit danken, auch weiterhin an einer Vielzahl von Projekten mitzuwirken und so diverse neue Möglichkeiten der nicht-invasiven Herzbildgebung kennenzulernen. Besonders danken möchte ich ihm dafür, dass er sich dafür eingesetzt hat, mir einen Forschungsaufenthalt an der „University of Chicago“ zu ermöglichen. So lernte ich Dr. Patel und Dr. Mor-Avi kennen. Beide verhalfen mir zu einer äußerst lehrreichen Zeit in Chicago. Sie haben mir viel über die Verfassung eines Manuskriptes und über Forschungsthemen in der kardialen Magnetresonanztomographie sowie über die Präsentation von Forschung auf Kongressen beigebracht

Auch bei den Teams aus dem „CMR Core-Lab“ des Deutschen Herzzentrums und der „University of Chicago“ und den tatkräftigen medizinisch-technischen Assistent*innen möchte ich mich herzlich bedanken. All diese Projekte zu vollenden hat uns zusammen viel Kraft und Teamarbeit gekostet. Ich konnte währenddessen von allen viel lernen und habe nicht nur wundervolle Kolleg*innen kennengelernt, sondern auch wahre Freundschaften schließen können.

Zuletzt möchte ich mich bei meiner Familie, meinen Freund*innen und meinem Lebenspartner für die stetige moralische Unterstützung und Motivation bedanken.